

DUDLEY KNOX LIBRARY
NAVAL POSTGRADUATE SCHOOL
MONTEREY, CALIFORNIA 93943

RELEASABLE TO NPS INTERNATIONAL AFFILIATES

(Ref.: Memo, T702 NC4(0142) dtd 21 Mar 88

NAVAL POSTGRADUATE SCHOOL

Monterey, California



RELEASABLE TO NPS INTERNATIONAL AFFILIATES

(Ref.: Memo, T702 NC4(0142) dtd 21 Mar 88

THESIS

NUMERICAL COMPUTATION OF THE SCATTERING
COEFFICIENTS OF AN INDUCTIVE
STRIP IN A FIN-LINE

by

John C. Deal

March 1984

Thesis Advisor:

J. B. Knorr

Special Distribution

T217394

RELEASABLE TO NPS INTERNATIONAL AFFILIATES

(Ref.: Memo, T702 NC4(0142) dtd 21 Mar 88

REPORT DOCUMENTATION PAGE		READ INSTRUCTIONS BEFORE COMPLETING FORM
1. REPORT NUMBER	2. GOVT ACCESSION NO.	3. RECIPIENT'S CATALOG NUMBER
4. TITLE (and Subtitle) Numerical Computation of the Scattering Coefficients of an Inductive Strip in a Fin-Line		5. TYPE OF REPORT & PERIOD COVERED Master's Thesis; March 1984
7. AUTHOR(s) John C. Deal		6. PERFORMING ORG. REPORT NUMBER
9. PERFORMING ORGANIZATION NAME AND ADDRESS Naval Postgraduate School Monterey, California 93943		8. CONTRACT OR GRANT NUMBER(s)
11. CONTROLLING OFFICE NAME AND ADDRESS Naval Postgraduate School Monterey, California 93943		10. PROGRAM ELEMENT, PROJECT, TASK AREA & WORK UNIT NUMBERS
14. MONITORING AGENCY NAME & ADDRESS (if different from Controlling Office)		12. REPORT DATE March 1984
		13. NUMBER OF PAGES 178
		15. SECURITY CLASS. (of this report) UNCLASSIFIED
		15a. DECLASSIFICATION/DOWNGRADING SCHEDULE
16. DISTRIBUTION STATEMENT (of this Report) Special Distribution		
17. DISTRIBUTION STATEMENT (of the abstract entered in Block 20, if different from Report)		
18. SUPPLEMENTARY NOTES		
19. KEY WORDS (Continue on reverse side if necessary and identify by block number) Microwave Septums Millimeter Wave Discontinuities Integrated Circuits Fin-Line Inductive Strips		
20. ABSTRACT (Continue on reverse side if necessary and identify by block number) Fin-line is well recognized as a viable transmission structure for millimeter waves. The theoretical analysis of fin-line has received considerable attention and has been discussed in the literature by numerous authors. The spectral domain method of analysis has been established as a powerful and versatile approach to computing the characteristics of fin-line derived structures. This thesis describes the application of the spectral domain		

technique to the solution of the problem of end coupled fin-line cavities. Galerkin's method is used to compute the odd and even mode resonant lengths which are then used to calculate the scattering coefficients of the inductive strip separating the two cavities. Results are compared with experimental measurements.

Special Distribution

Numerical Computation of the Scattering Coefficients
of an Inductive Strip in a Fin-Line

by

John C. Deal
Captain(P), United States Army
B.A., University of Alaska, 1973

Submitted in partial fulfillment of the
requirements for the degree of

MASTER OF SCIENCE IN ELECTRICAL ENGINEERING

from the

NAVAL POSTGRADUATE SCHOOL
March 1984

Thesis
D.18254
C.1

ABSTRACT

Fin-line is well recognized as a viable transmission structure for millimeter waves. The theoretical analysis of fin-line has received considerable attention and has been discussed in the literature by numerous authors. The spectral domain method of analysis has been established as a powerful and versatile approach to computing the characteristics of fin-line derived structures. This thesis describes the application of the spectral domain technique to the solution of the problem of end coupled fin-line cavities. Galerkin's method is used to compute the odd and even mode resonant lengths which are then used to calculate the scattering coefficients of the inductive strip separating the two cavities. Results are compared with experimental measurements.

TABLE OF CONTENTS

I.	INTRODUCTION-----	15
II.	SINGLE CAVITY RESONANT LENGTH AND EQUIVALENT REACTANCE OF A SHORTING SEPTUM-----	17
A.	THEORY-----	17
B.	NUMERICAL ANALYSIS AND RESULTS-----	22
III.	COUPLED CAVITIES RESONANT LENGTHS FOR ODD AND EVEN MODES-----	27
A.	THEORY-----	27
B.	NUMERICAL ANALYSIS AND RESULTS-----	31
IV.	INDUCTIVE STRIP SCATTERING PARAMETERS-----	37
A.	THEORY-----	37
B.	NUMERICAL ANALYSIS AND RESULTS-----	38
V.	CONCLUSIONS AND RECOMMENDATIONS-----	43
APPENDIX A -	THEORETICAL ANALYSIS OF THE SINGLE RESONANT CAVITY-----	46
APPENDIX B -	NUMERICAL RESULTS FOR THE SINGLE RESONANT CAVITY-----	55
APPENDIX C -	THEORETICAL ANALYSIS OF THE COUPLED RESONANT CAVITIES-----	60
APPENDIX D -	NUMERICAL RESULTS FOR THE SINGLE AND COUPLED RESONANT CAVITIES-----	72
APPENDIX E -	THEORETICAL ANALYSIS OF THE SCATTERING PARAMETERS OF THE FIN-LINE INDUCTIVE STRIP-----	76
APPENDIX F -	NUMERICAL RESULTS FOR THE SCATTERING PARAMETERS OF THE FIN-LINE INDUCTIVE STRIP-----	83
APPENDIX G -	FINCAV, PROGRAM LISTING FOR THE SINGLE RESONANT CAVITY-----	139
APPENDIX H -	FINSTRP, PROGRAM LISTING FOR THE COUPLED RESONANT CAVITIES-----	151

LIST OF REFERENCES----- 176

INITIAL DISTRIBUTION LIST----- 178

LIST OF FIGURES

II-1	Fin-line Structure Geometry (end on view)-----	21
II-2	Fin-line Resonant Cavity Geometry (sideview and z dependence of the electric field)-----	21
II-3	Convergence Test for the Single Resonant Cavity for $w/b=0.5$, $t/D=16.0$, $f=12$ GHz-----	24
III-1	Coupled Fin-line Cavities and Basis Functions Field Distributions (side view)-----	28
III-2	Convergence Test for the Coupled Resonant Cavities for $w/b=1.0$, $t/D=1.0$, and $f=8.0$, 10.0, and 12.0 GHz-----	33
III-3	Equivalent Electrical Length of an Inductive Strip-----	34
IV-1	$ S_{11} $ Convergence Test for the Inductive Strip for $w/b=1.0$, $t/d=1.0$, and $f=8, 10$, and 12 GHz-----	39
B-1	Normalized Septum Reactance v.s. Frequency for $\epsilon_{r_2}=1.0$ and $w/b=1.0$ as the Inductive Strip Width $T \rightarrow \infty$ -----	55
B-2	Normalized Septum Reactance v.s. Frequency for $\epsilon_{r_2}=1.0$ and $w/b=0.5$ as the Inductive Strip Width $T \rightarrow \infty$ -----	56
B-3	Normalized Septum Reactance v.s. Frequency for $\epsilon_{r_2}=1.0$ and $w/b=0.1$ as the Inductive Strip Width $T \rightarrow \infty$ -----	57
B-4	Normalized Septum Reactance v.s. Septum Length $T/2$ in Inches for $w/b=1.0$ and $\epsilon_{r_2}=1.0$ for 8, 10, and 12 GHz-----	58
B-5	Normalized Septum Reactance v.s. Normalized Frequency for $\epsilon_{r_2}=2.2$, $b/a=0.5$, $h_1/a=0.5$, $D/a=0$, as $T \rightarrow \infty$ -----	59

B-6	Normalized Septum Reactance v.s. Normalized Frequency for $\epsilon_{r_2}=2.2$, $b/a=0.5$, $h_1/a=0.5$ $D/a=0.05$, as $T \rightarrow \infty$ -----	60
B-7	Normalized Septum Reactance v.s. Normalized Frequency for $\epsilon_{r_2}=2.2$, $b/a=0.5$, $D/a=0.1$, as $T \rightarrow \infty$ ----- r_2 -----	61
D-1	Odd and Even Mode Resonant Lengths for the Unilaterally Coupled Fin-line Resonant Cavities for $w/b=1.0$, $t/D=0.05$, 0.1 , 0.2 , 0.5 , 1.0 , 2.0 , 5.0 , 10.0 , and 16.0 , $D=0.1$ inch, $\epsilon_{r_2}=1.0$, and for 8 through 12 GHz----- r_2 -----	73
D-2	Resonant Lengths for the Single Fin-line Resonant Cavity for $w/b=1.0$, $t/D=0.2$, 0.5 , 1.0 , 2.0 , 5.0 , 10.0 , and 16.0 , $D=0.1$ inch, $\epsilon_{r_2}=1.0$, and for 8 through 12 GHz-----	75
F-1	$ S_{11} $ v.s. Frequency for $T=.02$ inch Inductive Strip, $w/b=1.0$, and $\epsilon_{r_2}=1.0$ -----	83
F-2	$ S_{11} $ v.s. Frequency for $T=.05$ inch Inductive Strip, $w/b=1.0$, and $\epsilon_{r_2}=1.0$ -----	84
F-3	$ S_{11} $ v.s. Frequency for $T=0.1$ inch Inductive Strip, $w/b=1.0$, and $\epsilon_{r_2}=1.0$ -----	85
F-4	$ S_{11} $ v.s. Frequency for $T=0.2$ inch Inductive Strip, $w/b=1.0$, and $\epsilon_{r_2}=1.0$ -----	86
F-5	$ S_{11} $ v.s. Frequency for $T=0.5$ inch Inductive Strip, $w/b=1.0$, and $\epsilon_{r_2}=1.0$ -----	87
F-6	$ S_{11} $ v.s. Frequency for $T=1.0$ inch Inductive Strip, $w/b=1.0$, and $\epsilon_{r_2}=1.0$ -----	88
F-7	θ_{11} v.s. Frequency for $T=.02$ inch Inductive Strip, $w/b=1.0$, and $\epsilon_{r_2}=1.0$ -----	89

F-8	θ_{11} v.s. Frequency for T=.05 inch Inductive Strip, w/b=1.0, and $\epsilon_{r_2}=1.0$ -----	90
F-9	θ_{11} v.s. Frequency for T=0.1 inch Inductive Strip, w/b=1.0, and $\epsilon_{r_2}=1.0$ -----	91
F-10	θ_{11} v.s. Frequency for T=0.2 inch Inductive Strip, w/b=1.0, and $\epsilon_{r_2}=1.0$ -----	92
F-11	θ_{11} v.s. Frequency for T=0.5 inch Inductive Strip, w/b=1.0, and $\epsilon_{r_2}=1.0$ -----	93
F-12	θ_{11} v.s. Frequency for T=1.0 inch Inductive Strip, w/b=1.0, and $\epsilon_{r_2}=1.0$ -----	94
F-13	$ S_{21} $ v.s. Frequency for T=.02 inch Inductive Strip, w/b=1.0, and $\epsilon_{r_2}=1.0$ -----	95
F-14	$ S_{21} $ v.s. Frequency for T=.05 inch Inductive Strip, w/b=1.0, and $\epsilon_{r_2}=1.0$ -----	96
F-15	$ S_{21} $ v.s. Frequency for T=0.1 inch Inductive Strip, w/b=1.0, and $\epsilon_{r_2}=1.0$ -----	97
F-16	$ S_{21} $ v.s. Frequency for T=0.2 inch Inductive Strip, w/b=1.0, and $\epsilon_{r_2}=1.0$ -----	98
F-17	$ S_{21} $ v.s. Frequency for T=0.5 inch Inductive Strip, w/b=1.0, and $\epsilon_{r_2}=1.0$ -----	99
F-18	$ S_{21} $ v.s. Frequency for T=1.0 inch Inductive Strip, w/b=1.0, and $\epsilon_{r_2}=1.0$ -----	100

F-19	θ_{21} v.s. Frequency for T=.02 inch Inductive Strip, w/b=1.0, and $\epsilon_{r_2}=1.0$ -----	101
F-20	θ_{21} v.s. Frequency for T=.05 inch Inductive Strip, w/b=1.0, and $\epsilon_{r_2}=1.0$ -----	102
F-21	θ_{21} v.s. Frequency for T=0.1 inch Inductive Strip, w/b=1.0, and $\epsilon_{r_2}=1.0$ -----	103
F-22	θ_{21} v.s. Frequency for T=0.2 inch Inductive Strip, w/b=1.0, and $\epsilon_{r_2}=1.0$ -----	104
F-23	θ_{21} v.s. Frequency for T=0.5 inch Inductive Strip, w/b=1.0, and $\epsilon_{r_2}=1.0$ -----	105
F-24	θ_{21} v.s. Frequency for T=1.0 inch Inductive Strip, w/b=1.0, and $\epsilon_{r_2}=1.0$ -----	106
F-25	$ S_{11} $ v.s. Frequency for T=.05 inch Inductive Strip, w/b=0.5, and $\epsilon_{r_2}=1.0$ -----	107
F-26	$ S_{11} $ v.s. Frequency for T=0.1 inch Inductive Strip, w/b=0.5, and $\epsilon_{r_2}=1.0$ -----	108
F-27	$ S_{11} $ v.s. Frequency for T=0.2 inch Inductive Strip, w/b=0.5, and $\epsilon_{r_2}=1.0$ -----	109
F-28	$ S_{11} $ v.s. Frequency for T=0.5 inch Inductive Strip, w/b=0.5, and $\epsilon_{r_2}=1.0$ -----	110
F-29	$ S_{11} $ v.s. Frequency for T=.05 inch Inductive Strip, w/b=.25, and $\epsilon_{r_2}=1.0$ -----	111

F-30	$ S_{11} $ v.s. Frequency for T=0.1 inch Inductive Strip, w/b=.25, and $\epsilon_{r_2}=1.0$ -----	112
F-31	$ S_{11} $ v.s. Frequency for T=0.2 inch Inductive Strip, w/b=.25, and $\epsilon_{r_2}=1.0$ -----	113
F-32	$ S_{11} $ v.s. Frequency for T=0.5 inch Inductive Strip, w/b=.25, and $\epsilon_{r_2}=1.0$ -----	114
F-33	$ S_{11} $ v.s. Frequency for T=.05 inch Inductive Strip, w/b=.2, and $\epsilon_{r_2}=1.0$ -----	115
F-34	$ S_{11} $ v.s. Frequency for T=0.1 inch Inductive Strip, w/b=.2, and $\epsilon_{r_2}=1.0$ -----	116
F-35	$ S_{11} $ v.s. Frequency for T=0.2 inch Inductive Strip, w/b=.2, and $\epsilon_{r_2}=1.0$ -----	117
F-36	$ S_{11} $ v.s. Frequency for T=0.5 inch Inductive Strip, w/b=.2, and $\epsilon_{r_2}=1.0$ -----	118
F-37	$ S_{11} $ v.s. Frequency for T=.05 inch Inductive Strip, w/b=.1, and $\epsilon_{r_2}=1.0$ -----	119
F-38	$ S_{11} $ v.s. Frequency for T=0.1 inch Inductive Strip, w/b=.1, and $\epsilon_{r_2}=1.0$ -----	120
F-39	$ S_{11} $ v.s. Frequency for T=0.2 inch Inductive Strip, w/b=.1, and $\epsilon_{r_2}=1.0$ -----	121
F-40	$ S_{11} $ v.s. Frequency for T=0.5 inch Inductive Strip, w/b=.1, and $\epsilon_{r_2}=1.0$ -----	122

F-41	θ_{11} v.s. Frequency for T=.05 inch Inductive Strip, w/b=.5, and $\epsilon_{r_2}=1.0$ -----	123
F-42	θ_{11} v.s. Frequency for T=0.1 inch Inductive Strip, w/b=.5, and $\epsilon_{r_2}=1.0$ -----	124
F-43	θ_{11} v.s. Frequency for T=0.2 inch Inductive Strip, w/b=.5, and $\epsilon_{r_2}=1.0$ -----	125
F-44	θ_{11} v.s. Frequency for T=0.5 inch Inductive Strip, w/b=.5, and $\epsilon_{r_2}=1.0$ -----	126
F-45	θ_{11} v.s. Frequency for T=.05 inch Inductive Strip, w/b=.25, and $\epsilon_{r_2}=1.0$ -----	127
F-46	θ_{11} v.s. Frequency for T=0.1 inch Inductive Strip, w/b=.25, and $\epsilon_{r_2}=1.0$ -----	128
F-47	θ_{11} v.s. Frequency for T=0.2 inch Inductive Strip, w/b=.25, and $\epsilon_{r_2}=1.0$ -----	129
F-48	θ_{11} v.s. Frequency for T=0.5 inch Inductive Strip, w/b=.25, and $\epsilon_{r_2}=1.0$ -----	130
F-49	θ_{11} v.s. Frequency for T=.05 inch Inductive Strip, w/b=.2, and $\epsilon_{r_2}=1.0$ -----	131
F-50	θ_{11} v.s. Frequency for T=0.1 inch Inductive Strip, w/b=.2, and $\epsilon_{r_2}=1.0$ -----	132
F-51	θ_{11} v.s. Frequency for T=0.2 inch Inductive Strip, w/b=.2, and $\epsilon_{r_2}=1.0$ -----	133

F-52	θ_{11} v.s. Frequency for T=0.5 inch Inductive Strip, w/b=.2, and $\epsilon_{r_2}=1.0$ -----	134
F-53	θ_{11} v.s. Frequency for T=.05 inch Inductive Strip, w/b=.1, and $\epsilon_{r_2}=1.0$ -----	135
F-54	θ_{11} v.s. Frequency for T=0.1 inch Inductive Strip, w/b=.1, and $\epsilon_{r_2}=1.0$ -----	136
F-55	θ_{11} v.s. Frequency for T=0.2 inch Inductive Strip, w/b=.1, and $\epsilon_{r_2}=1.0$ -----	137
F-56	θ_{11} v.s. Frequency for T=0.5 inch Inductive Strip, w/b=.1, and $\epsilon_{r_2}=1.0$ -----	138

ACKNOWLEDGMENTS

I would like to thank Professor Jeffery B. Knorr for his continued support, guidance, and most of all faith. I would also like to thank Dr. Yi-Chi Shih for his counsel and inspirational suggestions and Dr. H. M. Lee for his continued interest and provoking questions. Most importantly, I would like to thank my wife, Colleen, for her assistance in preparing the figures and graphs contained within and proofing the draft and final document. Her continued emotional support has made the completion of this research possible.

I. INTRODUCTION

The need and advantages, as well as difficulties, of going to millimeter waves (30-300 GHz) are recognized. As a consequence, numerous transmission media have been developed in an effort to take advantage of present technology and overcome the drawbacks. The objectives of these new designs are low attenuation, single mode operation, containment of spurious emissions, ease of production, and compatibility with integrated circuit technology. One such design which appears very attractive is the Fin-Line transmission structure [Refs. 1, 2].

The Spectral Domain technique of analyzing Fin-Line structures is well established in the research community [Refs. 3-11]. A review of these references shows that difficulties lie in the viable choice of basis functions to represent the fields within the Fin-line structure. Two papers of prime importance in the establishment of the spectral domain technique for analyzing Fin-Line structures are by Knorr and Shayda in July 1980 [Ref. 4] and Peter-Schmidt and Itoh in September 1980 [Ref. 5]. Both addressed the proper choice of basis functions and accurately determined the Fin-Line guide wavelength and characteristic impedance. What is important is that their methods and approach have set the standard in Fin-Line analysis.

The purpose of this thesis is to analyze the inductive discontinuity (strip) in a Fin-Line structure. This problem was first addressed in November 1981 by Knorr [Ref. 7]. Therefore, this thesis is a direct extension of Knorr's work. The analysis was accomplished in three phases. First, an extended set of basis functions were chosen and the results presented in Reference 7 were reproduced. This was the evaluation of the resonant length of a single resonant cavity. Second, another set of basis functions was chosen and the odd and even resonant lengths of two unilaterally coupled Fin-Line cavities were evaluated. Third, with the odd and even mode resonant lengths obtained and treating the inductive discontinuity as a lossless two-port network, the S-parameters were evaluated in terms of the odd and even resonant lengths. The numerical results were then compared with the experimental results obtained by Miller [Ref. 12]. This thesis will discuss both the theoretical and numerical aspects of the analysis.

II. SINGLE CAVITY RESONANT LENGTH AND EQUIVALENT REACTANCE OF A SHORTING SEPTUM

The following is broken down into two parts: theory and numerical analysis and results. The theory covers the method of moments, Galerkin's method, Fin-Line structure and selected basis set, implementation of Galerkin's method, and definition of inner product and equivalent reactance. The numerical analysis and results cover the search method, functional singularities, limits of summation, convergence, and comparison with other numerical and experimental results.

A. THEORY

Harrington in Reference 13 provides a full and complete discussion of the computation of fields by the method of moments. Briefly, if $L(f) = g$ represents an equation where L is a linear operator, g is a known function (or possibly unknown) and f is a function which represents the solution to be determined, allowing f to be represented by a series of basis functions f_n a solution may be arrived at in the following manner:

Given

$$L(f) = g \tag{1}$$

Let

$$f = \sum_n a_n f_n \tag{2}$$

where the α_n 's are to be determined. Substituting (2) into (1) yields

$$\sum_n \alpha_n L(f_n) = g$$

Multiplying by W_m ,

$$\sum \alpha_n w_m L(f_n) = w_m g$$

where w_m is some weight function to be determined.

Taking the inner product, $\langle a, b \rangle$, of both sides:

$$\sum \alpha_n \langle w_m, L(f_n) \rangle = \langle w_m, g \rangle$$

where the inner product is to be determined. Allowing

$$w_m = f_m:$$

$$\sum \alpha_n \langle f_m, L(f_n) \rangle = \langle f_m, g \rangle .$$

This is known as Galerkin's Method.

In matrix algebra format, the above becomes:

$$[\langle f_i, L(f_j) \rangle] \begin{bmatrix} \alpha_1 \\ \vdots \\ \alpha_n \end{bmatrix} = [\langle f_i, g \rangle]$$

where $i=1$ to m and $j=1$ to n .

The theoretical analysis of the single resonant cavity begins by continuing with Eq. (12), Reference 7, and making the assumption that $E_z \approx 0$ leaving:

$$\langle G_{11} E_x, E_x \rangle = 0$$

where the script represent the Fourier transform of the x-directed electric field, and G_{11} is the dyadic Green's function obtained by the application of the Helmholtz Equation and Boundary Conditions to the Fin-Line geometry as depicted in Figure II-1. Here "a" is the width of the guide, "b" is the height of the guide, D is the dielectric thickness, h_1 and h_2 represent the fins location relative to the side walls of the guide and w is the gap width.

ϵ_{r1} , ϵ_{r2} , and ϵ_{r3} are the relative dielectric constants for regions 1, 2, and 3 respectively.

The following assumption is made in the transform (spectral) domain:

$$E_x(\alpha_n, \xi_k) = E_x^X(\alpha_n) E_x^Z(\xi_u)$$

where α_n and ξ_k are the transform variables with respect to x and z and are defined by Equations (4) and (5), Reference 7. Next step is the choice of basis functions.

The x component of the electric field is defined as:

$$e_x(x,z) = A \sum_{m=1}^M B_m \cos \frac{(2m-1)\pi z}{\ell}$$

$$\text{for } |x| \leq w/2, \quad |z| \leq \ell/2.$$

The geometries for the fin-line resonant cavity and the z-dependence of the x-directed electric field, $e_x(x,z)$ are as depicted by Figure II-2.

In the transform (spectral) domain,

$$F\{e_x(x,z)\} = E_x^x(\alpha_n) \sum_{m=1}^M B_m E_{x_m}^z(\xi_k)$$

where

$$E_x^x(\alpha_n) = AW \frac{\sin \frac{1}{2}(\alpha_n D)(\frac{w}{D})}{\frac{1}{2}(\alpha_n D)(\frac{w}{D})}$$

and

$$E_{x_m}^z(\xi_k) = (-1)^m \frac{(2m-1)}{2}(\ell\pi) \frac{\cos(\xi_k D)(\ell/2D)}{(\xi_k D)^2(\frac{\ell}{2D})^2 - [\frac{(2m-1)\pi}{2}]^2} \cdot$$

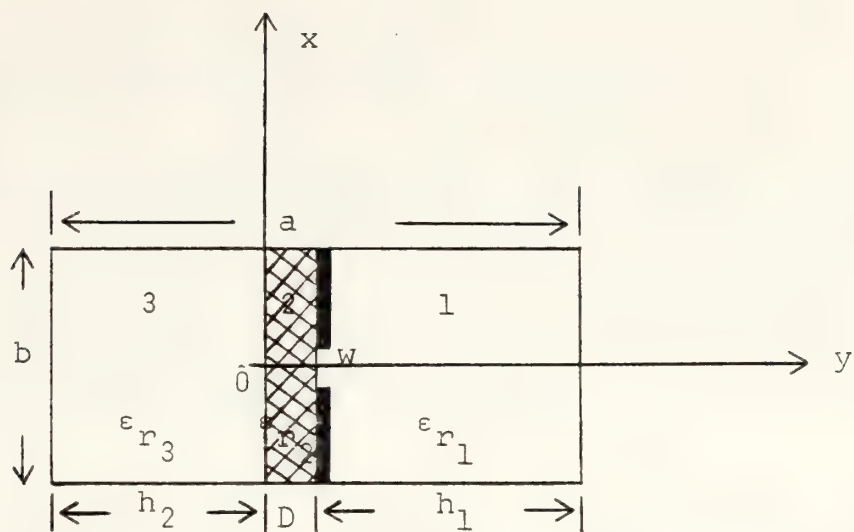


Figure II-1 Fin-Line Structure Geometry
(end on view)

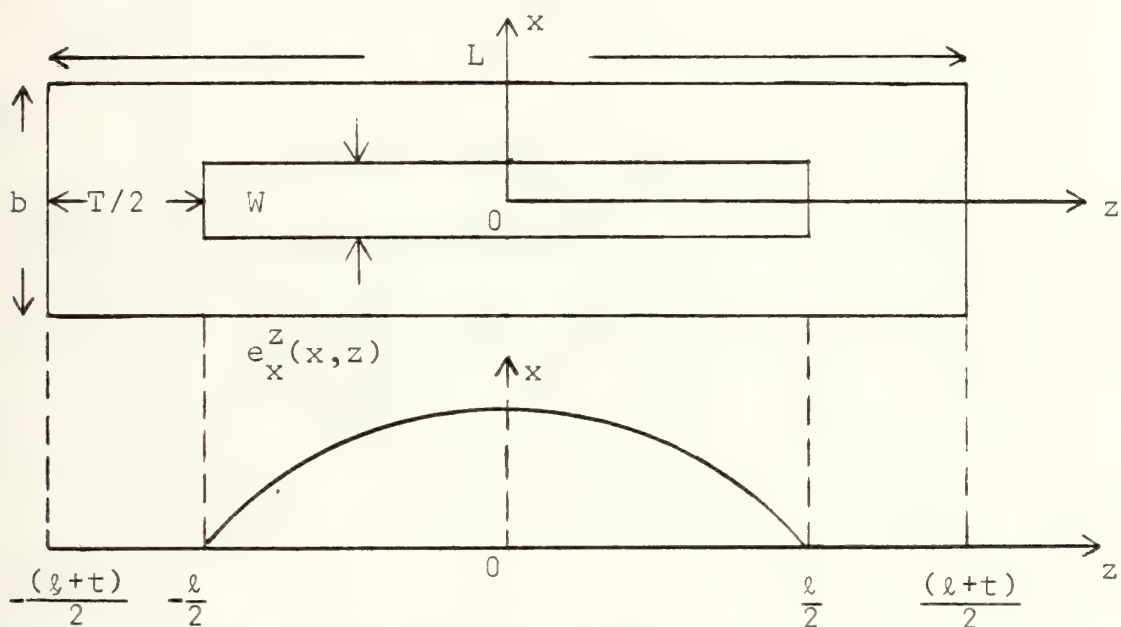


Figure II-2 Fin-Line Resonant Cavity Geometry
(side view and z -dependence of the
electric field)

Finally, applying the Galerkin's Method yields:

$$\langle B_j [E_x^x(\alpha_n)]^2 G_{11} E_{x_i}^z(\xi_k) E_{x_j}^z(\xi_k) \rangle = 0$$

$$[\langle [E_x^x(\alpha_n)]^2 G_{11} E_{x_i}^z(\xi_k) E_{x_j}^z(\xi_k) \rangle] [\tilde{B}_j] = 0$$

where $i = 1$ to M and $j = 1$ to M . And the inner produce is defined as

$$\sum_{n=-\infty}^{\infty} \sum_{k=-\infty}^{\infty} G_{11}(\alpha_n, \xi_k) [E_x^x(\alpha_n)]^2 E_{x_i}^z(\xi_k) E_{x_j}^z(\xi_k) \quad [\text{Ref. 13}].$$

For a complete derivation see Appendix A.

B. NUMERICAL ANALYSIS AND RESULTS

The problem is to find the value of the resonant length for a given Fin-Line geometry and frequency which causes the determinant of the matrix of inner profuct terms to equal zero, since the B coefficients cannot be zero except in the trivial case.

For ease in numerical calculations and for programming purposes all geometric parameters and frequencies are normalized as follows:

D/λ Wavelength (frequency) of interest normalized with respect to D , the dielectric thickness
 h_1/D Fin location relative to the positive "y" side wall normalized with respect to D
 h_2/D Fin location relative to the negative "y" side wall normalized with respect to D
 b/D Guide height normalized with respect to D
 t/D Inductive Strip width normalized with respect to D .

The resonant length normalized to the guide wavelength is defined as ℓ/λ' where λ' , the guide wavelength, is numerically determined in the same manner as described in Reference 4. A simple bisectional search is used to determine the value of ℓ/λ' for which the determinant goes to zero. The residue is .0001, therefore, the uncertainty of ℓ/λ' is $\pm .0001$. Increasing the size of the matrix (number of basis functions used) continually improves the result until a limit is reached where no further improvement is realized. This is depicted by the convergence test of Figure II-3.

Two other numerical considerations are singularities in the $E_x^X(\alpha_n)$ and $E_x^Z(\xi_k)$ functions and the limits of summation over α_n and ξ_k . Both are derived and resolved in Appendix A. The documented program is found in Appendix G.

Numerical results for a single cavity (Figure II-2) are graphed and may be found in Appendix B. The figures of Appendix B are of the same form as Figures 7 through 12 of Reference 7, hence comparison is made with those results.

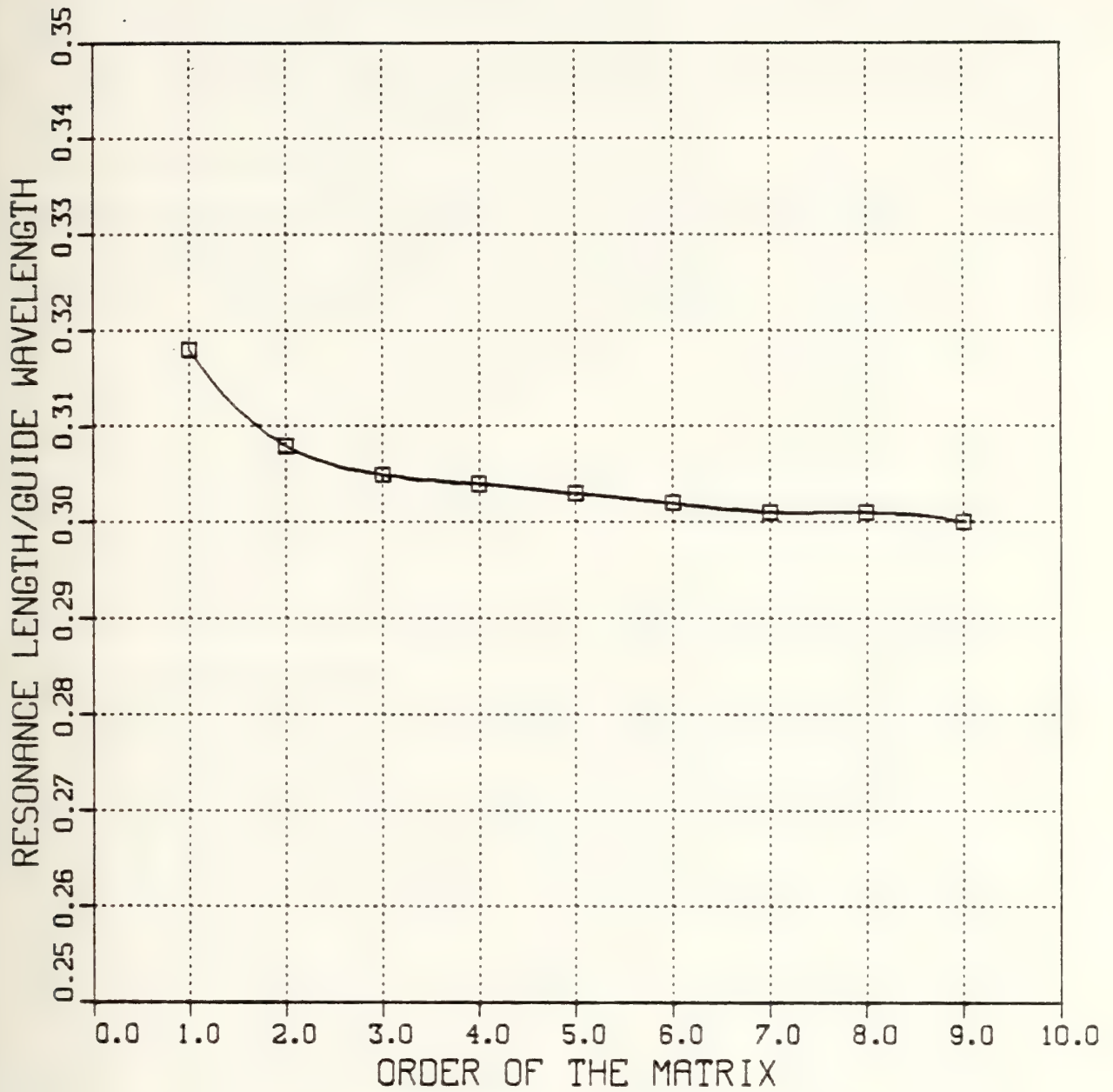


Figure II-3 Convergence Test for the Single Resonant Cavity for $w/b=0.5$, $t/D=16.0$, and $f=12$ GHz

The solid curves and circled crosses in these graphs are the numerical and experimental results respectively from Reference 7. The dashed curves are the numerical results obtained by the method of moments with the expanded set of cosine functions.

As can be seen, the difference between the experimental and numerical results of Reference 7 and the numerical results obtained herein ranges from 0% to 2%. The normalized septum reactance is defined as

$$x = \tan 2\pi \Delta\ell/\lambda'$$

where $\Delta\ell/\lambda' = \frac{1}{2}(\frac{1}{2} - \ell/\lambda')$, [Ref. 7]. Figure B-4 shows the variation of the normalized reactance and in turn, the normalized resonant length, with respect to the length of the inductive septum.

The dimension of the matrix was chosen to be 7x7 based upon a convergence test in which the matrix order was iterated until the resonant length was no more than 0.001 (typically less than 0.5%). Given a particular fin-line geometry and frequency, the solutions converged with matrix dimensions ranging from 5x5 to 8x8. The numerical calculations for Figures B-1 through B-4 were for WR(90) waveguide with centered fins for 8.0 to 12.0 GHz, normalized gap width $w/b = 1.0, 0.5, \text{ and } 0.1$, dielectric thickness $D=0.1$ inch,

$a = 0.9$ inch, $b = 0.4$ inch, and for a dielectric constant, $\epsilon_{r_2} = 1.0$. The numerical calculations for Figures B-5 through B-7 were for normalized frequencies $2a/\lambda = 1.2$ to 1.8 normalized gap width $w/b = 1.0, 0.5, 0.2$ and 0.1 , $b/a = 0.5$, and $D/a = 0.1, 0.05$, and 0.1 respectively for $\epsilon_{r_2} = 1.0$ and 2.2 .

The conclusion based upon this phase of the analysis is that an expanded set of basis functions works extremely well and that the choice of the cosine basis functions to represent the z -variation of the x -directed electric field was proper and viable. This set the stage for phase two of the analysis.

III. COUPLED CAVITIES RESONANT LENGTHS FOR ODD AND EVEN MODES

The following is broken down into two parts, theory and numerical analysis and results. The theory will cover the geometry of the two coupled fin-line cavities, the selected basis set, odd and even mode field distribution, and implementation of Galerkin's Method. The numerical analysis and results will cover convergence and three tests of the results for correctness.

A. THEORY

The theoretical analysis of the two coupled cavities is an extension of the single cavity. The geometrical structure of the coupled cavities and field distributions of the selected basis functions for the z-dependence of the x-directed electric field E_x^z for both odd and even modes are described in Figure III-1. The end walls are perfect shorts and the inductive discontinuity is in the center of the structure. The solid lines of the field distributions represent even modes and the dashed lines represent odd modes.

As can be seen the choice of basis functions are both sine and cosine. The x and z dependence of the electric field is given by

$$e_x(x,z) = A \sum_{q=1}^Q B_q F_q(z), \quad |x| \leq w/2, \quad t/2 \leq |z| \leq \ell + t/2$$

where

$$F_q(z) = \begin{cases} \sin \frac{q\pi z}{\ell}, & \text{for } q \text{ even.} \\ \cos \frac{q\pi z}{\ell}, & \text{for } q \text{ odd.} \end{cases}$$

For example, if $q = 4$, which is even,

$$F_4(z) = \sin \frac{4\pi z}{\ell}$$

and if $q = 7$, which is odd,

$$F_7(z) = \cos \frac{7\pi z}{\ell}.$$

And the spatially shifted basis functions as depicted in Figure III-1 are defined

$$F_q(z) = \begin{cases} - \sin \frac{q\pi}{\ell} [z + (\frac{\ell+t}{2})], & z < 0 \\ & q \text{ even} \\ \pm \sin \frac{q\pi}{\ell} [z - (\frac{\ell+t}{2})], & z > 0 \\ & q \text{ even} \\ \cos \frac{q\pi}{\ell} [z + (\frac{\ell+t}{2})], & z < 0 \\ & q \text{ odd} \\ \pm \cos \frac{q\pi}{\ell} [z - (\frac{\ell+t}{2})], & z > 0 \\ & q \text{ odd} \end{cases}$$

where for (+) the sine function, plus (+) = odd mode and minus (-) = even mode, and where for (+) the cosine function, plus (+) = even mode and minus (-) = odd mode.

In the transform domain,

$$F\{e_x(x,z)\} = E_x^x(\alpha_n) \cdot \sum_{q=1}^Q B_q E_{x_q}^z(\xi_k)$$

where α_n and ξ_k are the x and z transform variables respectively as defined by Eq. (4) & (5), Reference 7.

For q even:

$$E_{x_q}^z(\xi_k) = \begin{cases} (-1)^q \left(\frac{q\pi}{2} l_e\right) \frac{\sin \theta}{\theta^2 - \left(\frac{q\pi}{2}\right)^2} (2) \sin \xi_k \left(\frac{l_e + t}{2}\right) \\ \text{for Even Mode} \\ (-1)^q \left(\frac{q\pi}{2} l_o\right) \frac{\sin \theta}{\theta^2 - \left(\frac{q\pi}{2}\right)^2} (2j) \cos \xi_k \left(\frac{l_e + t}{2}\right) \\ \text{for Odd Mode} \end{cases}$$

and for q odd:

$$E_{x_q}^z(\xi_k) = \begin{cases} (-1)^q \frac{q}{2} (l_e \pi) \frac{\cos \theta}{\theta^2 - \left(\frac{q\pi}{2}\right)^2} (2) \cos \xi_k \left(\frac{l_e + t}{2}\right) \\ \text{for Even Mode} \\ (-1)^q \frac{q}{2} (l_o \pi) \frac{\cos \theta}{\theta^2 - \left(\frac{q\pi}{2}\right)^2} (2j) \sin \xi_k \left(\frac{l_o + t}{2}\right) \\ \text{for Odd Mode} \end{cases}$$

where $\theta = (\xi_k l)/2$.

Finally applying Galerkin's Method yields:

$$[<[E_x^x(\alpha_n)^2 G_{11} E_{x_i}^z (E_u) E_{x_j}^z (\xi_k)>] [\tilde{B}_j] = 0$$

where "i" and "j" = 1 to Q and $E_{x_i}^z$ and $E_{x_j}^z$ are sine or cosine functions depending on whether the index is odd or even.

The inner product is defined over α_n and ξ_k , as it was in the single cavity case. For a complete derivation see Appendix C.

B. NUMERICAL ANALYSIS AND RESULTS

The problem is to find the values of the odd and even mode resonant lengths of the coupled cavities for a given Fin-Line geometry and frequency which cause the determinant of the matrix of inner products to equal zero. The odd and even mode resonant lengths normalized to the guide wavelength are denoted by ℓ_o/λ' and ℓ_e/λ' , respectively. As in the single cavity case, a bisectional search is used with a residue of .0001, therefore the values of the odd and even resonant lengths are determined to within $\pm .0001$. Increasing the size of the matrix (number of basis functions used) continually improves the result until a numerical limit in computation is reached. That limit is a matrix of 12x12 dimension. However, the numerical results do converge with increasing order of the matrix. This is depicted by the

convergence test of Figure III-2. Therefore an order of 12 was used for all numerical results contained herein for the coupled cavities where $w/b=1.0$.

Three checks are used to determine the correctness of the numerical results. First, as the thickness of the inductive strip increases a point is reached where the two cavities become uncoupled and $\epsilon_e/\lambda' = \epsilon_o/\lambda'$. This is seen to occur in the numerical results of Appendix D for $w/b = 1.0$ where the Fin-Line gap equals the "b" dimension of the waveguide. As the thickness of the strip, normalized with respect to D, t/D (TOVD) approaches 16.0, ϵ_e/λ' (LE/LPR) equals ϵ_o/λ' (LO/LPR). Here $D = 0.1$ inch and D/λ (D/L) is the free space wavelength normalized with respect to D, the dielectric thickness, for 8.0 to 12.0 GHz in steps of 0.5 GHz. Second, as the thickness of the strip becomes very small ϵ_o/λ' approaches one half (0.5). Referring to Appendix D, this can be seen to occur. In fact, as $t/D = 0.1$, $\epsilon_o/\lambda' = 0.5$ for all frequencies from 8 to 12 GHz. The third check is noting that the odd mode resonant length is equal to the resonant length for the single cavity plus the equivalent electrical length of the inductive septum, as derived in the single cavity case. Graphically, this is depicted in Figure III-3.

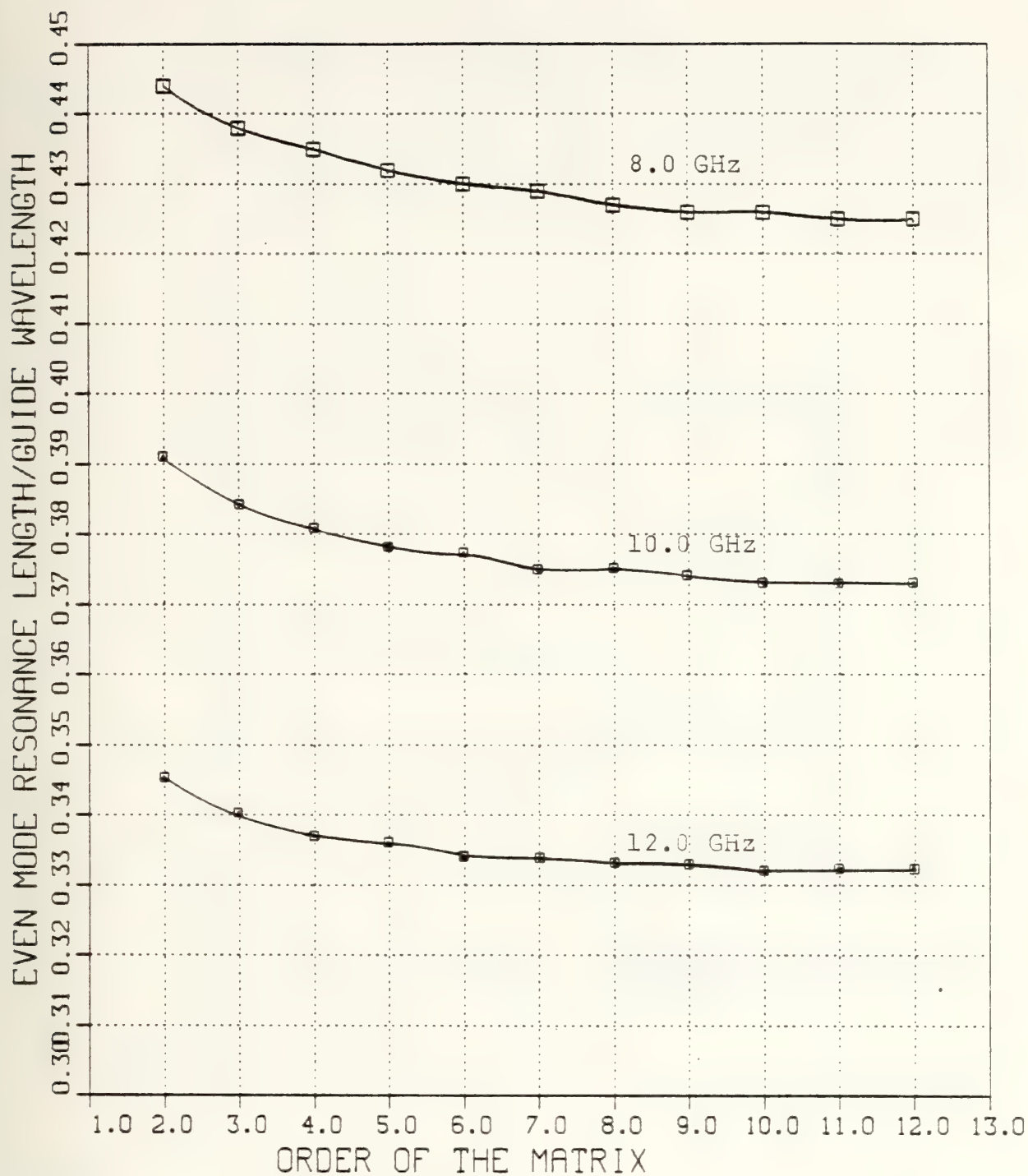
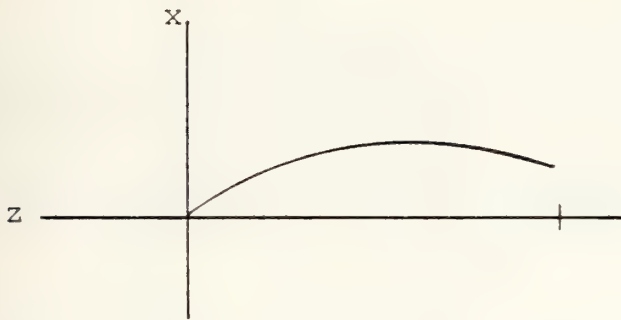


Figure III-2 Convergence Test for the Coupled Resonant Cavities for $w/b=1.0$, $t/D=1.0$ and $f=8.0$, 10.0 , and 12.0 GHz

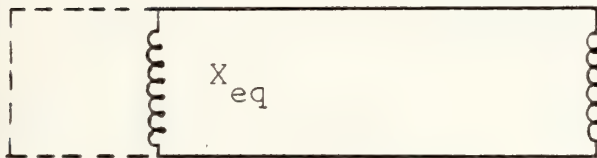
Short
Circuit →



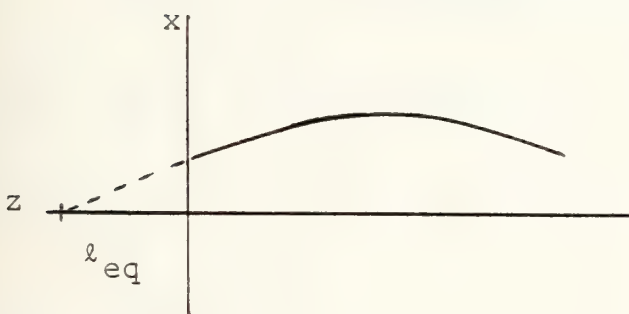
One Cavity of the
Coupled Resonant
Cavities



Resonant Field



Single Resonant
Cavity



Resonant Field and
Equivalent Electrical
Length

Figure III-3 Equivalent Electrical Length of an Inductive

Therefore, $\ell_o/\lambda' = \ell/\lambda' + \ell_{eq}/\lambda'$

$$x_{eq} = \tan 2\pi \ell_{eq}/\lambda'$$

$$\ell_{eq}/\lambda' = \frac{1}{2\pi} \tan^{-1} x_{eq}$$

where x_{eq} = XSC as derived in the single cavity case and is included in Appendix D.

As an example, consider 8 GHz for $w/b = 1.0$, and $t/D = 1.0$:

$$\ell_o/\lambda' = .487 \qquad x_{eq} = .098$$

$$\ell/\lambda' = .469 \qquad \ell_{eq}/\lambda' = \frac{1}{2\pi} \tan^{-1} .098$$

$$.487 \approx .469 + .0155$$

$$\approx .4845, \quad \text{mean relative error} = 0.5\%$$

As a second example, consider 12 GHz for $w/b = 1.0$ and $t/D = 5.0$:

$$\ell_o/\lambda' = .406 \qquad x_{eq} = .688$$

$$\ell/\lambda' = .308 \qquad \ell_{eq}/\lambda' = \frac{1}{2\pi} \tan^{-1} .688$$

$$.406 \approx .308 + .096$$

$$\approx .404, \text{ mean relative error} = 0.5\%.$$

The mean relative error is defined as:

$$\text{M.R.E.} = \frac{(\ell_o/\lambda') - (\ell/\lambda' + \ell_{eq}/\lambda')}{\sqrt{(\ell_o/\lambda') (\ell/\lambda' + \ell_{eq}/\lambda')}}.$$

As with the single resonant cavity, two other numerical considerations are singularities in the $E_x^x(\alpha_n)$ and $E_x^z(\xi_k)$ functions and the limits of summation over α_n and ξ_k . Both are derived and resolved in Appendix C. The documented program is found in Appendix H.

The conclusion of this phase of the Fin-Line inductive strip analysis is that numerically the results are correct with regard to convergence and the three checks. Also, the choice of the sine and cosine basis functions was proper and viable. The final phase is to derive the scattering parameters for the inductive strip as a function of both odd and even mode resonant lengths and compare numerical and experimental results.

IV. INDUCTIVE STRIP SCATTERING PARAMETERS

A. THEORY

The final phase of the analysis of the Fin-Line inductive discontinuity consists of deriving its scattering parameters from basic microwave network circuit theory by treating the strip as a lossless two-port network and then comparing the numerically calculated scattering parameters with these determined through experiment. The complete derivation of the scattering parameters is found in Appendix E. Since the inductive strip is considered lossless, reciprocal, and symmetric, the scattering matrix is unitary, $S_{11} = S_{22}$ and $S_{21} = S_{12}$. The values of S_{11} and S_{12} are determined to be

$$S_{11} = -\exp(j2\pi[\frac{\ell_e}{\lambda_T} + \frac{\ell_o}{\lambda_T}]) \cos 2\pi (\frac{\ell_e}{\lambda_T} - \frac{\ell_o}{\lambda_T})$$

$$S_{12} = j\exp(j2\pi[\frac{\ell_e}{\lambda_T} + \frac{\ell_o}{\lambda_T}]) \sin 2\pi (\frac{\ell_e}{\lambda_T} - \frac{\ell_o}{\lambda_T})$$

and the equivalent circuit reactances for the inductive strip are determined to be

$$x_s = \frac{1}{2} [\tan 2\pi(\frac{1}{2} - \frac{\ell_e}{\lambda_T}) + \tan 2\pi(\frac{1}{2} - \frac{\ell_o}{\lambda_T})]$$

$$M = \frac{1}{2} [\tan 2\pi(\frac{1}{2} - \frac{\ell_e}{\lambda_T}) - \tan 2\pi(\frac{1}{2} - \frac{\ell_o}{\lambda_T})]. \quad [\text{Ref. 14}]$$

B. NUMERICAL ANALYSIS AND RESULTS

Using the odd and even mode resonant lengths numerically determined, the corresponding S_{11} and S_{12} parameters are calculated and checked for convergence. Figure IV-1 shows that convergence is achieved with an order of "10" for the $|S_{11}|$ for $t/D = 1.0$, $w/b = 1.0$, $\epsilon_{r_2} = 1.0$, and for 8, 10, and 12 GHz, as an example. Similar convergences were obtained for various other geometric parameters and frequencies for S_{11} , θ_{11} , S_{12} , and θ_{12} .

The numerical results obtained herein for S_{11} , θ_{11} , S_{12} , and θ_{12} are compared with the experimental measurements by Miller [Ref. 15] and graphically depicted in Appendix F. Referring to Appendix F, the solid lines with circles are numerical data and the dashed lines with squares are the experimental measurements by Miller. Defining the mean relative error (MRE) between the experimental (EXP) and numerical (NUM) data as:

$$\text{M.Rel.Err.} = \left[\frac{(\text{NUM} - \text{EXP})^2}{(\text{NUM})(\text{EXP})} \right]^{1/2} \times 100\%,$$

the mean relative errors for the S_{11} parameters range from 0% up to 8.5% for the phase term θ_{11} for a septum thickness of 0.2 inch at 8 GHz. Errors for the S_{21} parameter are very large in many instances and very erratic.

As an example, for a septum thickness of 0.2 inch, $w/b = 1.0$ at 8 GHz the mean relative error for the $|S_{21}|$ is

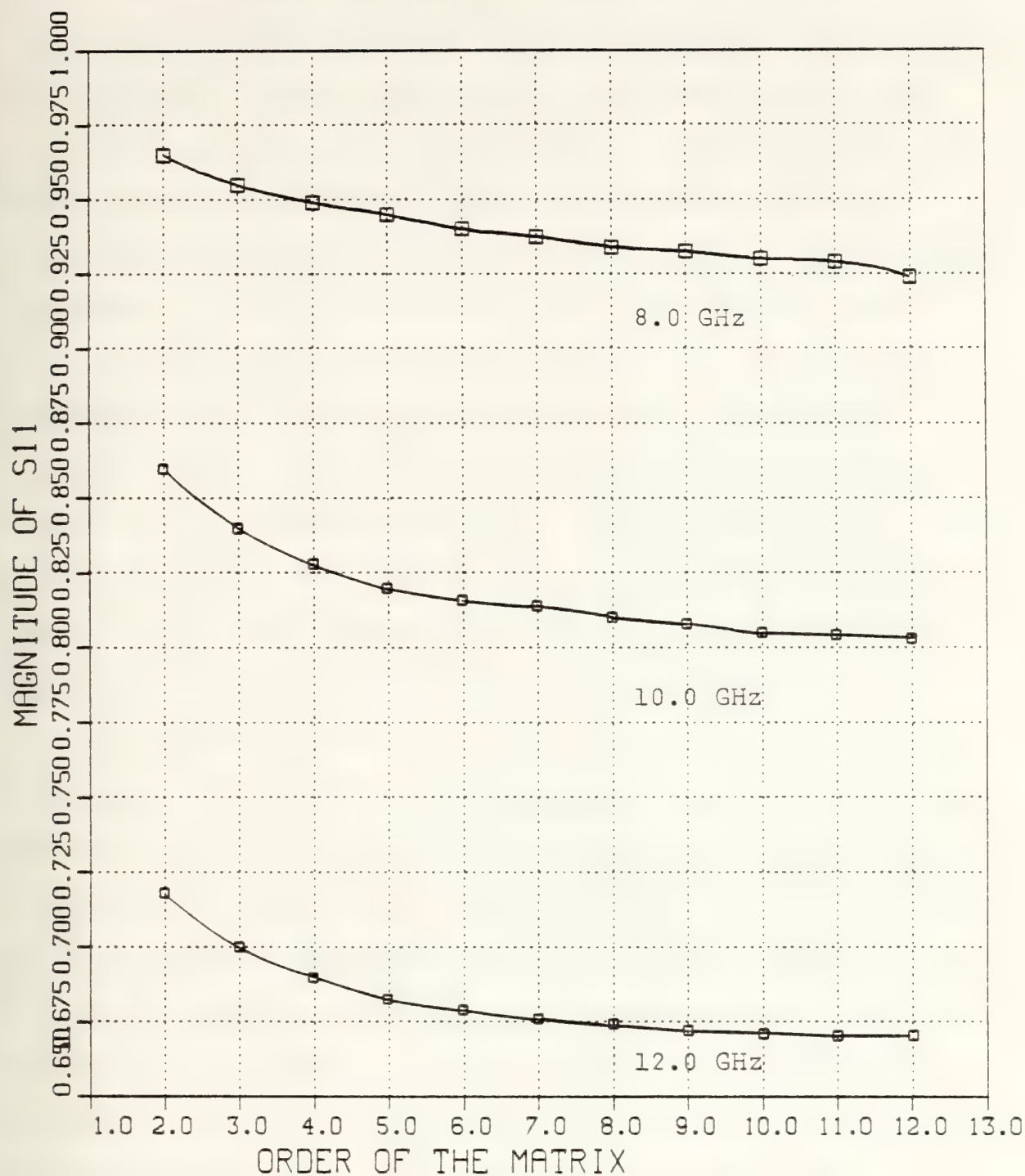


Figure IV-1 $|S_{11}|$ Convergence Test for the Inductive Strip for $w/b=1.0$, $t/D=1.0$, and $f=8.0$, 10.0 , and 12.0 GHz

51.4% and for the phase term θ_{21} the error is 86.66%. In view of these two extremes in agreement between experimental and numerical results, some general statements can be made.

For $|S_{11}|$ and θ_{11} , the mean relative error is generally less than 5% and deviations from this general rule are restricted to the lower frequencies near 8 GHz. For the S_{21} parameter, the error for the $|S_{21}|$ follow the same general rule of being less than 5% with the exception of the septum thickness of 0.2 inch which appears to be a measurement anomaly. However, such is not the case for the phase θ_{21} term of the S_{21} parameter where the mean relative error ranges from 0% to 86% with no median value regardless of frequency range. The closest agreement for the S_{21} parameter between experimental and numerical data can be seen to be for the septum thickness of 0.05 inch where the mean relative error ranges from 0% to 7% for the frequency range from 8.0 to 11.5 GHz and 70.7% for 12 GHz. If the inductive strip is indeed a loss less two-port network then the square root of the sum of the squares of the magnitudes of S_{11} and S_{21} should equal 1.0 and the phase terms of S_{11} and S_{21} should differ by 90° degrees, ($\theta_{11} - \theta_{21} = 90^\circ$). Considering the close agreement between the numerical and experimental data for the magnitude and phase of S_{11} , it is the author's belief that the experimental results for the magnitude and phase of S_{21} for the inductive strip as presented by Miller in Reference 15 are in error and Miller agrees with this fact in his

conclusions. Since the experimental and numerical data for the S_{11} parameters agree within a 5% error for $w/b = 1.0$, numerical calculations of the scattering parameter S_{11} were made and plotted for $w/b = 0.5, 0.25, 0.2$, and 0.1 and are presented in Figures F-25 through F-56 of Appendix F. Values for the S_{21} parameters can be obtained from these curves by noting that:

$$S_{21} = \sqrt{1 - |S_{11}|^2}$$

$$\theta_{21} = \theta_{11} - 90^\circ$$

These curves should prove useful in design and comparison with experimental measurements for $w/b < 1.0$. The numerical results for $w/b < 1.0$ presented were obtained using a matrix of order 8, which corresponds to the use of 8 basis functions to represent the electric field spatial distribution, and restricting the maximum limits of summation for the inner product terms which are the elements of the matrix for which a singularity is sought. This was done in the interest of computation time and may represent an error as high as 2% from that which could be obtained from an order of 10 or higher and unrestricted limits of summation over α_n and ξ_k . The numerical results appear physically sound. Comparison of the $|S_{11}|$ reflection coefficient for a specified strip

width t/D for $w/b = 1.0$ with $w/b = 0.5$ and 0.25 shows that the $|S_{11}|$ increases in magnitude with decreasing gap width w/b . This is physically reasonable in that as the gap becomes smaller the strip width relative to the gap appears electrically wider and the fields in the two cavities become more uncoupled. Comparison of the $|S_{11}|$ for $w/b = 0.25$ with 0.2 and 0.1 reveals that the magnitude drops for $w/b = 0.2$ and then begins to rise again for $w/b = 0.1$. This may be explained by noting that as the gap becomes smaller the electric field strength within the gap increases and is essentially constant and the multiple reflections of the decaying exponential tails between the two cavities on the strip may increase in strength, correspondingly. Hence, as coupling increases the $|S_{11}|$ decreases. However, experimental measurements must be made in order to determine the "correctness" of the numerical results presented here.

V. CONCLUSIONS AND RECOMMENDATIONS

The spectral domain technique used in conjunction with Galerkin's method and the choice of an expanded set of cosine and sine basis functions to represent the spatial distribution has been demonstrated to be proper, viable, and produce accurate results in the analysis of the fin-line inductive strip. For the single resonant cavity, agreement between previously published numerical and experimental results and the numerical results obtained herein is within 2%. For the coupled cavities using the odd and even mode resonant lengths to determine S_{11} for the inductive strips of various widths the agreement at several checkpoints is within 5%, in general.

Numerical computation time, especially for $w/b < 1.0$ can be quite large if high accuracy is sought. Numerical accuracy is a function of the number of basis functions used (matrix order), limits of summation over α_n and ξ_k , and the residue decision to determine the end of a search iteration. These three factors, along with search interval directly impact on computation time. As the order of the matrix goes up, so must the accuracy of the elements of matrix which can only be obtained by increasing the limits of summation for the inner product terms. This is due to the fact that as the determinant of the matrix approaches its singularity, which is what is sought, it becomes "ill-conditioned". If the

elements of the matrix contain a small error then an incorrect value of the determinant will result. As the matrix becomes very ill-conditioned, numerically, exponential underflow or overflow will exceed the capabilities of the available IBM 3033 used. Therefore, a trade must be made between accuracy and computation time.

Four recommendations are offered in conclusion. First, due to the computation time required for highly accurate numerical results, it is recommended that the programs contained herein be transferred to a personal minicomputer. Second, experimental measurements should be made for $w/b < 1.0$ and compared with the numerical results presented herein. Third, the use of other basis functions should be investigated in depth. Two basis functions are recommended. The close numerical agreement between the basis functions used in this thesis and the cosine with the exponential end correction used by Knorr in Reference 7 indicate that using a single cosine function with a sum of exponentials representing the decaying tails of higher order modes may prove to be very accurate. The second basis set recommended is formed from the Chebyshev polynomials of the first kind, $T_n(x)$, presented here as

$$F_n(x) = xT_n(x) - T_{n+1}(x).$$

This is a modified Chebyshev polynomial of the second kind, defined over the interval of -1 to $+1$ and is zero at these two points regardless of order. This function has the advantage of being even or odd depending on the value of the index "n". The fourth and final recommendation is that a faster search routine be sought. The bisectional search used herein is the most accurate and reliable but has the burden of being the slowest. The Newton-Gregory search method is offered for consideration.

APPENDIX A

THEORETICAL ANALYSIS OF THE SINGLE RESONANT CAVITY

Derivation of the Single Resonant Cavity Problem

Begin with
$$G_{11}E_x + G_{12}E_z = J_x$$

$$G_{21}E_x + G_{22}E_z = J_z$$

where all terms are in the frequency domain and the G_{11} , G_{12} , G_{21} , and G_{22} are the dyadic Green's functions as obtained from Knorr [7].

Mult by E_x and E_z and taking the inner product:

$$\langle G_{11} E_x, E_x \rangle + \langle G_{12} E_z, E_x \rangle = \langle J_x, E_x \rangle$$

$$\langle G_{21} E_x, E_z \rangle + \langle G_{22} E_z, E_z \rangle = \langle J_z, E_z \rangle$$

Next assuming $E_z \approx 0$

$$\langle G_{11} E_x, E_x \rangle = \langle J_x, E_x \rangle$$

Here the inner product is defined as

$$\langle a, b \rangle = \sum_{n=-\infty}^{\infty} \sum_{k=-\infty}^{\infty} a(\alpha_n, \xi_k) b^*(\alpha_n, \xi_k)$$

Substituting $E_x = \sum B'_n E_{x_n}$ into the inner product equation and multiplying by E_{x_m} :

$$\langle E_{x_m}, G_{ll} \sum B'_n E_{x_n} \rangle = \langle J_x, E_{x_m} \rangle = 0$$

which reduces to

$$\begin{bmatrix} \langle E_{x_i}, G_{ll} E_{x_j} \rangle \\ \vdots \\ \langle E_{x_M}, G_{ll} E_{x_j} \rangle \end{bmatrix} \begin{bmatrix} B'_1 \\ B'_2 \\ \vdots \\ B'_M \end{bmatrix} = 0$$

i and j
go from 1 to M

Clearly, if all B' 's are zero a trivial solution results \therefore solve the characteristic equation

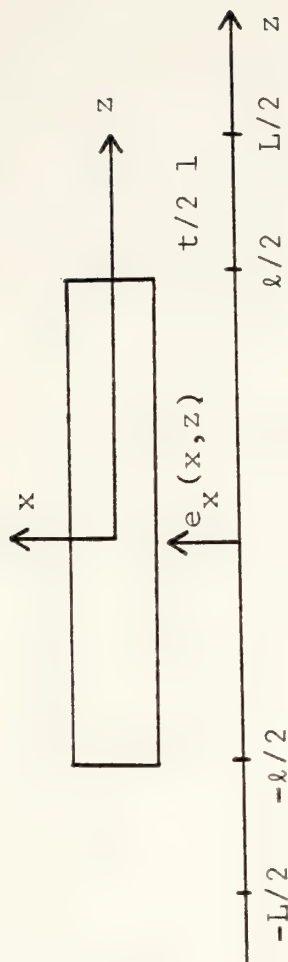
$$\det[\langle \quad \rangle] = 0$$

Assume: $E_x(\alpha_n, \xi_k) = E_x^x(\alpha_n) E_x^z(\xi_k) = \Sigma B_m' E_{x_m}(\alpha_n, \xi_k)$

Let $e_x(x, z) = A \Sigma_{m=1}^M B_m \cos \frac{(2m-1)\pi z}{\ell}$

for $|x| \leq w/2$

$|z| \leq \ell/2$



$L = \ell + t$

Define

$$E_x^x(\alpha_n) = F[e_x^x(x, z)] = \int_{-w/2}^{w/2} A e^{j\alpha_n x} dx = AW \frac{\sin \frac{1}{2}(\alpha_n D)(w/D)}{\frac{1}{2}(\alpha_n D)(w/D)}$$

Define

$$\Sigma B_m E_x^z(\xi_k) = F[e_x^z(x, z)] = \int_{-\ell/2}^{\ell/2} \Sigma B_m \cos \frac{(2m-1)\pi z}{\ell} e^{j\xi_k z} dz$$

$$\Sigma_{m=1}^M B_m (-1)^m \frac{(2m-1)}{2} \ell \pi \frac{\cos(\xi_k D)(\ell/2D)}{(\xi_k D)^2 (\ell/2D)^2 - [\frac{(2m-1)\pi}{2}]^2}$$

Determining the actual value of B'_m to be discarded:

$$E_{x_m} = \sum_n AW \left[\frac{\sin \frac{1}{2}(\alpha_n w)}{\frac{1}{2}(\alpha_n w)} \right] B'_m (-1)^m \frac{(2m-1)}{2} \ell \pi$$

$$\times \frac{\cos \frac{1}{2}(\xi_k \ell)}{(\xi_k \ell / 2)^2 - \left[\frac{(2m-1)\pi}{2} \right]^2}$$

Therefore, $B'_m = \frac{1}{2} AW B_m \ell \pi$.

And the inner product for the ij th term becomes

$$\sum_{n=-\infty}^{\infty} \sum_{k=-\infty}^{\infty} G_{11} \left[\frac{\sin \frac{1}{2}(\alpha_n w)}{\frac{1}{2}(\alpha_n w)} \right]^2 (-1)^{i+j} (2i-1)(2j-1) \frac{\cos \frac{1}{2}(\xi_k \ell)}{(\xi_k \ell / 2)^2 - \left[\frac{(2i-1)\pi}{2} \right]^2}$$

$$\times \frac{\cos \frac{1}{2}(\xi_k \ell)}{(\xi_k \ell / 2)^2 - \left[\frac{(2j-1)\pi}{2} \right]^2}$$

The inner product in expanded form can be written as:

$$\sum_{n=-\infty}^{\infty} \sum_{k=-\infty}^{\infty} f(\alpha_n, \xi_k) = f(\alpha_0, \xi_0) + 2 \sum_{n=1}^{n_{\max}} f(\alpha_n, \xi_0) + 2 \sum_{k=1}^{k_{\max}} f(\alpha_0, \xi_k)$$

$$+ 4 \sum_{n=1}^{n_{\max}} \sum_{k=1}^{k_{\max}} F(\alpha_n, \xi_k)$$

which can be reduced to:

$$\sum_{k=1}^{k_{\max}} \sum_{n=1}^{n_{\max}} f(\alpha_n, \xi_k) + 4 \sum_{n=1}^{n_{\max}} \sum_{k=1}^{k_{\max}} f(\alpha_n, \xi_k), \text{ if } f \text{ is even.}$$

$$N_{\max} \text{ is determined by noting } |E_x^x(\alpha_n)| \sim \frac{1}{\frac{1}{2} \alpha_n^w}$$

$$\text{Letting } \frac{1}{2} \alpha_n^w = \frac{x_{\text{const}}}{2} \quad \text{where } \alpha_n = \frac{n 2\pi}{b}$$

$$\text{yields } N_{\max} = \frac{x_{\text{const}}}{2\pi} \frac{b}{w}$$

And K_{\max} is determined by noting that

$$|E_x^2(\xi_k)| \sim \frac{1}{\theta^2 - \left[\frac{(2m-1)\pi}{2}\right]^2} \quad \text{where} \quad \theta = \xi_k \ell/2$$

$$\text{Letting } \theta^2 - \frac{(2m-1)^2 \pi^2}{4} = z \text{const } \pi^2$$

$$\text{and } \xi_k = (2k-1)\pi/L \quad \text{where } L = \ell + t$$

$$\text{yields } K_{\max} = \frac{1}{2} + \left[z \text{const} + \frac{(2m-1)^2 \ell/2}{4} \right] (1 + t/\ell)$$

The singularities of the E_x^x and E_x^z functions are determined via L'Hospital's Rule:

$$\lim_{\phi \rightarrow 0} \frac{\sin \phi}{\phi} = 1.0, \quad \text{where } \phi = \frac{1}{2} \alpha_n w$$

$$\lim_{\theta \rightarrow \frac{(2m-1)\pi}{2}} \frac{\cos \theta}{\theta^2 - \left[\frac{(2m-1)\pi}{2}\right]^2} = \frac{(-1)^m}{(2m-1)\pi}, \quad \text{where } \theta = \xi_k \ell/2$$

The G_{11} dyadic Green's function obtained from Knorr, notes for Reference 7, is defined as

$$G_{11} = g_{11}^a + g_{11}^b + g_{11}^c + g_{11}^d + g_{11}^e$$

$$g_{11}^a = -j \frac{(k_{c1} D)^2}{(\omega \mu D)(\gamma_1 D) \tanh[(\gamma_1 D)(h_1/D)]}$$

$$g_{11}^b = -j \frac{(k_{c2} D) d_{12}}{d_{11} d_{22} - d_{21} d_{12}} \left(\frac{(\alpha_n D)(\beta D)(k_{c2} D)^2 (\gamma_2 D) \tanh(\gamma_2 D)}{(\omega \mu D)(\gamma_2 D)^2 (k_{c3} D)^2} \right)$$

$$g_{11}^c = j \frac{d_{12} (k_{c2} D)^2}{d_{11} d_{22} - d_{21} d_{12}} \left(\frac{(\alpha_n D)(\beta D)(\gamma_2 D) \tanh(\gamma_2 D)}{(\omega \mu D)(\gamma_2 D)^2} \right)$$

$$g_{11}^d = -j \frac{d_{11} (k_{c2} D)^2}{d_{11} d_{22} - d_{21} d_{12}} \left(\frac{(k_{c2} D)^2 (\gamma_3 D) \tanh[(\gamma_3 D)(h_2/D)]}{(k_{c3} D)^2 (\gamma_2 D)^2} \right)$$

$$g_{11}^e = -j \left(\frac{(k_{c2})^2 d_{11}}{(d_{11}d_{22} - d_{21}d_{12})(\gamma_2 D) \tanh(\gamma_2 D)} \right)$$

where

$$d_{11} = -(k_{c2})^2 \left[1 + \frac{(\omega \epsilon_3 D)(\gamma_3 D)(k_{c2})^2 \tanh(\gamma_2 D)}{(\omega \epsilon_2 D)(\gamma_2 D)(k_{c2})^2 \tanh[(\gamma_3 D)(h_2/D)]} \right]$$

$$d_{12} = (k_{c2})^2 \left[\frac{(\alpha_n D)(\beta D)}{(\omega \epsilon_2 D)(\gamma_2 D)} \right] \left[\frac{(k_{c2})^2}{(k_{c3})^2} - 1 \right]$$

$$d_{21} = -(\alpha_n D)(\beta D) \left[\frac{(k_{c2})^2}{(k_{c1})^2} + \frac{(\omega \epsilon_3 D)(\gamma_3 D)(k_{c2})^2 \tanh(\gamma_2 D)}{(\omega \epsilon_2 D)(\gamma_2 D)(k_{c3})^2 \tanh[(\gamma_3 D)(h_2/D)]} \right]$$

$$d_{22} = (\omega \mu D) \left[1 + \frac{(\gamma_3 D)(k_{c2})^2 \tanh[(\gamma_3 D)(h_2/D)]}{(\gamma_2 D)(k_{c3})^2 \tanh(\gamma_2 D)} + \frac{(\alpha_n D)(\beta D)}{(\omega \mu D)(\gamma_2 D)} \right]$$

$$\times \left(\frac{(\alpha_n D)(\beta D)(k_{c2})^2}{(\omega \epsilon_2 D)(\gamma_2 D)(k_{c3})^2} - \frac{(\alpha_n D)(\beta D)}{(\omega \epsilon_2 D)(\gamma_2 D)^2} \right)$$

$$(k_{c_1D})^2 = (2\pi)^2 [\epsilon_{r_1} - (\lambda/\lambda')^2](D/\lambda)^2$$

$$(k_{c_2D})^2 = (2\pi)^2 [\epsilon_{r_2} - (\lambda/\lambda')^2](D/\lambda)^2$$

$$(k_{c_3D})^2 = (2\pi)^2 [\epsilon_{r_3} - (\lambda/\lambda')^2](D/\lambda)^2$$

$$\text{Assume } \mu_1 = \mu_2 = \mu_3 = \mu_0$$

$$\gamma_1^D)^2 = (\alpha_n^D)^2 + (2\pi)^2 [(\lambda/\lambda')^2 - \epsilon_{r_1}](D/\lambda)^2$$

$$(\gamma_2^D)^2 = (\alpha_n^D)^2 + (2\pi)^2 [(\lambda/\lambda')^2 - \epsilon_{r_2}](D/\lambda)^2$$

$$(\gamma_3^D)^2 = (\alpha_n^D)^2 + (2\pi)^2 [(\lambda/\lambda')^2 - \epsilon_{r_3}](D/\lambda)^2$$

$$\beta_D = -\xi_K^D$$

$$\alpha_n^D = 2n\pi(D/b), \text{ see Reference 7}$$

$$\xi_K^D = (2k-1)\pi/(L/D), \text{ see Reference 7}$$

$$\omega_{\mu D} = 240^2 (D/\lambda)$$

$$\omega_{\epsilon_1^D} = r_1 / 60 (D/\lambda)$$

$$\omega_{\epsilon_2^D} = r_2 / 60 (D/\lambda)$$

$$\omega_{\epsilon_3^D} = r_3 / 60 (D/\lambda)$$

$$\left. \begin{array}{l} \text{If } (\gamma_i^D) < 0 \\ \text{then define} \\ (\gamma_1^D)^2 = -(\gamma_1^D)^2 \\ (\gamma_2^D)^2 = -(\gamma_2^D)^2 \\ (\gamma_3^D)^2 = -(\gamma_3^D)^2 \end{array} \right\}$$

APPENDIX B
NUMERICAL RESULTS FOR THE SINGLE RESONANT CAVITY

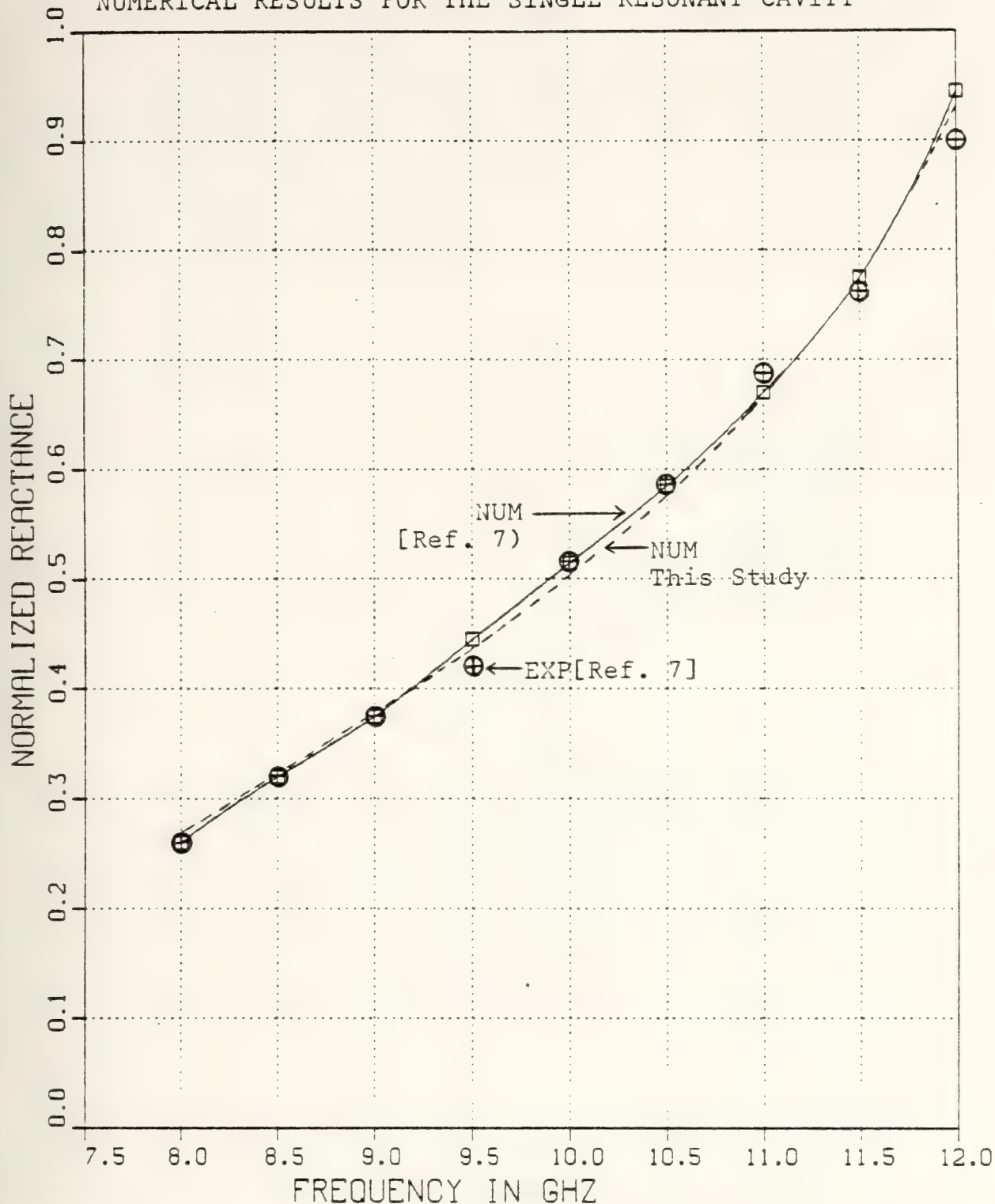


Figure B-1 Normalized Septum Reactance v.s. Frequency for $\epsilon_r = 1.0$, and $w/b = 1.0$ as the Inductive Strip Width $T \rightarrow \infty$

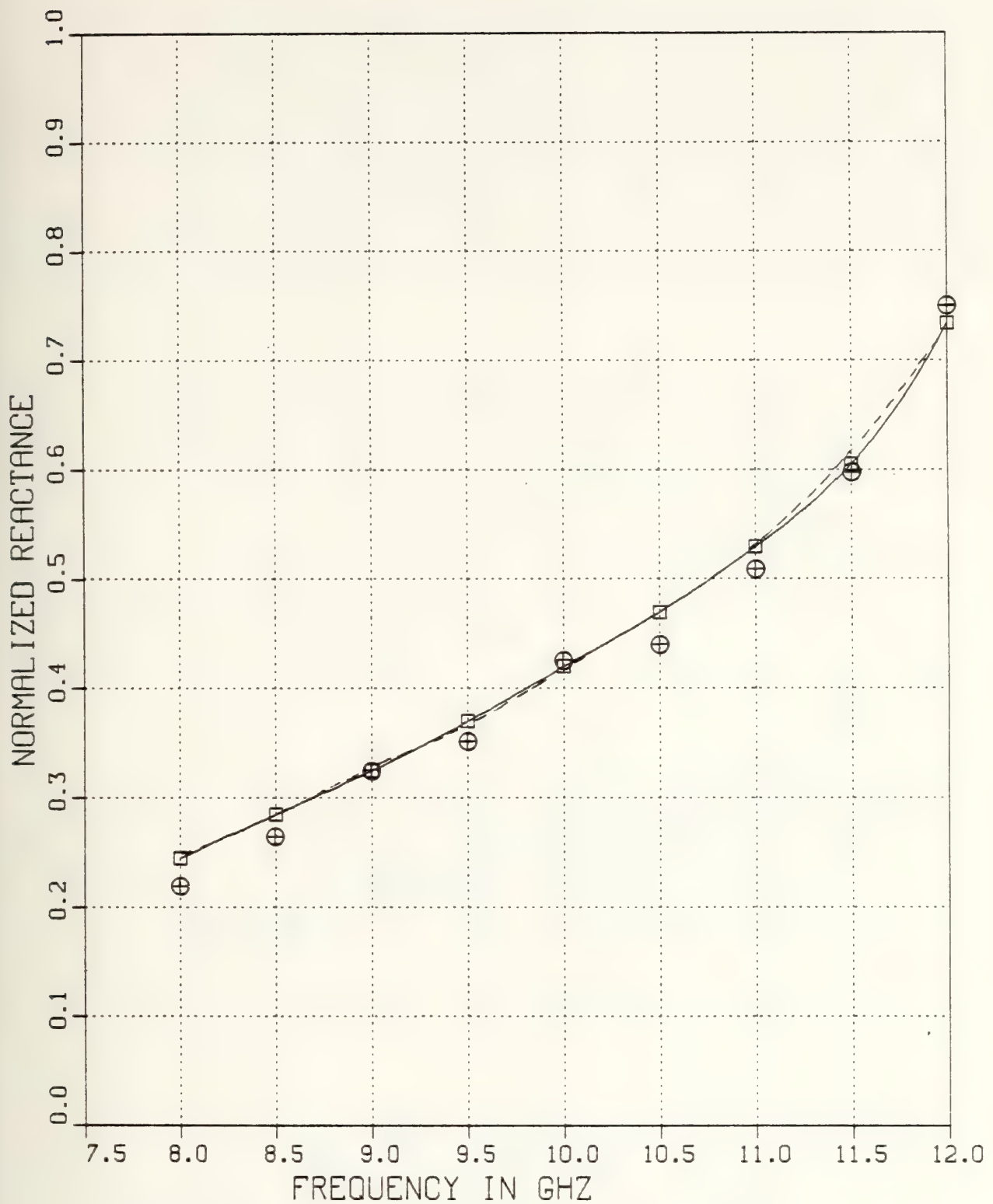


Figure B-2 Normalized Septum Reactance v.s. Frequency for $\epsilon_{r2}=1.0$ and $w/b=0.5$ as the Inductive Strip Width $T \rightarrow \infty$

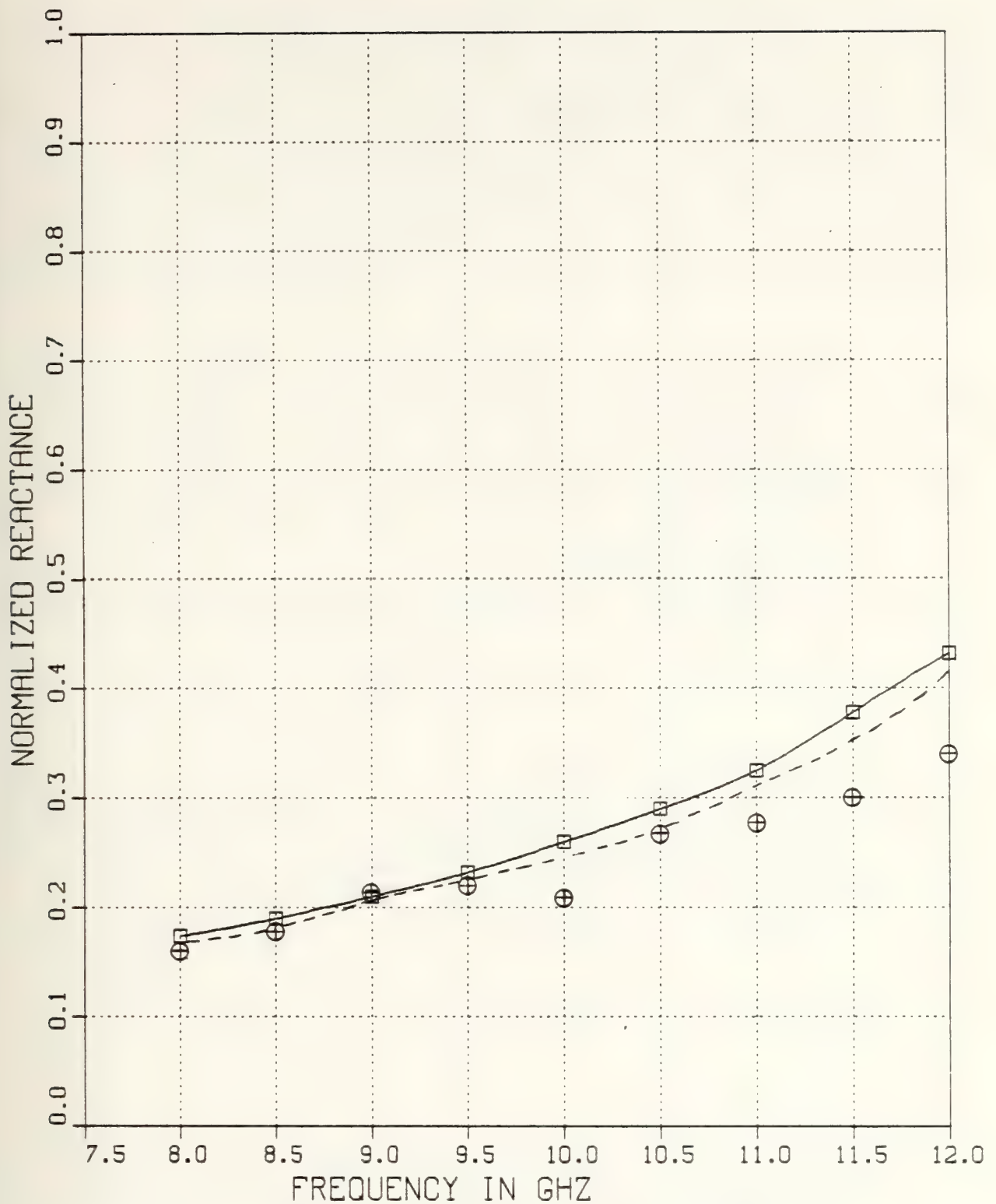


Figure B-3 Normalized Septum Reactance v.s. Frequency for $\epsilon_r = 1.0$ and $w/b = 0.1$ as the Inductive Strip Width $T \rightarrow \infty$

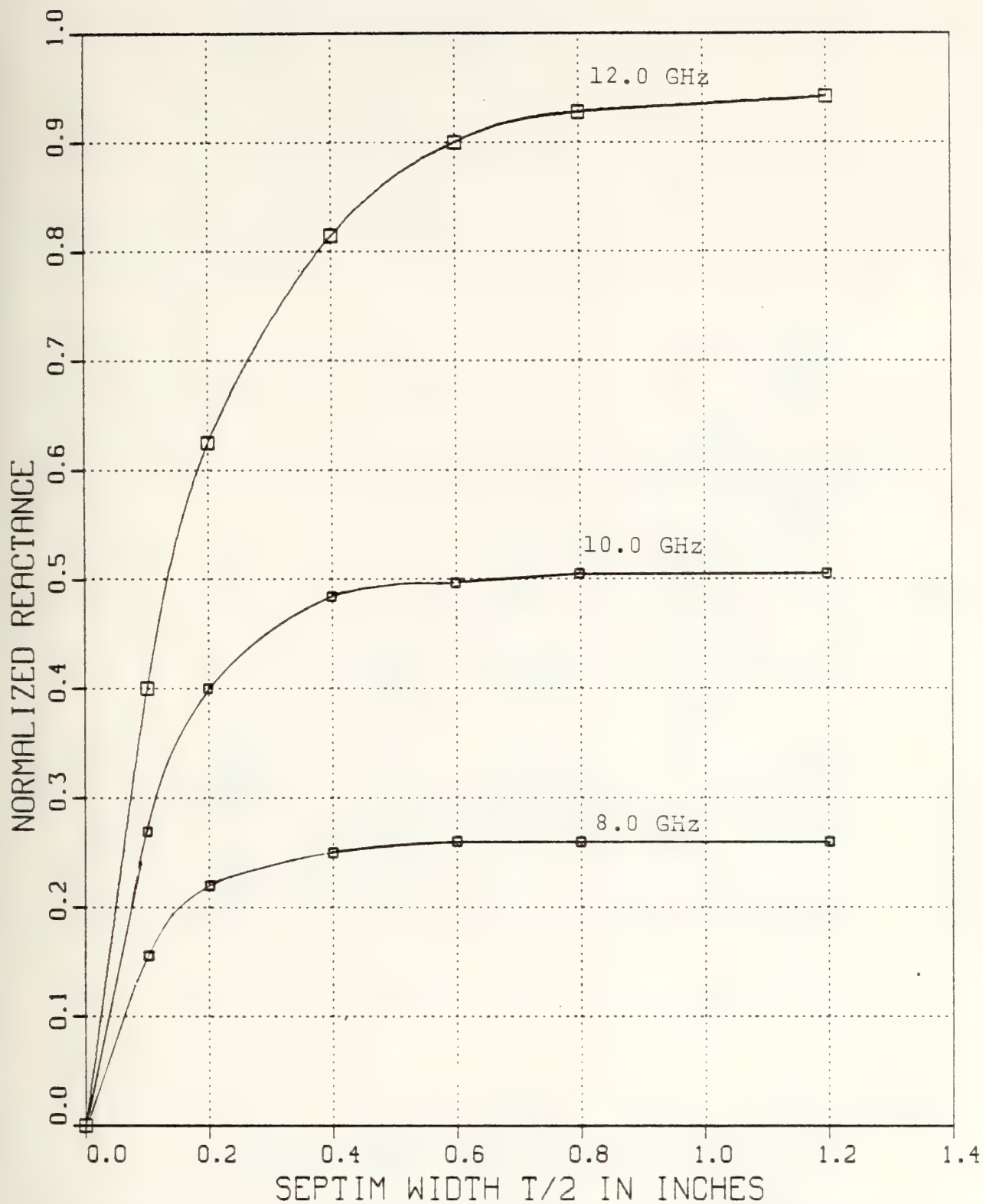


Figure B-4 Normalized Septum Reactance v.s. Septum Length $T/2$ in Inches for $w/b=1.0$ and $\epsilon_{r2}=1.0$ for 8, 10, and 12 GHz

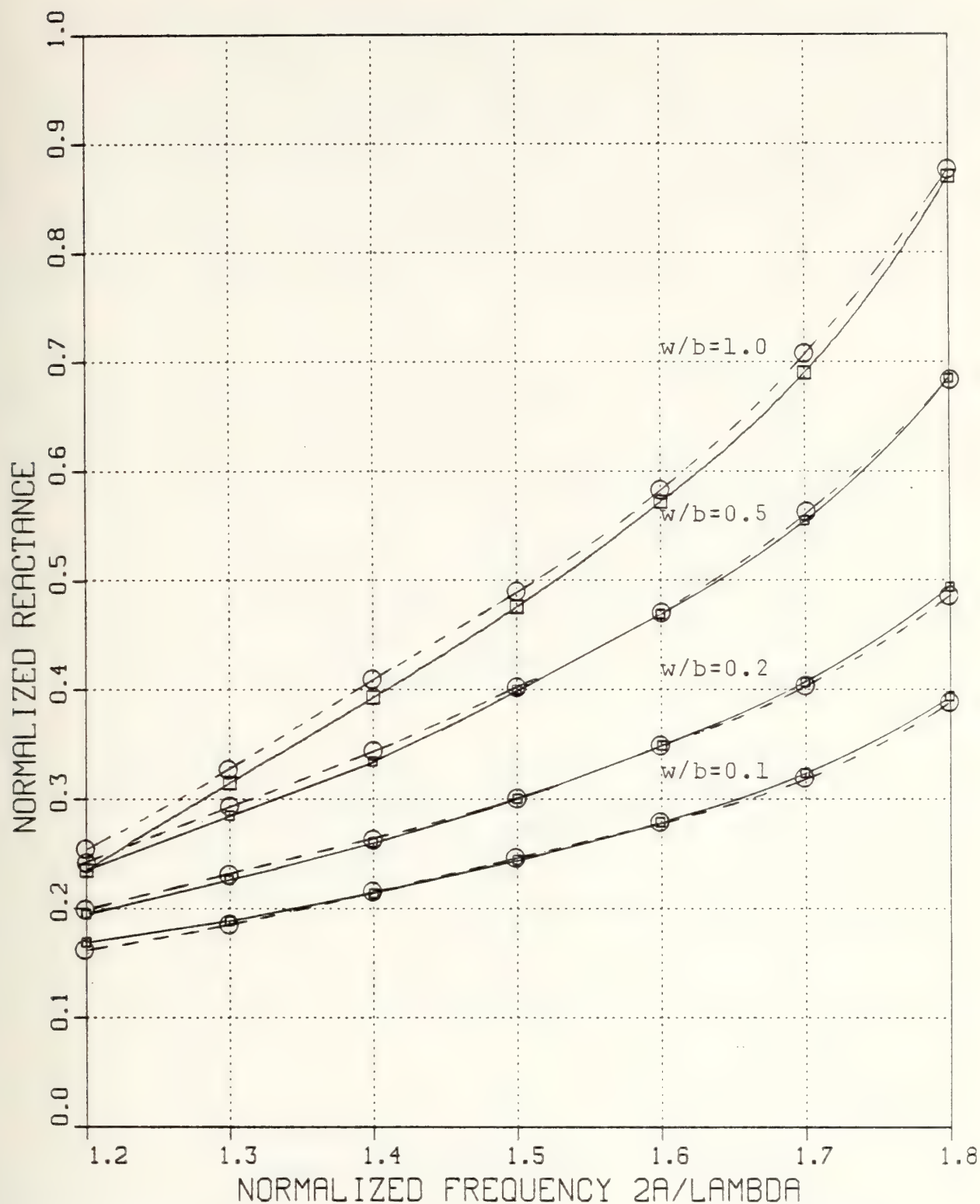


Figure B-5 Normalized Septum Reactance v.s. Normalized Frequency for $\epsilon_r = 2.2$, $b/a = 0.5$, $h_1/a = 0.5$, $D/a = 0$, as $T \rightarrow \infty$ r_2

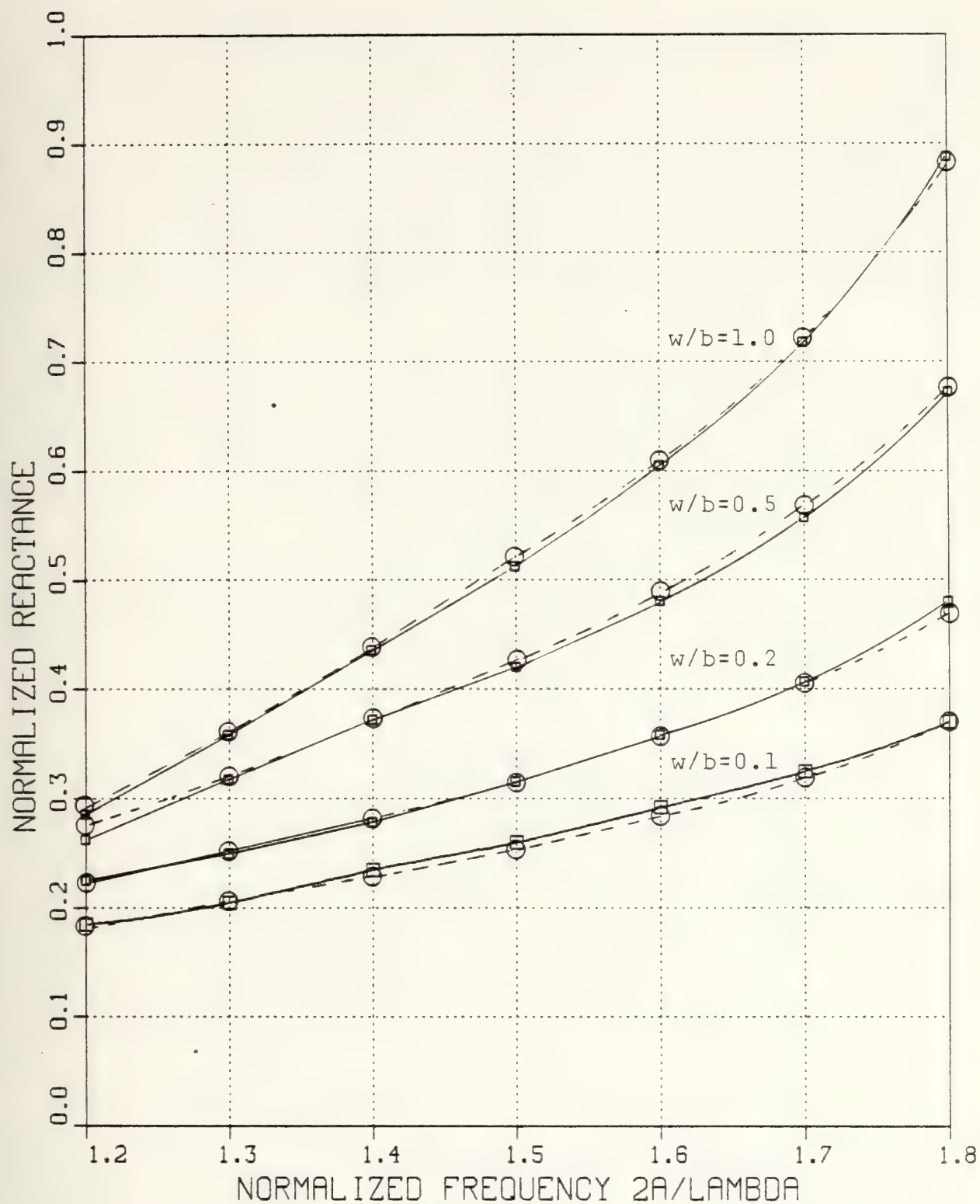


Figure B-6 Normalized Septum Reactance v.s. Normalized Frequency for $\epsilon_r = 2.2$, $b/a = 0.5$, $h_1/a = 0.5$, $D/a = 0.05$, as $T \rightarrow \infty$

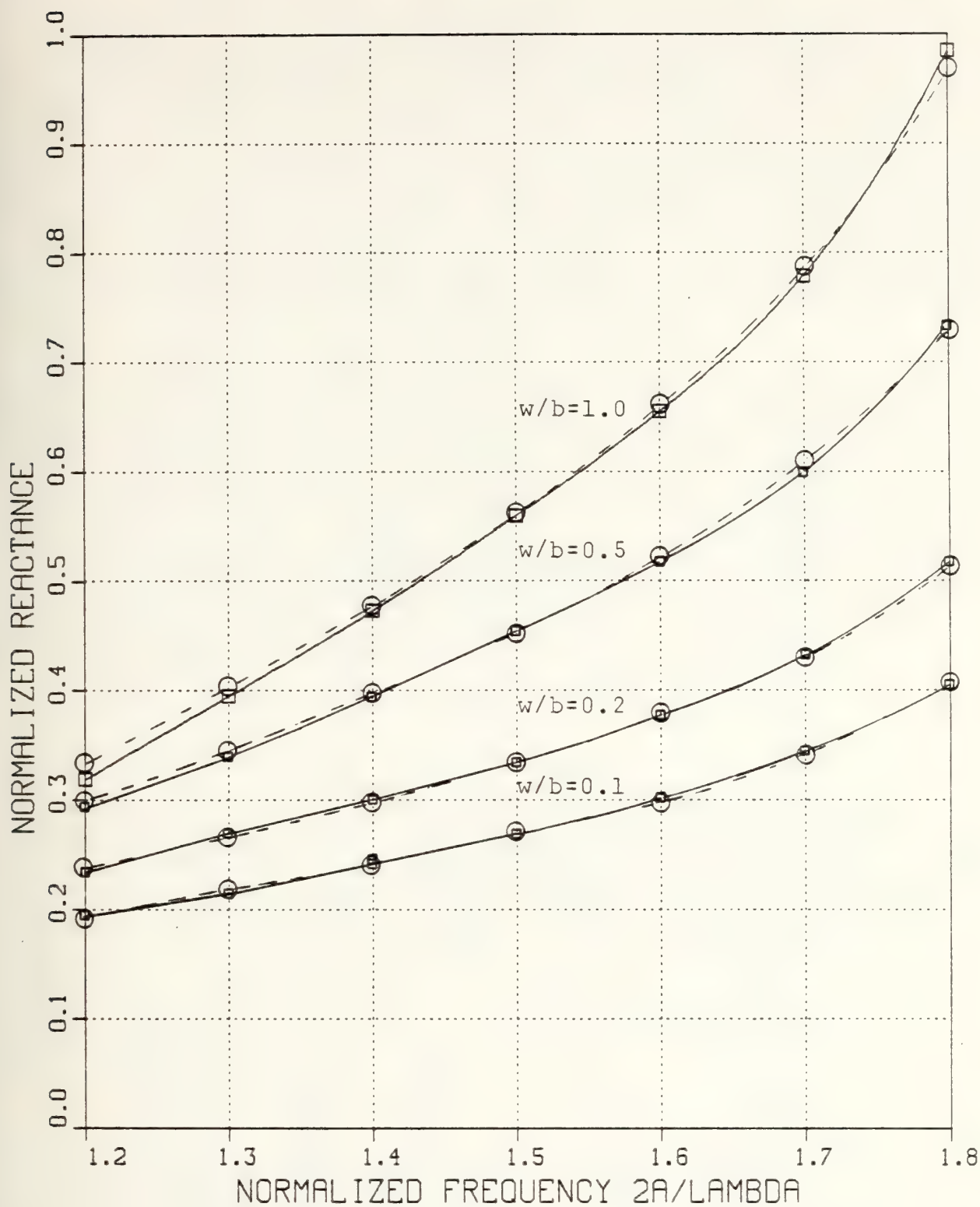


Figure B-7 Normalized Septum Reactance v.s. Normalized Frequency for $\epsilon_r = 2.2$, $b/a = 0.5$, $h_1/a = 0.5$, $D/a = 0.1$, as $T \rightarrow \infty$

THEORETICAL ANALYSIS OF THE COUPLED RESONANT CAVITIES

Derivation of the Coupled Resonant Cavities Problem

For the two coupled cavities, two basis functions are used for the odd and even modes where

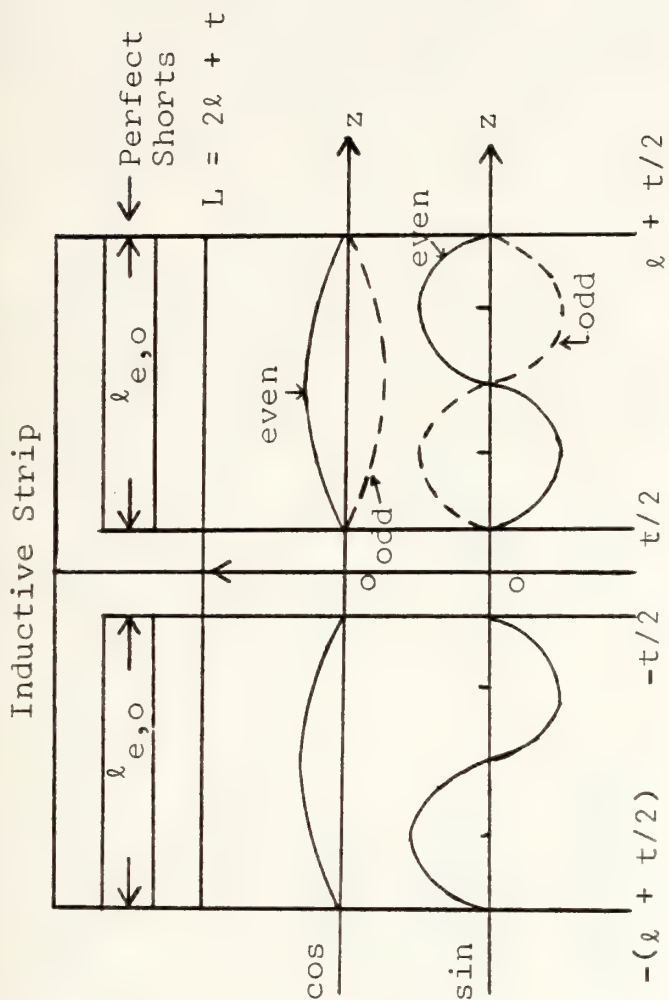
$$\xi_k = (2k-1)\pi/L \quad \text{for even mode}$$

$$\xi_k = k2\pi/L \quad \text{for odd mode}$$

as specified in Reference 7.

Here

$$e(x, z) = A \sum_{q=1}^Q B_q F_q(z), \quad |x| \leq w/x, \quad t/2 \leq |z| \leq \ell + t/2$$



where

$$\begin{aligned}
 F_q(z) = & \left\{ \begin{aligned} & \cos \frac{q\pi}{\ell} \left[z + \left(\frac{\ell + t}{2} \right) \right] , \quad z < 0 \\ & + \cos \frac{q\pi}{\ell} \left[z - \left(\frac{\ell + t}{2} \right) \right] , \quad z > 0 \\ & \text{for } q \text{ odd} \\ & + \text{even mode} \quad - \text{odd mode} \\ & - \sin \frac{q\pi}{\ell} \left[z + \left(\frac{\ell + t}{2} \right) \right] , \quad z < 0 \\ & + \sin \frac{q\pi}{\ell} \left[z - \left(\frac{\ell + t}{2} \right) \right] , \quad z > 0 \\ & \text{for } q \text{ even} \\ & + \text{even mode} \quad - \text{odd mode} \end{aligned} \right.
 \end{aligned}$$

The Fourier transform of $e_x(x)$, (x dependence), gives the same $E_x^x(\alpha_n)$ as in the single cavity case.

Define $E_{x_q}^z(\xi_k)$ as the Fourier Transform of F for the cosine basis function

$E_{x_q}^z(\xi_k)$ as the Fourier Transform of F for the sine basis function

Noting that $f(t+T) \leftrightarrow F(f)e^{j2\pi fT}$

$$f(t-T) \leftrightarrow F(f)e^{-j2\pi fT}$$

and that the Fourier Transform of the z-component is defined the same as in the single cavity base, for the cosine function:

$$E_{x_q}^z(\xi_k) = (-1)^q \frac{1}{2} \frac{\cos(\xi_k \ell/2)}{(\xi_k \ell/2)^2 - (\frac{q\pi}{2})^2} e^{j\xi_k(\frac{\ell+t}{2})}$$

for $z < 0$

$$E_{x_q}^{z_c(\xi_k)} = + \frac{(-1)^q}{2} \frac{\ell \pi}{\cos(\xi_k \ell/2)} \frac{e^{-j\xi_k(\frac{\ell+t}{2})}}{(\xi_k \ell/2)^2 - (\frac{q\pi}{2})^2}$$

for $z > 0$

Therefore, for the even mode:

$$E_{x_q}^{z_c} = \frac{(-1)^q}{2} \frac{\ell \pi}{\cos(\xi_k \ell/2)} \left[e^{j\xi_k(\frac{\ell+t}{2})} - j\xi_k(\frac{\ell+t}{2}) + e^{-j\xi_k(\frac{\ell+t}{2})} \right]$$

$$\text{or } [\quad] (2) \cos \xi_k(\frac{\ell+t}{2})$$

and for the
odd mode

$$E_{x_q}^{z_c} = [\quad] (2j) \sin \xi_k(\frac{\ell+t}{2})$$

obtained by summing the two transforms $E_{x_q}^{z_c}$'s for $z < 0$ and $z > 0$.

and for the sine function:

$$E_{x_q}^z s(\xi_k) = j(-1)^{q+1} \left(\frac{q\pi}{2}\right) \frac{\sin(\xi_k \ell/2)}{(\xi_k \ell/2)^2 - (\frac{q}{2}\pi)^2} e^{j\xi_k \left(\frac{\ell+t}{2}\right)} \quad \text{for } z < 0$$

$$E_{x_q}^z s(\xi_k) = + j(-1)^q \left(\frac{q\pi}{2}\right) \frac{\sin(\xi_k \ell/2)}{(\xi_k \ell/2)^2 - (\frac{q}{2}\pi)^2} e^{-j\xi_k \left(\frac{\ell+t}{2}\right)} \quad \text{for } z > 0$$

66

Therefore, for the even mode:

$$E_{x_q}^z s = (-1)^q \left(\frac{q}{2}\pi\right) \frac{\sin(\xi_k \ell/2)}{(\xi_k \ell/2)^2 - (\frac{q}{2}\pi)^2} \quad (2) \quad \sin \xi_k \left(\frac{\ell+t}{2}\right)$$

and for the odd mode

$$E_{x_q}^z s = [\quad] \quad (-2j) \cos \xi_k \left(\frac{\ell+t}{2}\right)$$

obtained by summing the two transforms $E_{x_q}^z s$, 's for $z < 0$ and $z > 0$.

Define $F[A \sum_{q=1}^Q B_q F_q(z)] = \sum_{q=1}^Q \tilde{B}_q E_q(\alpha_n, \xi_k)$

proceeding as in the single cavity case:

$$\langle E_{x_i}, G_{11} \sum_{j=1}^Q \tilde{B}_j E_{x_j} \rangle = 0, \quad i \text{ and } j = 1 \text{ to } Q$$

where $\tilde{B} = AB$

expanding

$$\begin{aligned} \langle E_{x_1}^x E_{x_1}^x G_{11} E_{x_1}^z, \tilde{B}_1 E_{x_1}^z \rangle + \dots \dots \dots \langle E_{x_1}^x E_{x_1}^x G_{11} E_{x_1}^z, \tilde{B}_Q E_{x_Q}^z \rangle &= 0 \\ \vdots & \\ \langle E_{x_1}^x E_{x_1}^x G_{11} E_{x_Q}^z, \tilde{B}_1 E_{x_1}^z \rangle + \dots \dots \dots \langle E_{x_1}^x E_{x_1}^x G_{11} E_{x_Q}^z, \tilde{B}_Q E_{x_Q}^z \rangle &= 0 \end{aligned}$$

substituting in the sine and cosine functions

$$\begin{aligned} \langle E_{x_1}^x E_{x_1}^x G_{11} E_{x_1}^z, \tilde{B}_1 E_{x_1}^z \rangle + \langle E_{x_1}^x G_{11} E_{x_1}^z \tilde{B}_2 E_{x_2}^z \rangle + \dots \dots \dots \langle E_{x_1}^x G_{11} E_{x_1}^z \tilde{B}_3 E_{x_3}^z \rangle \\ + \langle E_{x_1}^x G_{11} E_{x_1}^z \tilde{B}_4 E_{x_4}^z \rangle + \dots \dots \dots = 0 \end{aligned}$$

$$\begin{aligned} & \vdots \vdots \vdots \\ & \langle E_x^{x^2} G_{11x_Q}^{z_{s,c}} \tilde{B}_1 E_{x_1}^{z_c} \rangle + \dots \dots \dots \langle E_x^{x^2} G_{11x_Q}^{z_{s,c}} \tilde{B}_Q E_{x_Q}^{z_{s,c}} \rangle = 0 \end{aligned}$$

where $E_{x_q}^{z_{s,c}}$ is the transformed sine function if q is even and the transformed cosine function is q is odd

This expansion reduces to:

$$\left[\begin{array}{c} \langle E_x^{x^2} G_{11x_i}^{z_{s,c}} E_{x_j}^{z_{s,c}} \rangle \\ \vdots \\ \langle E_x^{x^2} G_{11x_Q}^{z_{s,c}} E_{x_Q}^{z_{s,c}} \rangle \end{array} \right] \left[\begin{array}{c} \tilde{B}_1 \\ \tilde{B}_2 \\ \vdots \\ \tilde{B}_Q \end{array} \right] = 0$$

where i and j run from 1 to Q.

As in the single cavity case, the problem reduces to

$$\det[\langle \cdot \rangle] = 0$$

Looking at each " ξ_k " inner product term for the even and odd modes, respectively:

For Even Mode:

$$E_{x_i}^{zs} E_{x_j}^{zc} = (\pi \ell)^2 [(-1)^i (i) \frac{\sin \theta}{\theta^2 - (\frac{j}{2}\pi)^2} \sin \phi (-1)^j (j) \frac{\cos \theta}{\theta^2 - (\frac{j}{2}\pi)^2} \cos \phi]$$

$$E_{x_i}^{zs} E_{x_j}^{ss} = (\pi \ell)^2 [(-1)^i (i) \frac{\sin \theta}{\theta^2 - (\frac{j}{2}\pi)^2} \sin \phi (-1)^j (j) \frac{\sin \theta}{\theta^2 - (\frac{j}{2}\pi)^2} \sin \phi]$$

$$E_{x_i}^{zc} E_{x_j}^{cc} = (\pi \ell)^2 [(-1)^i (i) \frac{\cos \theta}{\theta^2 - (\frac{j}{2}\pi)^2} \cos \phi (-1)^j (j) \frac{\cos \theta}{\theta^2 - (\frac{j}{2}\pi)^2} \cos \phi]$$

where $\theta = \xi_k \ell / 2$ and $\phi = \xi_k (\frac{\ell + t}{2})$

and $(\pi \ell)^2$ factors out of each element of the resulting matrix of inner product terms.

For the odd mode

$$E_{x_i x_j}^{z s c} = (\pi \ell)^2 [(-1)^i (i) \frac{\sin \theta}{\theta^2 - (\frac{i\pi}{2})^2} \cos \phi (-1)^j j \frac{\cos \theta}{\theta^2 - (\frac{j\pi}{2})^2} \sin \phi] \overbrace{(-j)(-j)}^{+j}$$

$$E_{x_i x_j}^{z s s} = (\pi \ell)^2 [(-1)^i (i) \frac{\sin \theta}{\theta^2 - (\frac{i\pi}{2})^2} \cos \phi (-1)^j j \frac{\sin \theta}{\theta^2 - (\frac{j\pi}{2})^2} \cos \phi] \overbrace{(-j)(-j)}^{-1}$$

$$E_{x_i x_j}^{z c c} = (\pi \ell)^2 [(-1)^i i \frac{\cos \theta}{\theta^2 - (\frac{i\pi}{2})^2} \cos \phi (-1)^j j \frac{\cos \theta}{\theta^2 - (\frac{j\pi}{2})^2} \cos \phi] \overbrace{(j)(j)}^{-1}$$

where $\theta = \xi_k \ell / 2$ and $\phi = \xi_k (\frac{\ell+t}{2})$

and $(\pi \ell)^2$ factors out of each element of the resulting matrix of the inner product terms. Note, each element of the matrix will be multiplied by $(-1)^{i+j+1}$ for the odd mode.

The singularities for the $E_x^x(\alpha_n)$ and $E_x^c(\xi_k)$ are the same as in the single cavity case. The singularity for $E_x^s(\xi_k)$ is found by

$$\lim_{\theta \rightarrow \frac{q\pi}{2}} \frac{\sin \theta}{\theta^2 - (\frac{q\pi}{2})^2} = \frac{(-1)^q}{q\pi}, \text{ for } q \text{ even.}$$

The inner product is defined the same as the single cavity case.

N_{\max} and K_{\max} are found in the same manner as in the single cavity case. N_{\max} remains unchanged. K_{\max} becomes

$$K_{\max} = \frac{1}{2} + (2 + t/\ell_e)[z\text{const} + (\frac{q}{2})^2]^{1/2}, \text{ even mode}$$

$$K_{\max} = (2 + t/\ell_o)[z\text{const} + (\frac{q}{2})^2]^{1/2}, \text{ odd mode}$$

APPENDIX D

NUMERICAL RESULTS FOR THE SINGLE AND COUPLED RESONANT CAVITIES

THIS IS THE FINSTRP PROGRAM TO DETERMINE THE ODD AND EVEN MODE RESONANT LENGTHS OF TWO UNILATERALLY COUPLED FIN-LINE RESONANT CAVITIES, THE CORRESPONDING EQUIVALENT CIRCUIT REACTANCES, AND THE SCATTERING PARAMETERS OF THE INDUCTIVE STRIP USING A BASIS SET OF SIN AND COS FUNCTIONS. THE DIMENSION OF THE MATRIX IS = 12
RESIDUE (ACCURACY) = 0.0001

FINLINE PARAMETERS FOR THE X-BAND WAVEGUIDE (8.0 TO 12.0 GHz)
ARE:

EPSR1 = 1.0 EPSR2 = 1.0 EPSR3 = 1.0
H1/D = 4.5 H2/D = 3.5 B/D = 4.0

W/B	W/C	D/L	LPR/L		
1.000	4.000	0.0677	1.747		
	TOVD	TOVW	LE/LPR	LO/LPR	XS
	0.050	0.012	0.373	0.500	0.511
	0.100	0.025	0.380	0.500	0.472
	0.200	0.050	0.389	0.500	0.419
	0.500	0.125	0.409	0.500	0.321
	1.000	0.250	0.425	0.487	0.295
	2.000	0.500	0.444	0.500	0.185
	5.000	1.250	0.458	0.464	0.251
	10.000	2.500	0.460	0.460	0.255
	16.000	4.000	0.460	0.460	0.256
1.000	4.000	0.0720	1.574		
	TOVD	TOVW	LE/LPR	LO/LPR	XS
	0.050	0.012	0.355	0.500	0.645
	0.100	0.025	0.361	0.500	0.595
	0.200	0.050	0.371	0.500	0.529
	0.500	0.125	0.390	0.491	0.443
	1.000	0.250	0.409	0.487	0.360
	2.000	0.500	0.430	0.470	0.332
	5.000	1.250	0.447	0.455	0.318
	10.000	2.500	0.451	0.451	0.318
	16.000	4.000	0.451	0.451	0.317
1.000	4.000	0.0762	1.461		
	TOVD	TOVW	LE/LPR	LO/LPR	XS
	0.050	0.012	0.342	0.500	0.706
	0.100	0.025	0.348	0.498	0.709
	0.200	0.050	0.358	0.497	0.634
	0.500	0.125	0.377	0.489	0.523
	1.000	0.250	0.396	0.480	0.446
	2.000	0.500	0.417	0.466	0.396
	5.000	1.250	0.438	0.448	0.375
	10.000	2.500	0.443	0.443	0.374
	16.000	4.000	0.443	0.443	0.374
1.000	4.000	0.0804	1.382		
	TOVD	TOVW	LE/LPR	LC/LPR	XS
	0.050	0.012	0.332	0.499	0.882
	0.100	0.025	0.338	0.498	0.816
	0.200	0.050	0.347	0.495	0.731
	0.500	0.125	0.365	0.487	0.604
	1.000	0.250	0.384	0.477	0.517
	2.000	0.500	0.406	0.462	0.459
	5.000	1.250	0.429	0.442	0.433
	10.000	2.500	0.435	0.436	0.432
	16.000	4.000	0.435	0.435	0.432
1.000	4.000	0.0847			

	TOVD	TOVW	1.325 LE/LPR	LC/LPR	XS
	0.050	0.012	0.324	0.499	1.004
	0.100	0.025	0.329	0.497	0.929
	0.200	0.050	0.338	0.494	0.834
	0.500	0.125	0.355	0.486	0.691
	1.000	0.250	0.372	0.474	0.599
	2.000	0.500	0.394	0.457	0.533
	5.000	1.250	0.418	0.434	0.502
	10.000	2.500	0.425	0.427	0.499
	16.000	4.000	0.426	0.426	0.500
1.000	4.000	0.0889			
	TCVD	TOVW	1.280 LE/LPR	LC/LPR	XS
	0.050	0.012	0.317	0.499	1.115
	0.100	0.025	0.322	0.497	1.032
	0.200	0.050	0.330	0.494	0.926
	0.500	0.125	0.346	0.485	0.777
	1.000	0.250	0.362	0.473	0.676
	2.000	0.500	0.382	0.454	0.608
	5.000	1.250	0.408	0.428	0.572
	10.000	2.500	0.417	0.419	0.569
	16.000	4.000	0.418	0.418	0.568
1.000	4.000	0.0931			
	TOVD	TOVW	1.246 LE/LPR	LC/LPR	XS
	0.050	0.012	0.311	0.498	1.236
	0.100	0.025	0.316	0.496	1.145
	0.200	0.050	0.323	0.493	1.032
	0.500	0.125	0.337	0.483	0.874
	1.000	0.250	0.351	0.470	0.773
	2.000	0.500	0.369	0.449	0.701
	5.000	1.250	0.395	0.421	0.659
	10.000	2.500	0.406	0.409	0.656
	16.000	4.000	0.408	0.408	0.655
1.000	4.000	0.0974			
	TOVD	TOVW	1.217 LE/LPR	LC/LPR	XS
	0.050	0.012	0.307	0.498	1.353
	0.100	0.025	0.311	0.496	1.258
	0.200	0.050	0.317	0.492	1.135
	0.500	0.125	0.329	0.482	0.977
	1.000	0.250	0.342	0.467	0.875
	2.000	0.500	0.357	0.445	0.806
	5.000	1.250	0.381	0.413	0.764
	10.000	2.500	0.394	0.400	0.758
	16.000	4.000	0.396	0.397	0.758
1.000	4.000	0.1016			
	TOVD	TOVW	1.195 LE/LPR	LC/LPR	XS
	0.050	0.012	0.302	0.498	1.475
	0.100	0.025	0.306	0.496	1.371
	0.200	0.050	0.312	0.492	1.248
	0.500	0.125	0.322	0.481	1.090
	1.000	0.250	0.332	0.465	0.998
	2.000	0.500	0.344	0.442	0.938
	5.000	1.250	0.365	0.406	0.902
	10.000	2.500	0.379	0.389	0.896
	16.000	4.000	0.383	0.385	0.895

Figure D-1 Odd and Even Mode Resonant Lengths for the Coupled Fin-Line Resonant Cavities for $w/b=1.0$, $t/D=0.05$, 0.1 , 0.2 , 0.5 , 1.0 , 2.0 , 5.0 , 10.0 , and 16.0 , $D=0.1$ inch, $\epsilon_{r2}=1.0$, and for 8 through 12 GHz

THIS IS THE FINCAV PROGRAM TO DETERMINE THE RESONANT
 LENGTH OF A SINGLE FIN-LINE RESONANT CAVITY, THE GUIDE
 WAVELENGTH, AND THE EQUIVALENT REACTANCE OF THE SHORTING
 SEPTUM (INDUCTIVE DISCONTINUITY)
 THE DIMENSION OF THE MATRIX IS = 12
 RESIDUE (ACCURACY) = 0.0001

FINLINE PARAMETERS FOR THE X-BAND WAVEGUIDE (8.0 TO 12.0 GHz)
 ARE:

EPSR1 = 1.0 EPSR2 = 1.0 EPSR3 = 1.0
 H1/D = 4.5 H2/D = 3.5 B/D = 4.0

W/B	W/D	D/L	LPR/L	TOVD	LRES/LPR
1.000	4.000	0.0577	1.747	0.200	0.493
				0.500	0.483
				1.000	0.469
				2.000	0.449
				5.000	0.424
				10.000	0.418
				16.000	0.417
1.000	4.000	0.0720	1.574	0.200	0.491
				0.500	0.479
				1.000	0.462
				2.000	0.438
				5.000	0.408
				10.000	0.400
				16.000	0.400
1.000	4.000	0.0762	1.461	0.200	0.490
				0.500	0.477
				1.000	0.457
				2.000	0.429
				5.000	0.394
				10.000	0.384
				16.000	0.383
1.000	4.000	0.0804	1.382	0.200	0.489
				0.500	0.474
				1.000	0.453
				2.000	0.421
				5.000	0.380
				10.000	0.368
				16.000	0.367
1.000	4.000	0.0847	1.325	0.200	0.488
				0.500	0.471
				1.000	0.448
				2.000	0.413
				5.000	0.366
				10.000	0.351
				16.000	0.350
1.000	4.000	0.0889	1.280	0.200	0.487
				0.500	0.469
				1.000	0.443
				2.000	0.405
				5.000	0.353
				10.000	0.334
				16.000	0.332

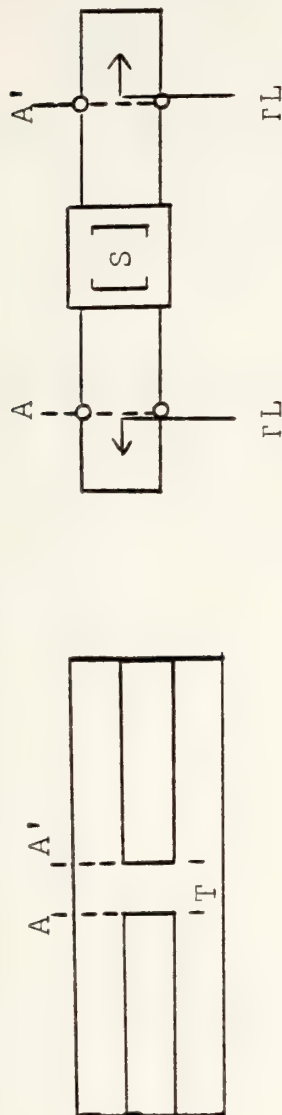
1.000	4.000	0.0931	1.246	0.200	0.486
				0.500	0.466
				1.000	0.438
				2.000	0.397
				5.000	0.338
				10.000	0.315
				16.000	0.312
1.000	4.000	0.0974	1.217	0.200	0.485
				0.500	0.464
				1.000	0.434
				2.000	0.389
				5.000	0.324
				10.000	0.295
				16.000	0.289
1.000	4.000	0.1016	1.195	0.200	0.483
				0.500	0.461
				1.000	0.430
				2.000	0.382
				5.000	0.308
				10.000	0.272
				16.000	0.262

Figure D-2 Resonant Lengths for the Single Fin-Line Resonant Cavity for $w/b=1.0$, $t/D=0.2, 0.5, 1.0, 2.0, 5.0, 10.0$, and 16.0 , $D=0.1$ inch, $\epsilon_{r2}=1.0$, and for 8 through 12 GHz

APPENDIX E THEORETICAL ANALYSIS OF THE SCATTERING PARAMETERS OF THE FIN-LINE INDUCTIVE STRIP

Solution of Inductive Discontinuity

Using S Parameters



This network is

- a) lossless
- b) symmetric with respect to reference planes A and A'
- c) reciprocal

As a result the scattering matrix of the network is

- a) unitary

$$b) S_{11} = S_{22}$$

$$c) \text{ symmetric } (S_{21} = S_{12})$$

Therefore

$$[S] = \begin{bmatrix} \overline{S_{11}} & \overline{S_{12}} \\ S_{12} & S_{11} \end{bmatrix}$$

$$S_{11}S_{11}^* + S_{12}S_{12}^* = 1$$

$$S_{11}S_{12}^* + S_{12}S_{11}^* = 0$$

Hence $|S_{12}| = \sqrt{1 - |S_{11}|^2}$

$$\theta_{12} = \theta_{11} - \pi/2, \text{ since the strip is inductive}$$

Γ_L is the reflection coefficient looking into the shorted fin-line at A or A'

$$\Gamma_L = -1 e^{-j2\beta\ell}$$

$$b_1 = S_{11}a_1 + S_{12}a_2$$

$$\text{and } a_1 = \Gamma_L b_1, a_2 = \Gamma_L b_2$$

$$b_2 = S_{12}a_1 + S_{11}a_2$$

Substituting: $b_1 = S_{11}r_L b_1 + S_{12}r_L b_2$

$$b_2 = S_{12}r_L b_1 + S_{11}r_L b_2$$

$$(1-S_{11}r_L)b_1 - (S_{12}r_L)b_2 = 0$$

$$-(S_{12}r_L)b_1 + (1-S_{11}r_L)b_2 = 0$$

eliminating the b's:

$$(1-S_{11}r_L)^2 + (S_{12}r_L)^2 = 0$$

$$(S_{11}^2 - S_{12}^2)r_L^2 - 2S_{11}r_L + 1 = 0$$

Solving for r_L with the quadratic formula

$$r_L = \frac{2S_{11} \pm \sqrt{(2S_{11})^2 - 4(S_{11}^2 - S_{12}^2)}}{2(S_{11} + S_{12})(S_{11} - S_{12})}$$

giving $r_L = \frac{S_{11} + S_{12}}{(S_{11} + S_{12})(S_{11} - S_{12})}$

$$\left. \begin{aligned} \text{and } \Gamma_{Le} &= \frac{1}{S_{11} - S_{12}} \\ \Gamma_{Lo} &= \frac{1}{S_{11} + S_{12}} \end{aligned} \right\}$$

$$S_{11} = \frac{1}{2} \left(\frac{\Gamma_e + \Gamma_o}{\Gamma_e \Gamma_o} \right)$$

$$S_{12} = \frac{1}{2} \left(\frac{\Gamma_e - \Gamma_o}{\Gamma_e \Gamma_o} \right)$$

$$\Gamma_{Le} = -e^{-j4\pi\ell e/\lambda'} \quad \text{and} \quad \Gamma_{Lo} = -e^{-j4\pi\ell o/\lambda'}$$

Substituting,

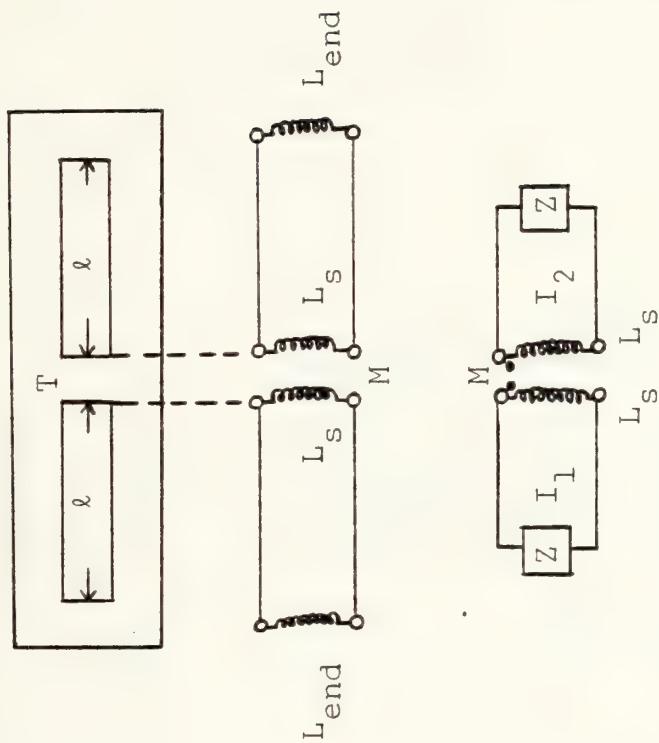
$$S_{11} = \frac{1}{2} \left[\frac{-e^{-j2\beta\ell e} - e^{-j2\beta\ell o}}{e^{-j2\beta(\ell e + \ell o)}} \right]$$

$$= -e^{j2\pi(\ell e/\lambda' + \ell o/\lambda')} \cos 2\pi(\ell e/\lambda' - \ell o/\lambda')$$

$$S_{12} = \frac{1}{2} \left[\frac{-e^{-j2\beta\ell e} + e^{-j2\beta\ell o}}{e^{-j2\beta(\ell e + \ell o)}} \right]$$

$$= j e^{j2\pi(\ell e/\lambda' + \ell o/\lambda')} \sin 2\pi(\ell e/\lambda' - \ell o/\lambda').$$

From Knorr, notes for reference 7, the equivalent circuit reactances are determined as follows:



$$\begin{aligned} x_{\text{end}} &= \omega L_{\text{end}} \\ Z_L &= j\omega L_s \\ Z_M &= j\omega M \end{aligned}$$

$$Z = Z_o \frac{Z_R + j Z_o \tan \beta \ell}{Z_o + j Z_R \tan \beta \ell} \quad x_{\text{end}} = \tan(\tan^{-1} x_{\text{end}})$$

$$z = \frac{j x_{\text{end}} + j \tan \beta \ell}{1 - x_{\text{end}} \tan \beta \ell} \quad \frac{Z_L}{Z_o} = j X_s = j \omega \frac{L_s}{Z_o}$$

$$z = j \frac{\tan(\tan^{-1}x_{\text{end}}) + \tan\beta\ell}{1 - \tan(\tan^{-1}x_{\text{end}})\tan\beta\ell}$$

$$\text{Noting } \tan(\alpha+\beta) = \frac{\tan\alpha + \tan\beta}{1 - \tan\alpha\tan\beta}$$

$$z = j \tan(\beta\ell + \tan^{-1}x_{\text{end}}) = jx$$

$$\text{At resonance: } zI_1 + j\omega L_s I_1 + j\omega m I_2 = 0$$

$$zI_2 + j\omega L_s I_2 + j\omega m I_1 = 0$$

$$\text{Normalizing } jx_s I_1 + jm I_2 = jx I_1$$

$$jm I_1 + jx_s I_2 = jx I_2$$

$$(x_s + m)(I_1 + I_2) = x(I_1 + I_2)$$

$$\text{Hence } x = x_s + m \quad \text{yielding } \quad \begin{cases} x_{\text{even}} = x_s + m \\ x_{\text{odd}} = x_s - m \end{cases}$$

Solving for x_s and m ;

$$x_s = \frac{1}{2}(x_{\text{even}} + x_{\text{odd}})$$

$$m = \frac{1}{2}(x_{\text{even}} - x_{\text{odd}})$$

and

$$x_s = \frac{1}{2}[\tan(2\pi \ell e/\lambda') + \tan^{-1}x_{\text{end}}) + \tan(2\pi \ell o/\lambda' + \tan^{-1}x_{\text{end}})]$$

$$= \frac{1}{2}[\tan(\pi - 2\pi \ell e/\lambda') + \tan(\pi - 2\pi \ell o/\lambda')]$$

$$m = \frac{1}{2}[\tan(\pi - 2\pi \ell e/\lambda') - \tan(\pi - 2\pi \ell o/\lambda')]$$

APPENDIX F
 NUMERICAL RESULTS FOR THE SCATTERING PARAMETERS
 OF THE FIN-LINE INDUCTIVE STRIP

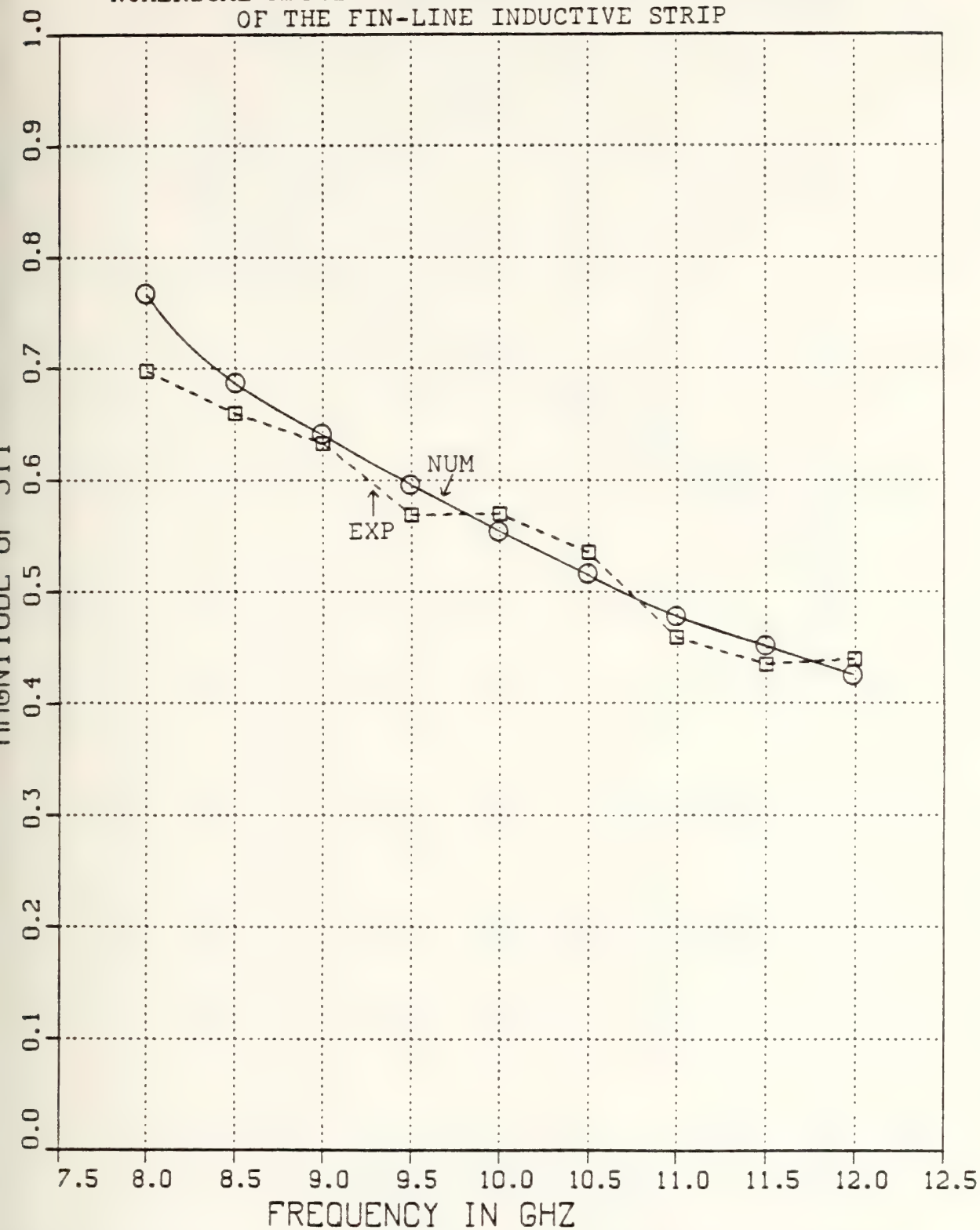


Figure F-1 $|S_{11}|$ v.s. Frequency for $T=.02$ inch Inductive Strip, $w/b=1.0$, and $\epsilon_{r2}=1.0$

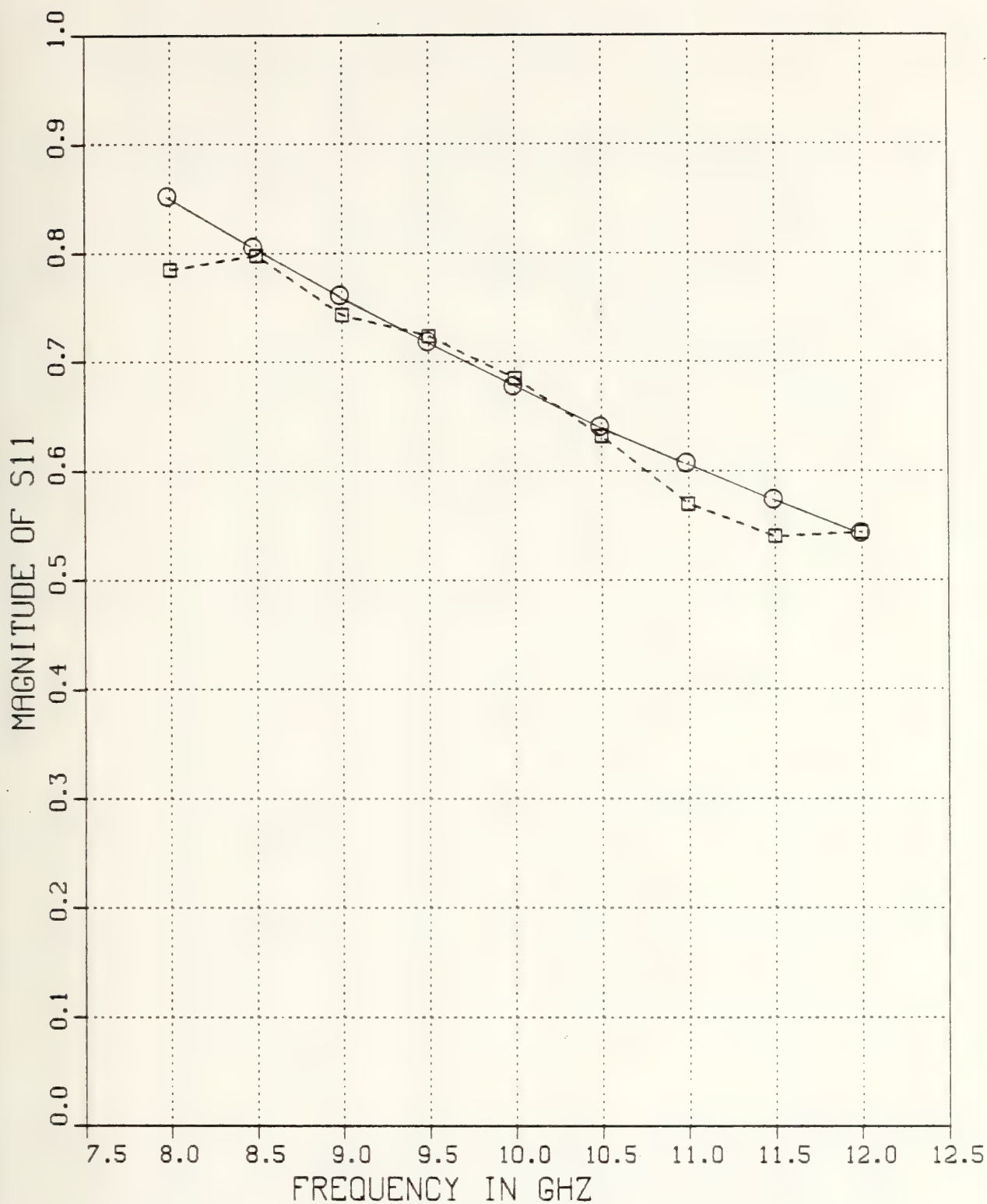


Figure F-2 $|S_{11}|$ v.s. Frequency for $T=.05$ inch Inductive Strip, $w/b=1.0$, and $\epsilon_{r_2}=1.0$

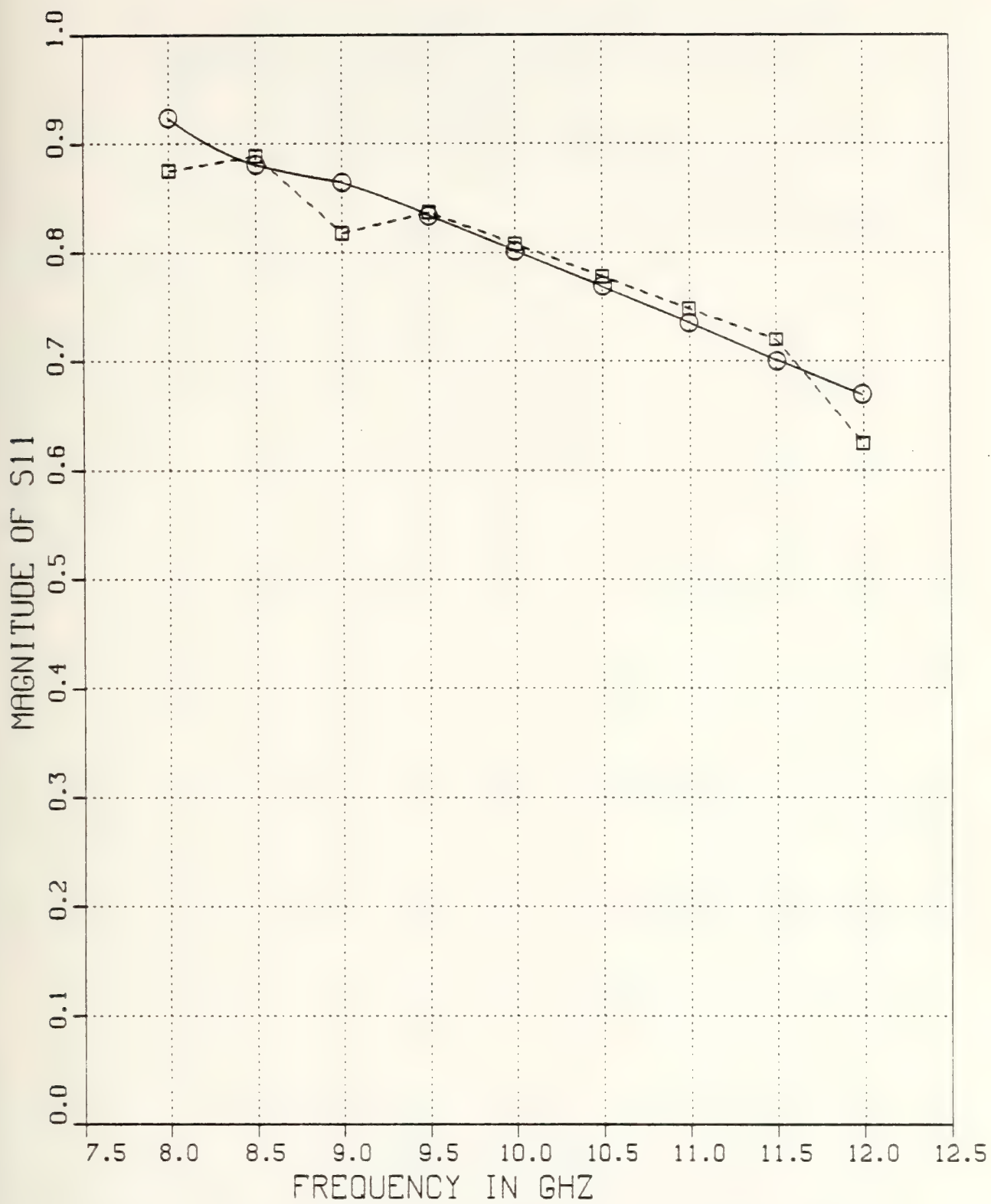


Figure F-3 $|S_{11}|$ v.s. Frequency for $T=0.1$ inch Inductive Strip, $w/b=1.0$, and $\epsilon_{r_2}=1.0$

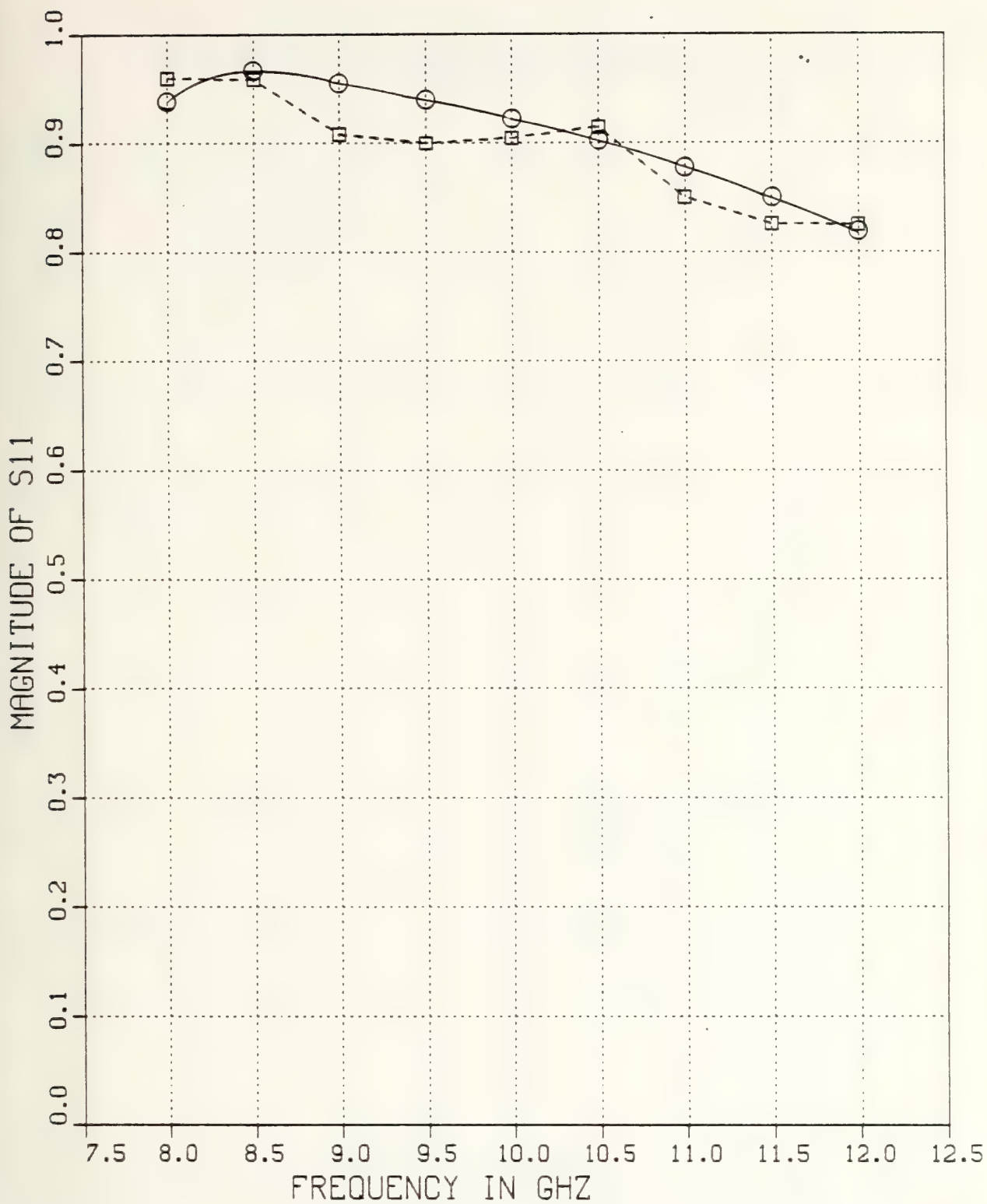


Figure F-4 $|S_{11}|$ v.s. Frequency for $T=0.2$ inch Inductive Strip, $w/b=1.0$, and $\epsilon_{r2}=1.0$

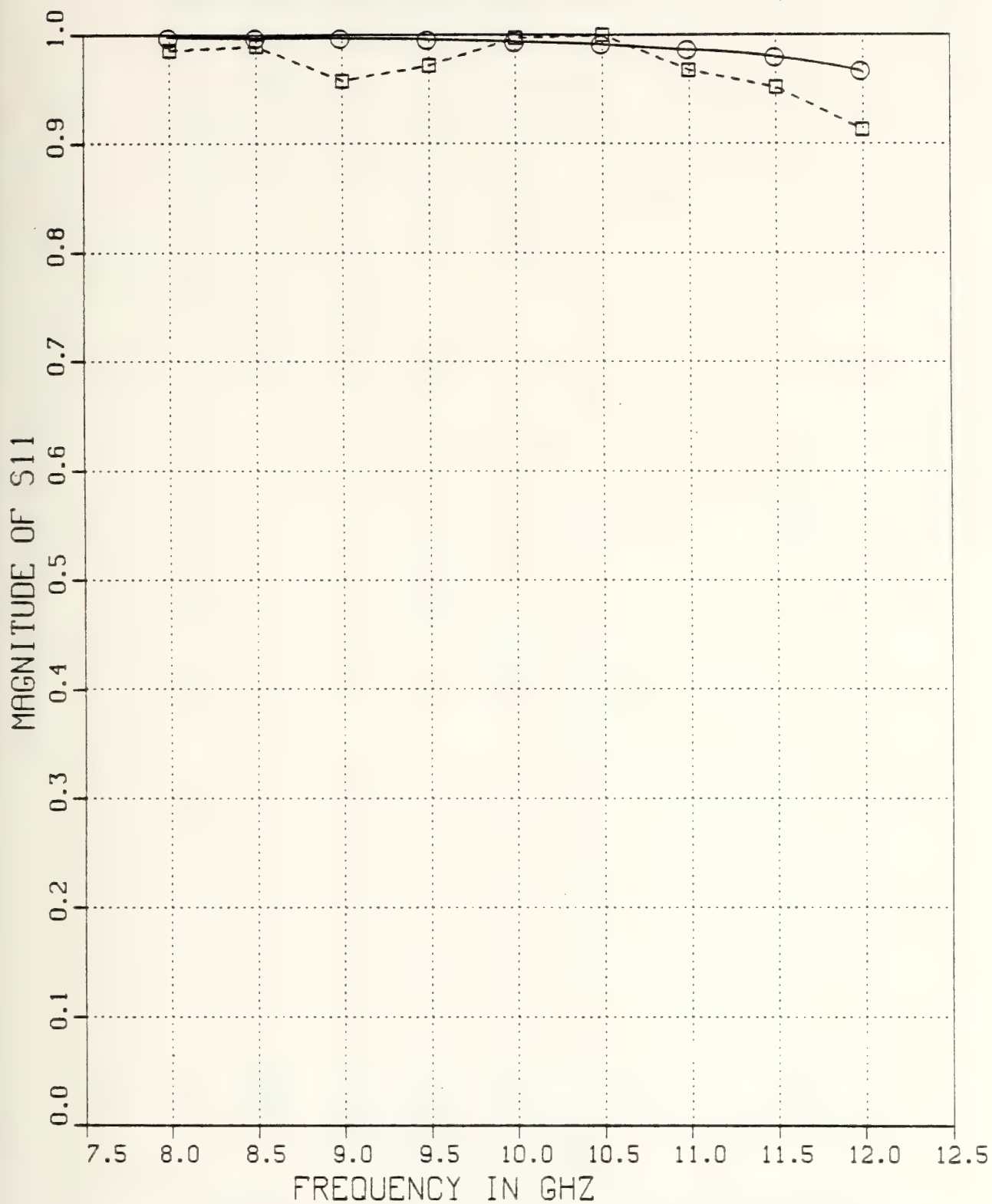


Figure F-5 $|S_{11}|$ v.s. Frequency for $T=0.5$ inch Inductive Strip, $w/b=1.0$, and $\epsilon_{r_2}=1.0$

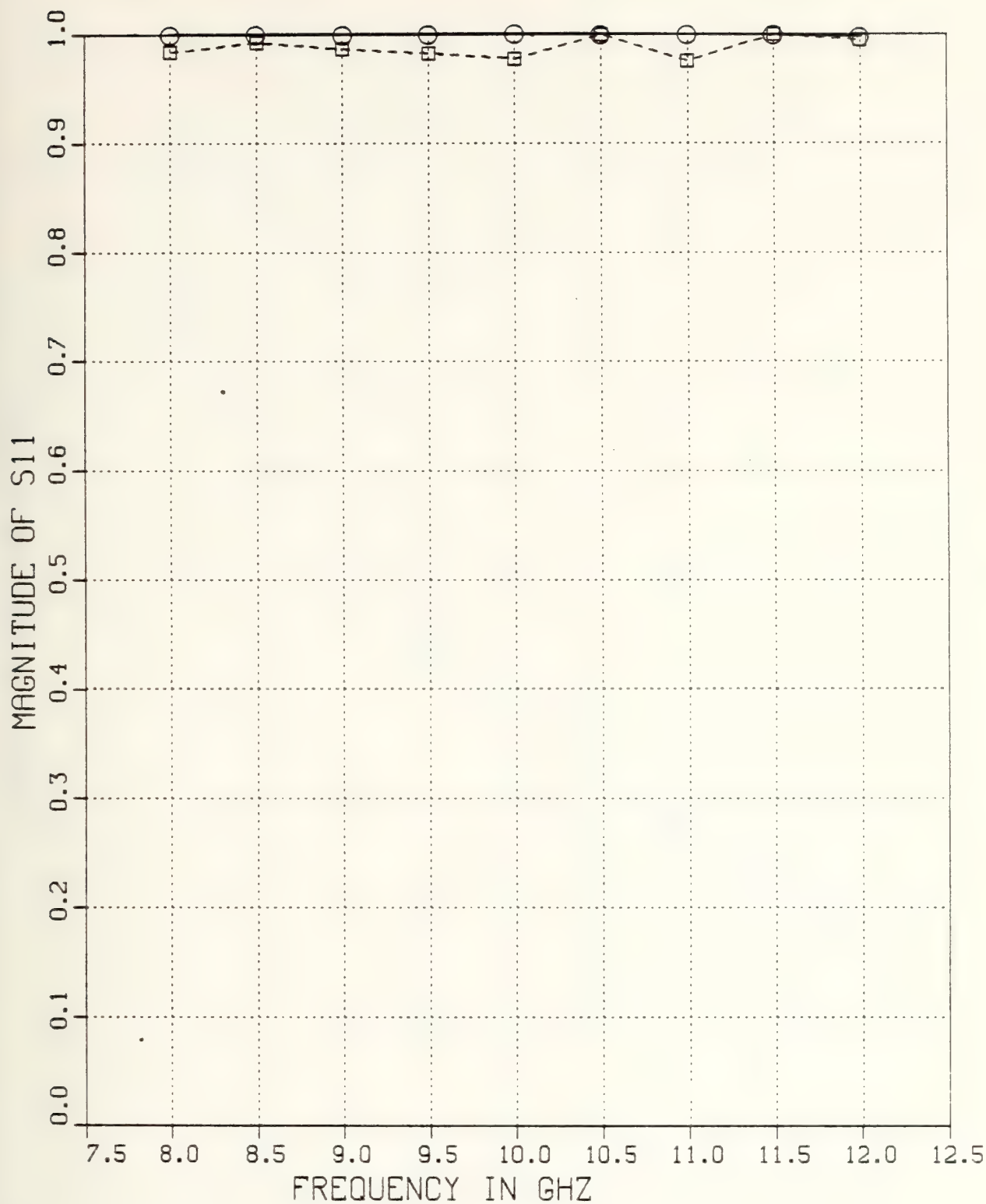


Figure F-6 $|S_{11}|$ v.s. Frequency for $T=1.0$ inch Inductive Strip, $w/b=1.0$, and $\epsilon_{r2}=1.0$

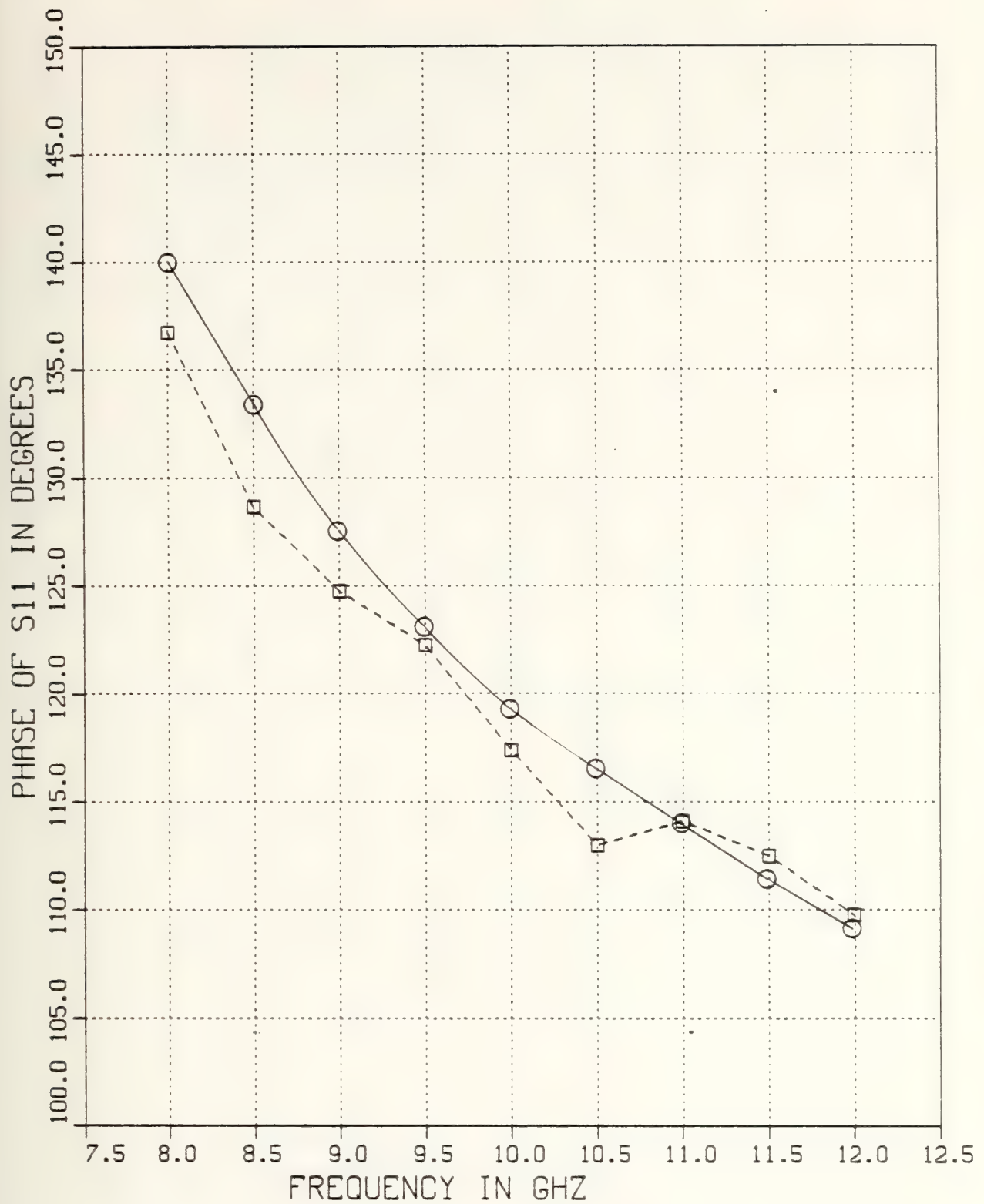


Figure F-7 θ_{11} v.s. Frequency for $T=.02$ inch Inductive Strip,
 $w/b=1.0$, and $\epsilon_{r_2}=1.0$

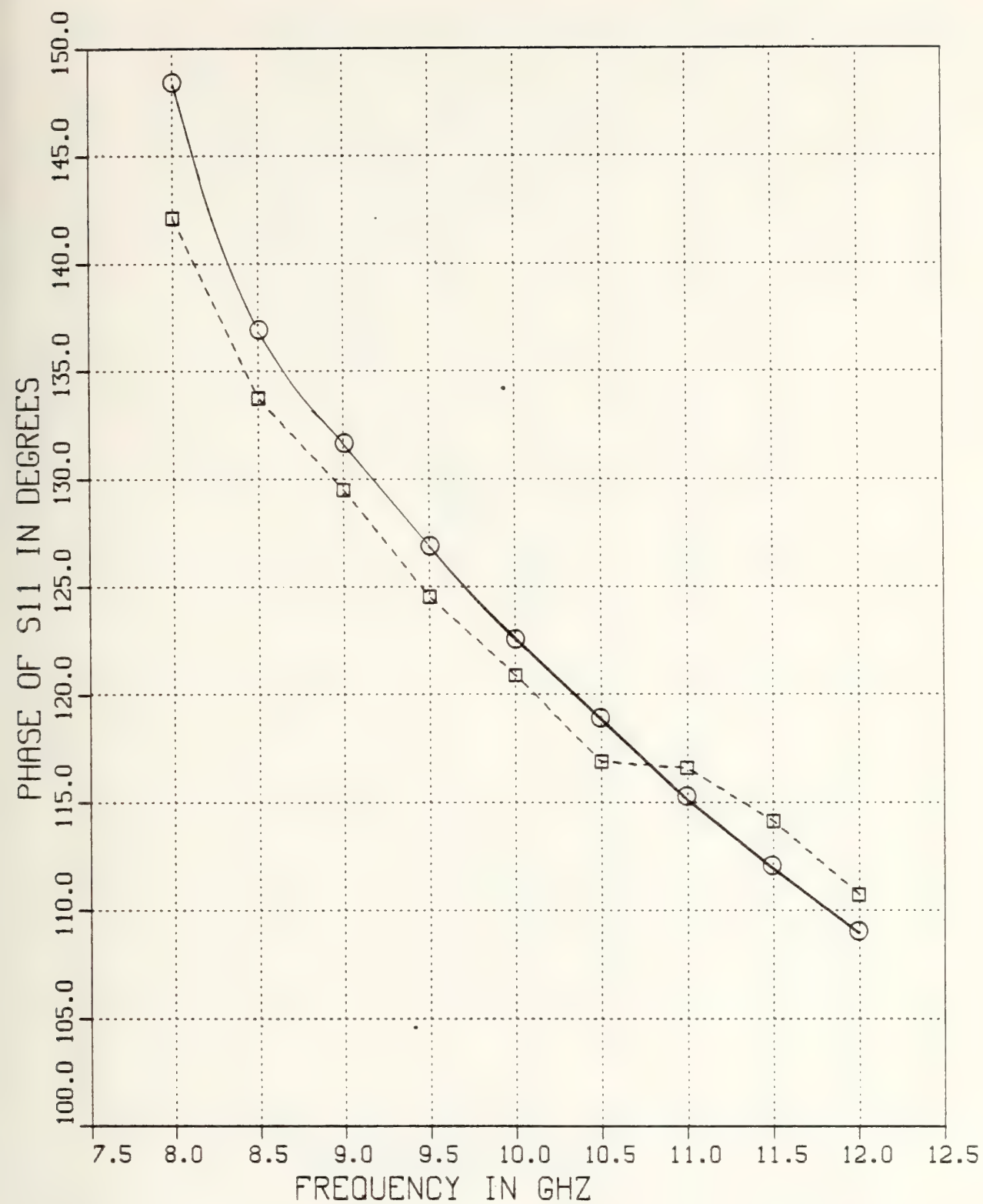


Figure F-8 θ_{11} v.s. Frequency for $T=.05$ inch Inductive Strip, $w/b=1.0$, and $\epsilon_{r2}=1.0$

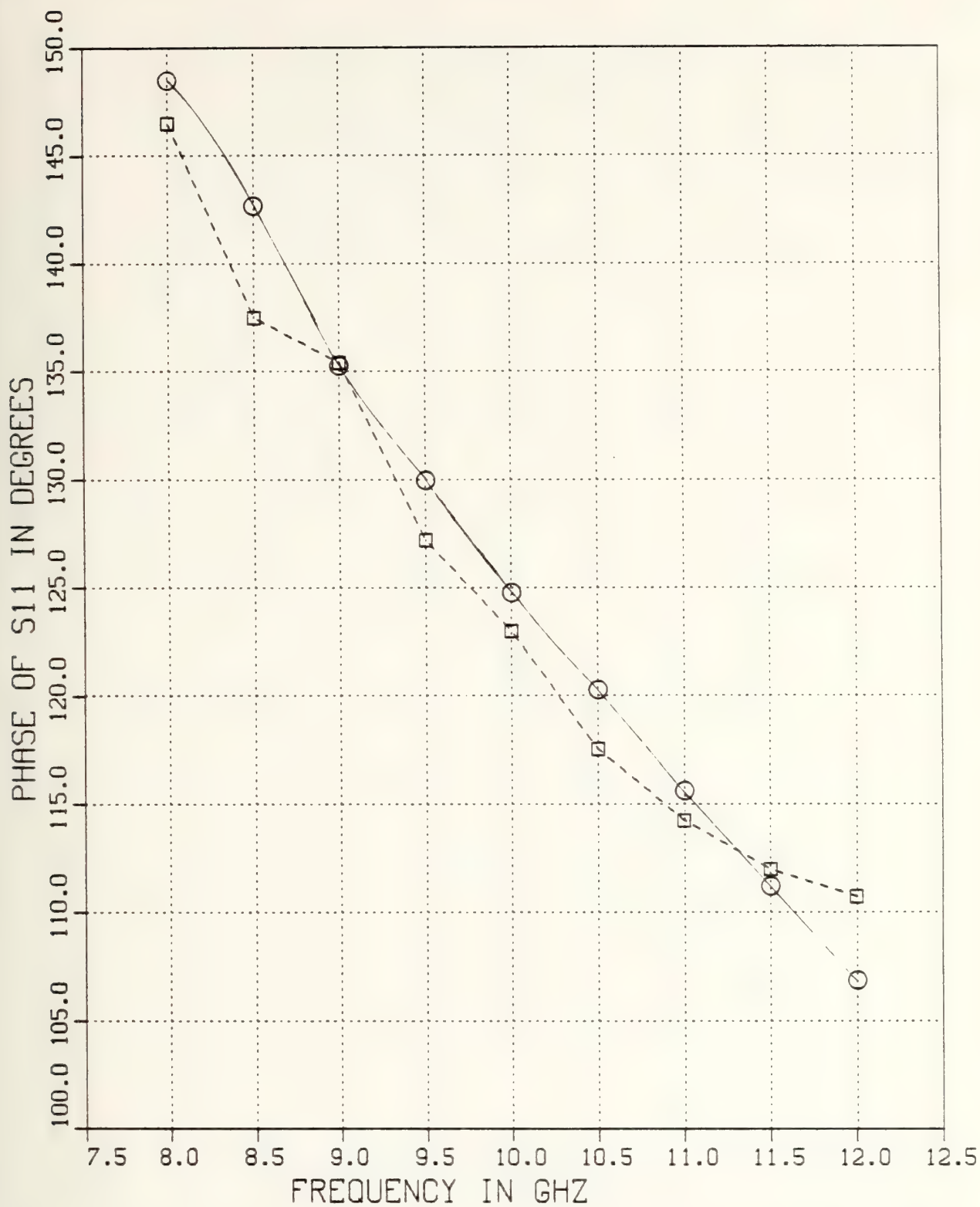


Figure F-9 θ_{11} v.s. Frequency for $T=0.1$ inch Inductive Strip,
 $w/b=1.0$, and $\epsilon_{r2}=1.0$

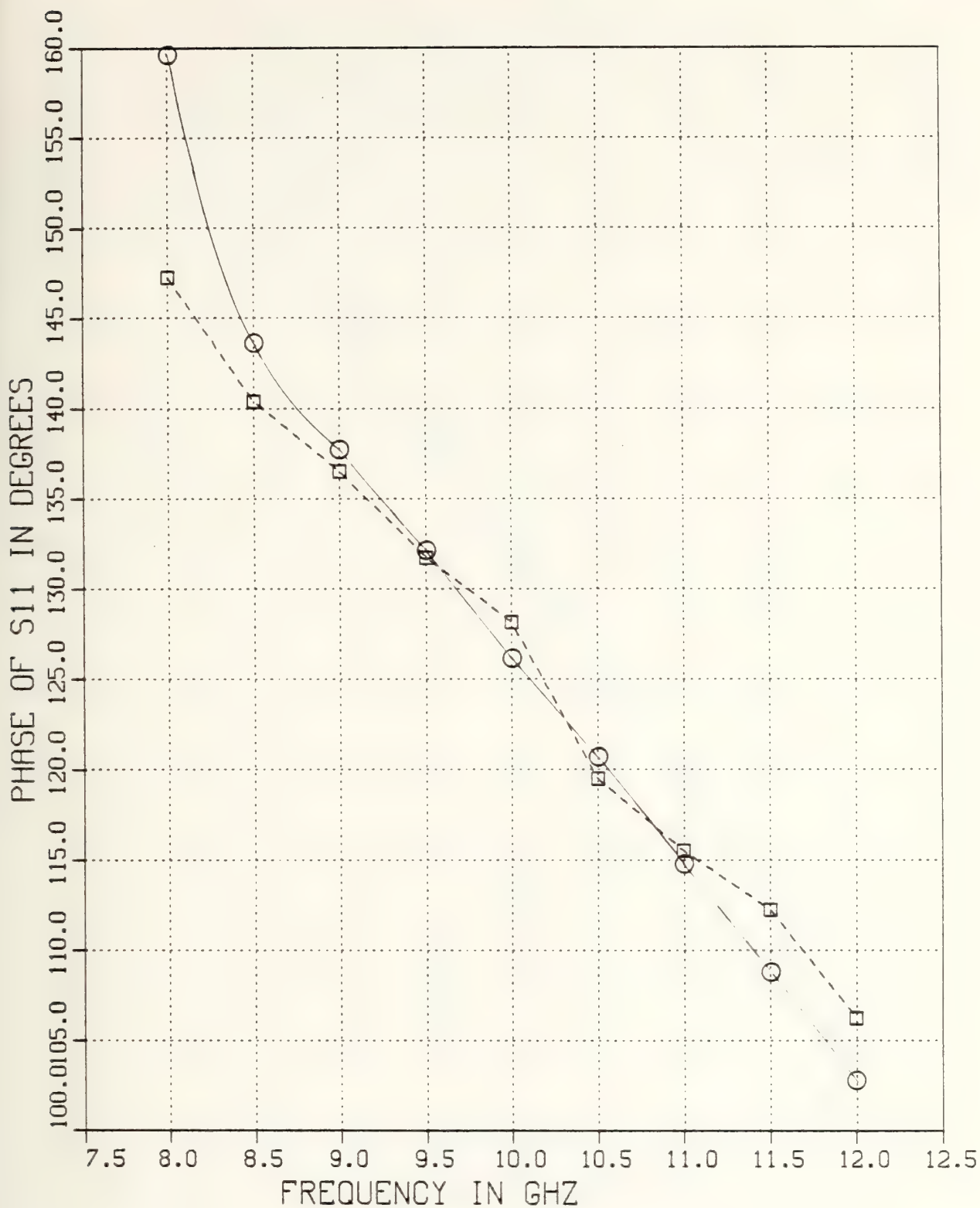


Figure F-10 θ_{11} v.s. Frequency for $T=0.2$ inch Inductive Strip, $w/b=1.0$, and $\epsilon_{r_2}=1.0$

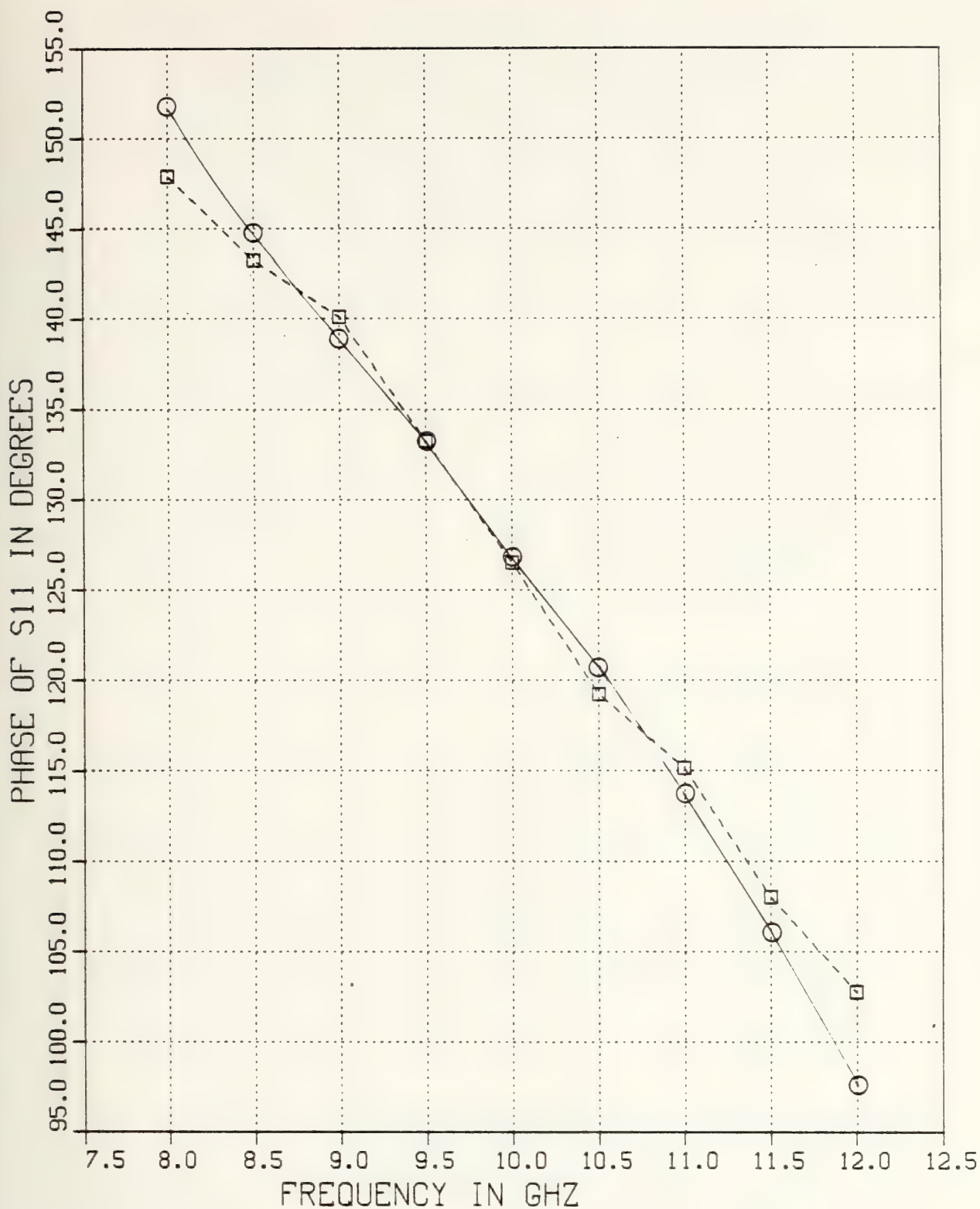


Figure F-11 θ_{11} v.s. Frequency for $T=0.5$ inch Inductive Strip, $w/b=1.0$, and $\epsilon_{r_2}=1.0$

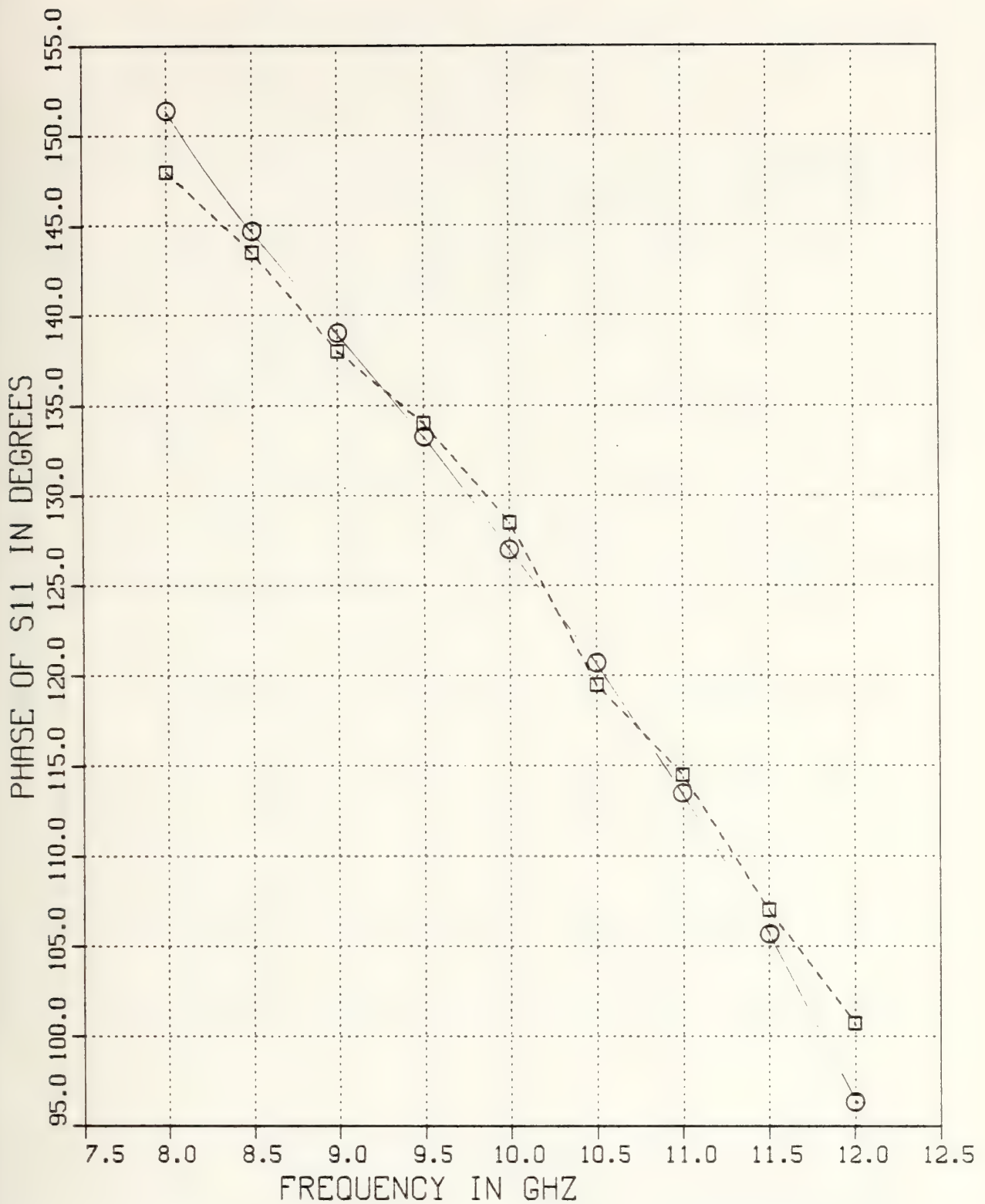


Figure F-12 θ_{11} v.s. Frequency for $T=1.0$ inch Inductive Strip, $w/b=1.0$, and $\epsilon_{r_2}=1.0$

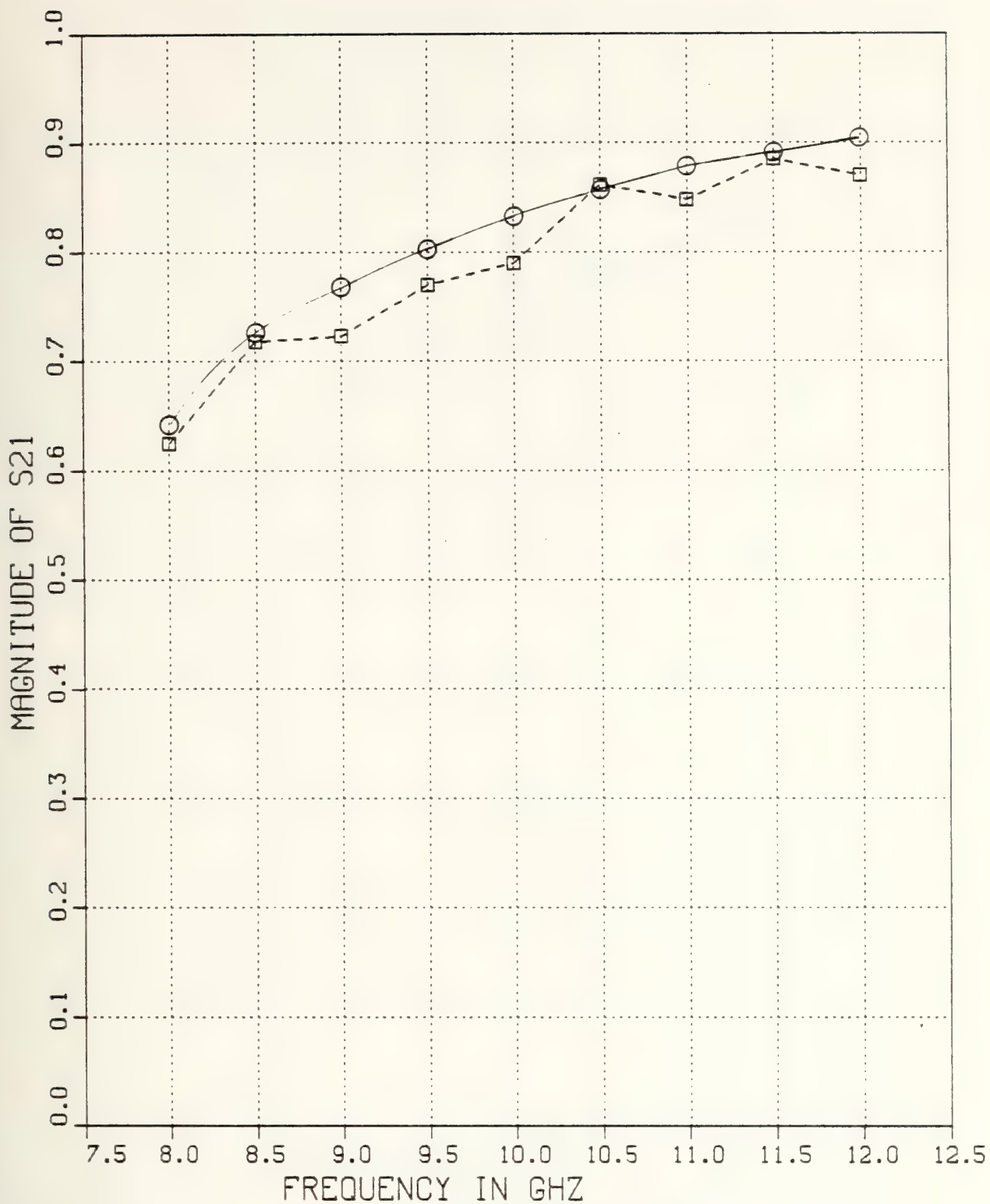


Figure F-13 $|S_{21}|$ v.s. Frequency for $T=.02$ inch Inductive Strip, $w/b=1.0$, and $\epsilon_{r_2}=1.0$

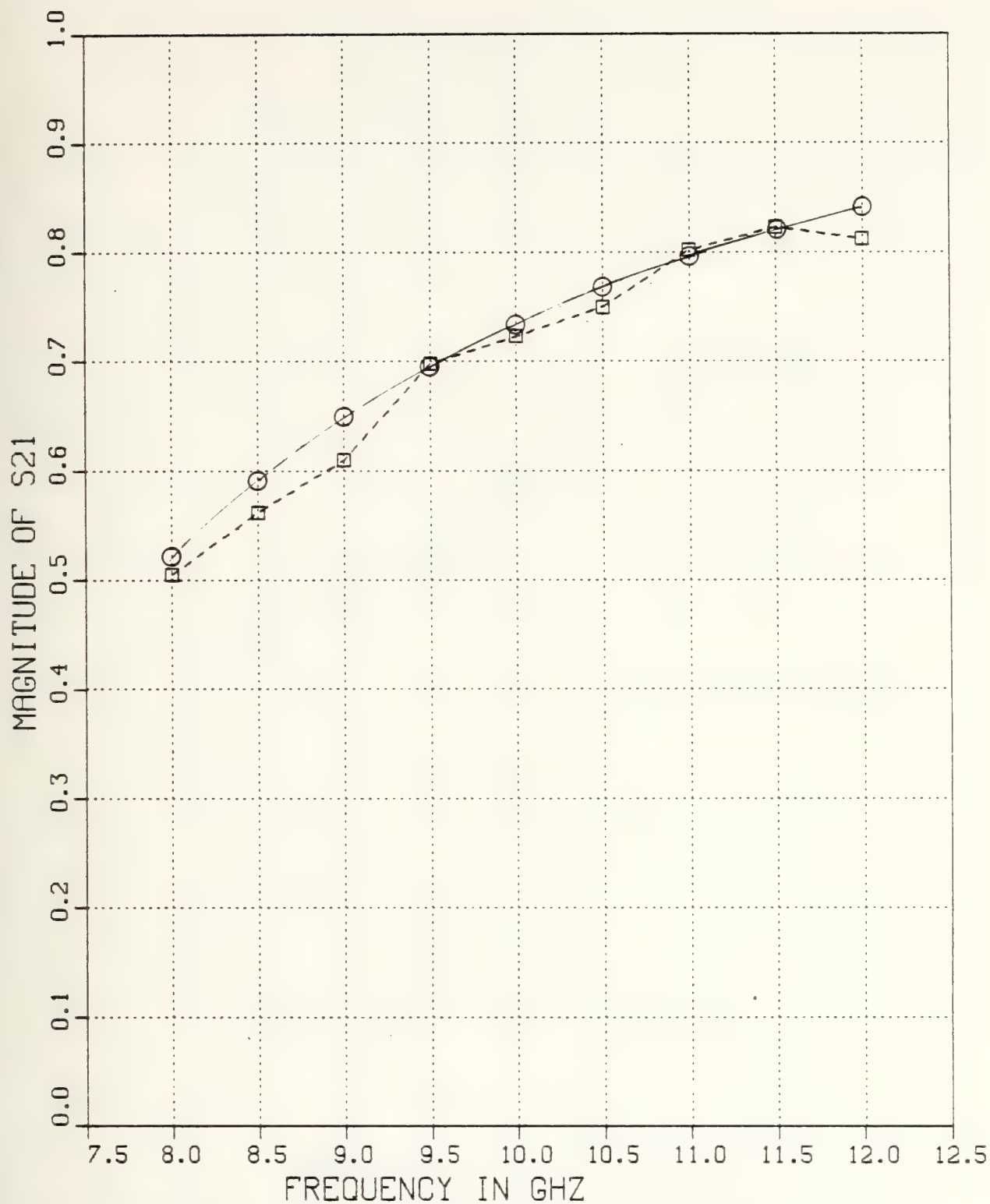


Figure F-14 $|S_{21}|$ v.s. Frequency for $T=.05$ inch Inductive Strip, $w/b=1.0$, and $\epsilon_{r_2}=1.0$

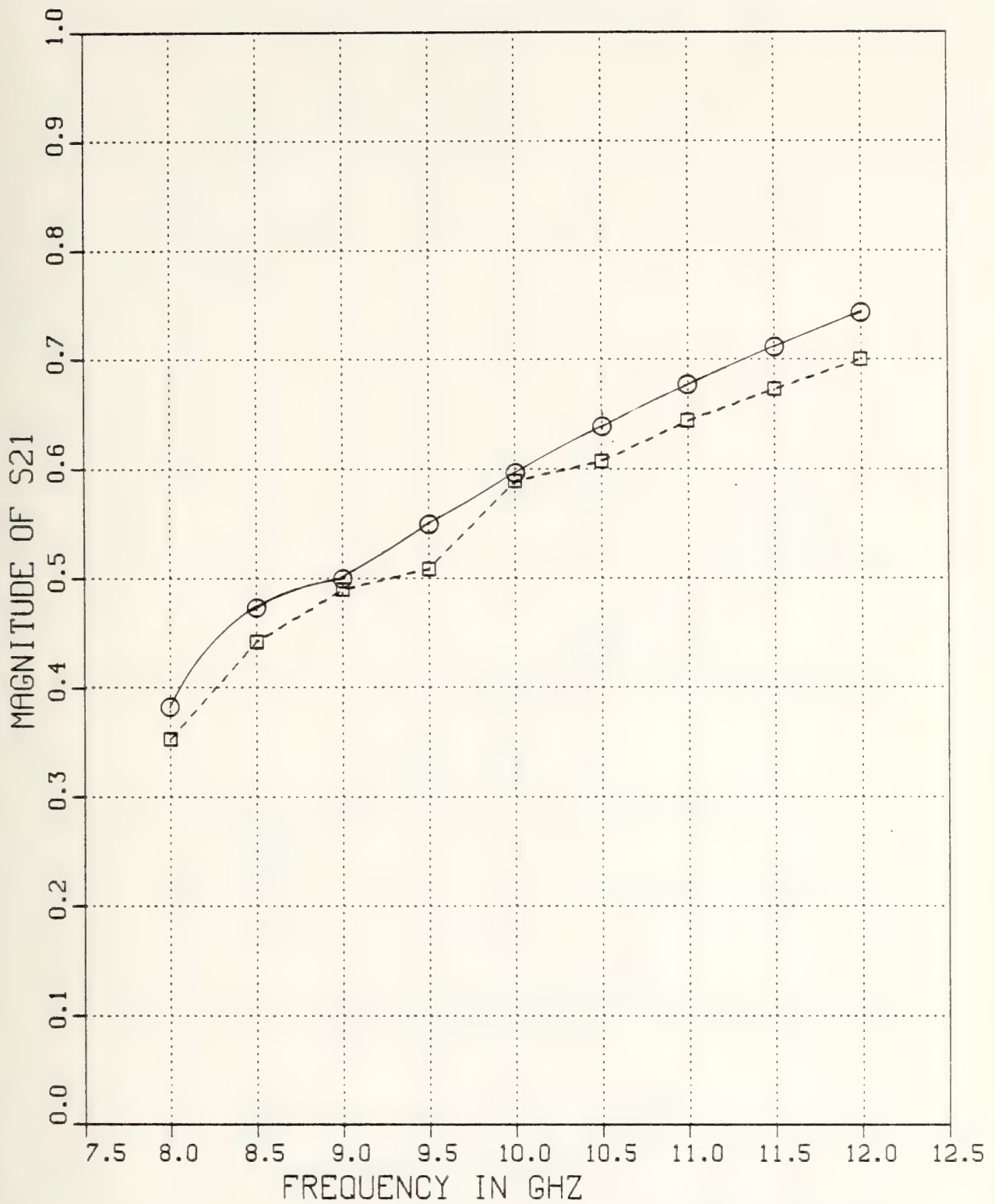


Figure F-15 $|S_{21}|$ v.s. Frequency for $T=0.1$ inch Inductive Strip, $w/b=1.0$, and $\epsilon_{r_2}=1.0$

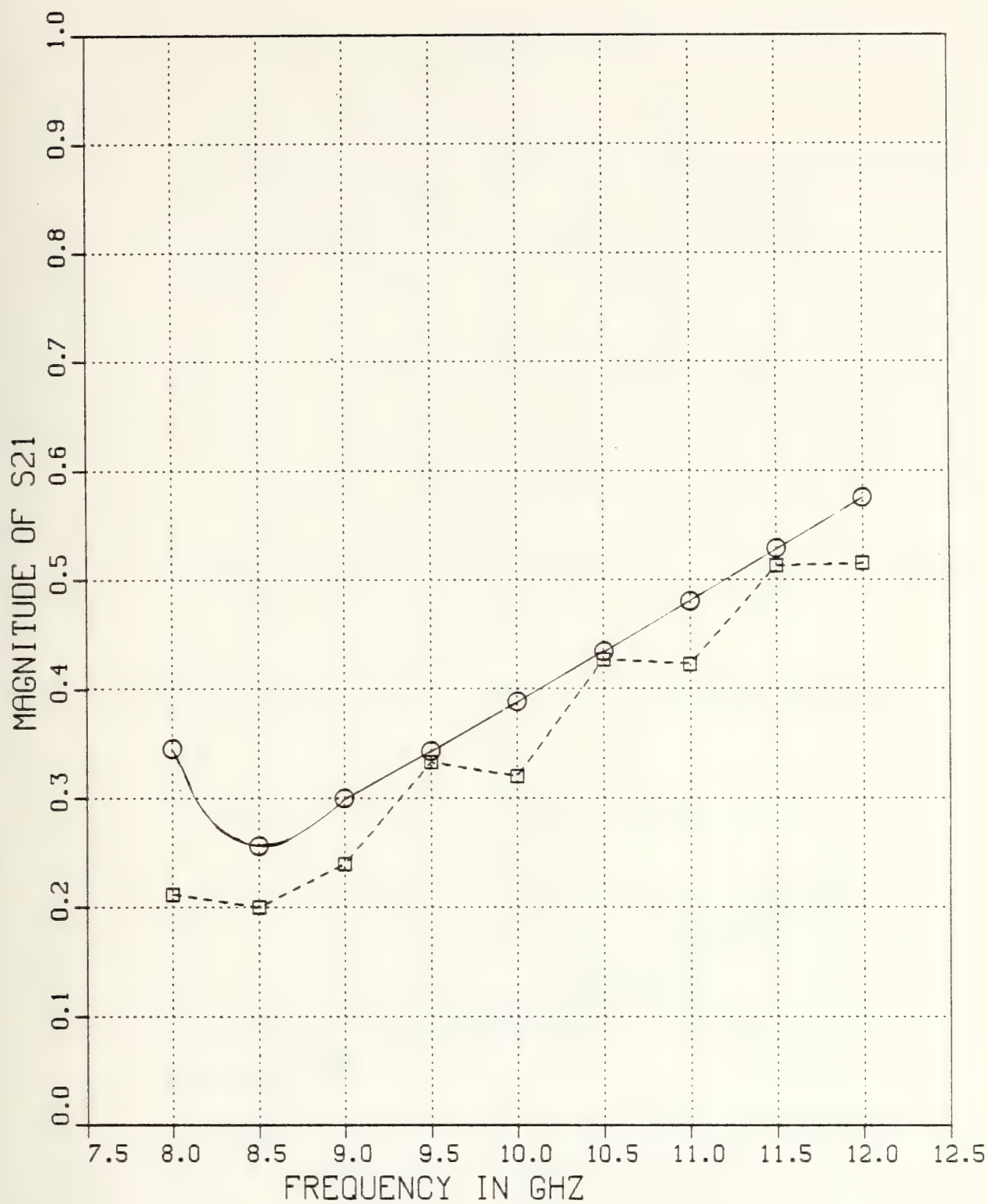


Figure F-16 $|S_{21}|$ v.s. Frequency for $T=0.2$ inch Inductive Strip, $w/b=1.0$, and $\epsilon_{r_2}=1.0$

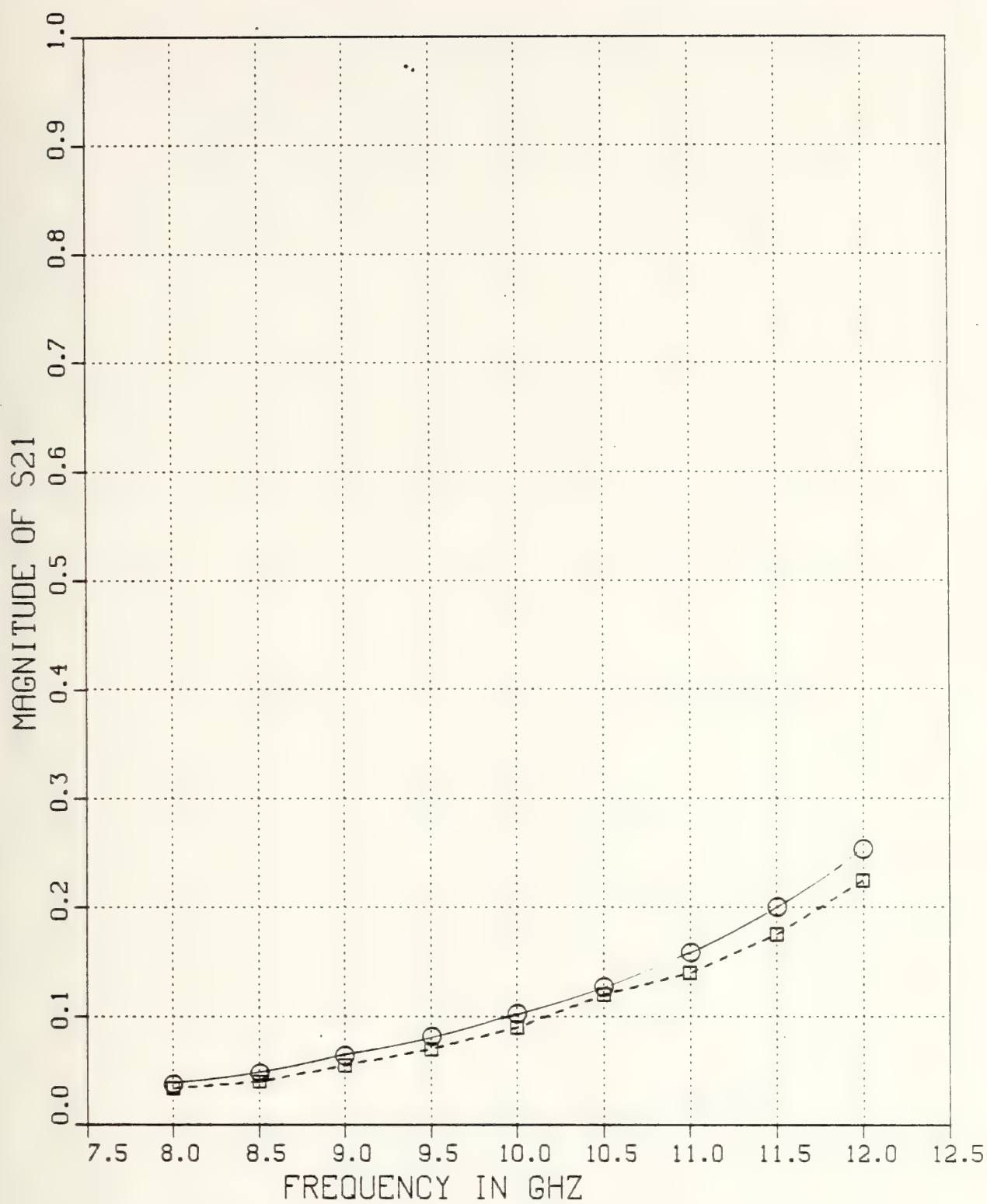


Figure F-17 $|S_{21}|$ v.s. Frequency for $T=0.5$ inch Inductive Strip, $w/b=1.0$, and $\epsilon_{r_2}=1.0$

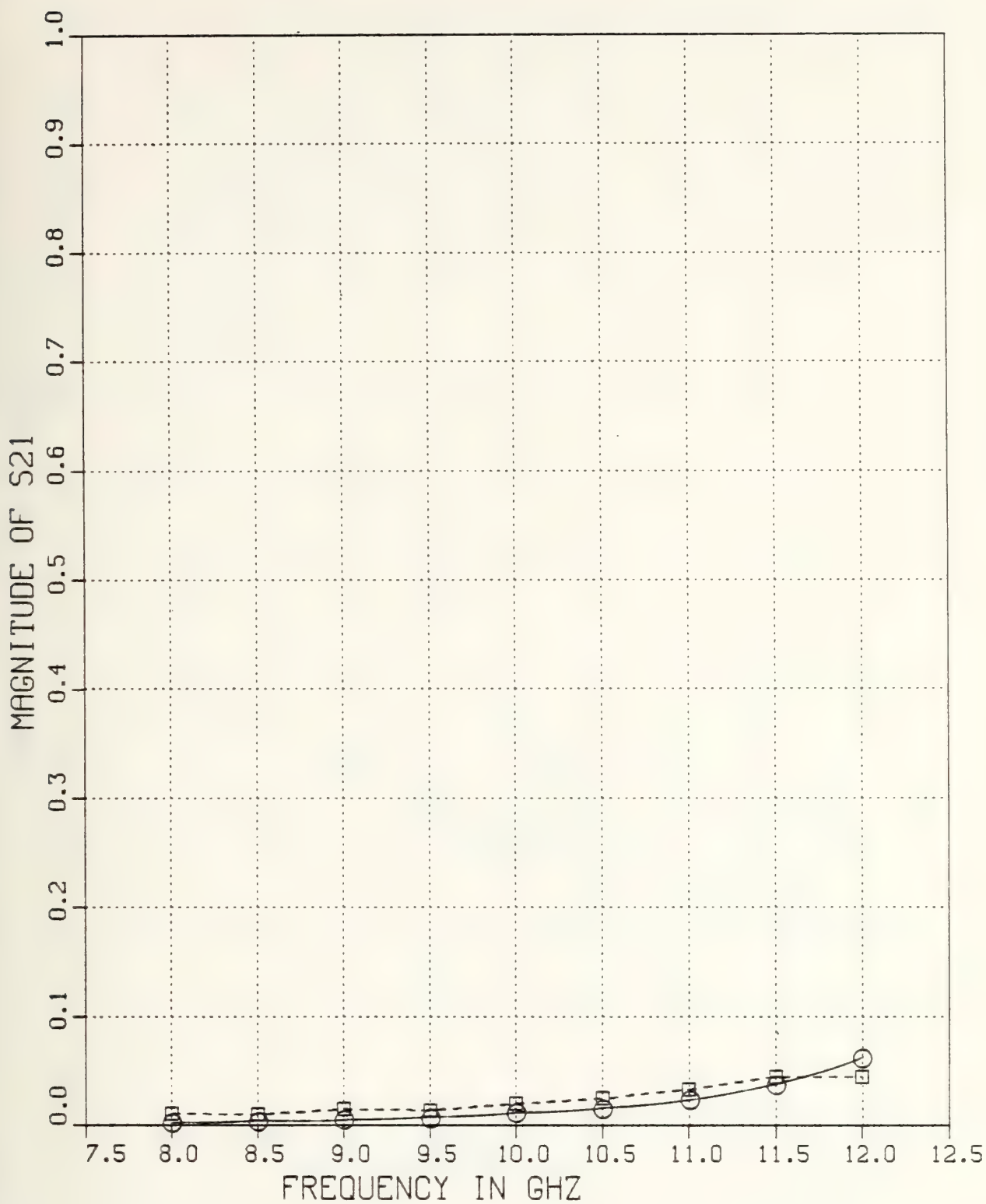


Figure F-18 $|S_{21}|$ v.s. Frequency for $T=1.0$ inch Inductive Strip, $w/b=1.0$, and $\epsilon_{r_2}=1.0$

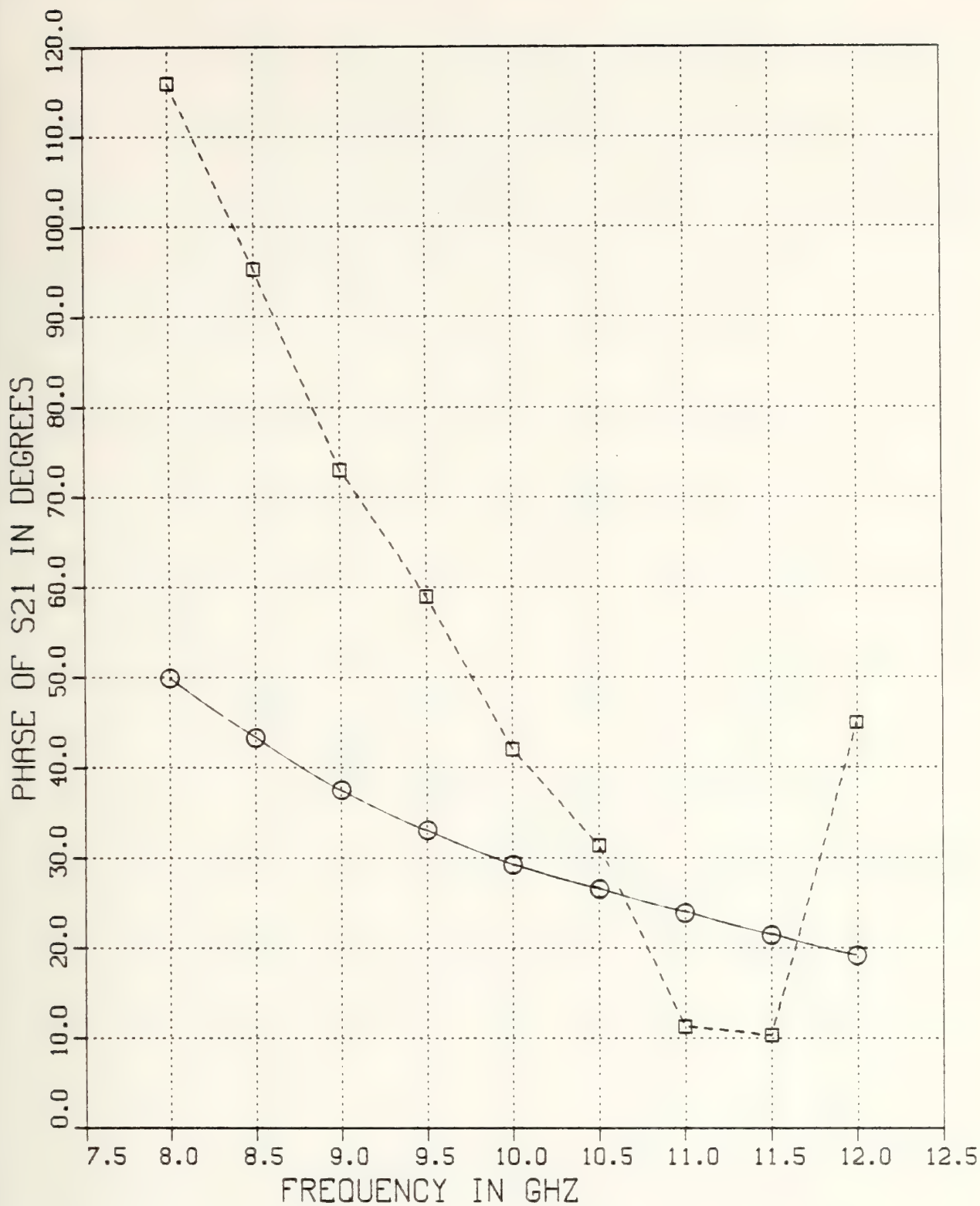


Figure F-19 θ_{21} v.s. Frequency for $T=.02$ inch Inductive Strip, $w/d=1.0$, and $\epsilon_{r_2}=1.0$

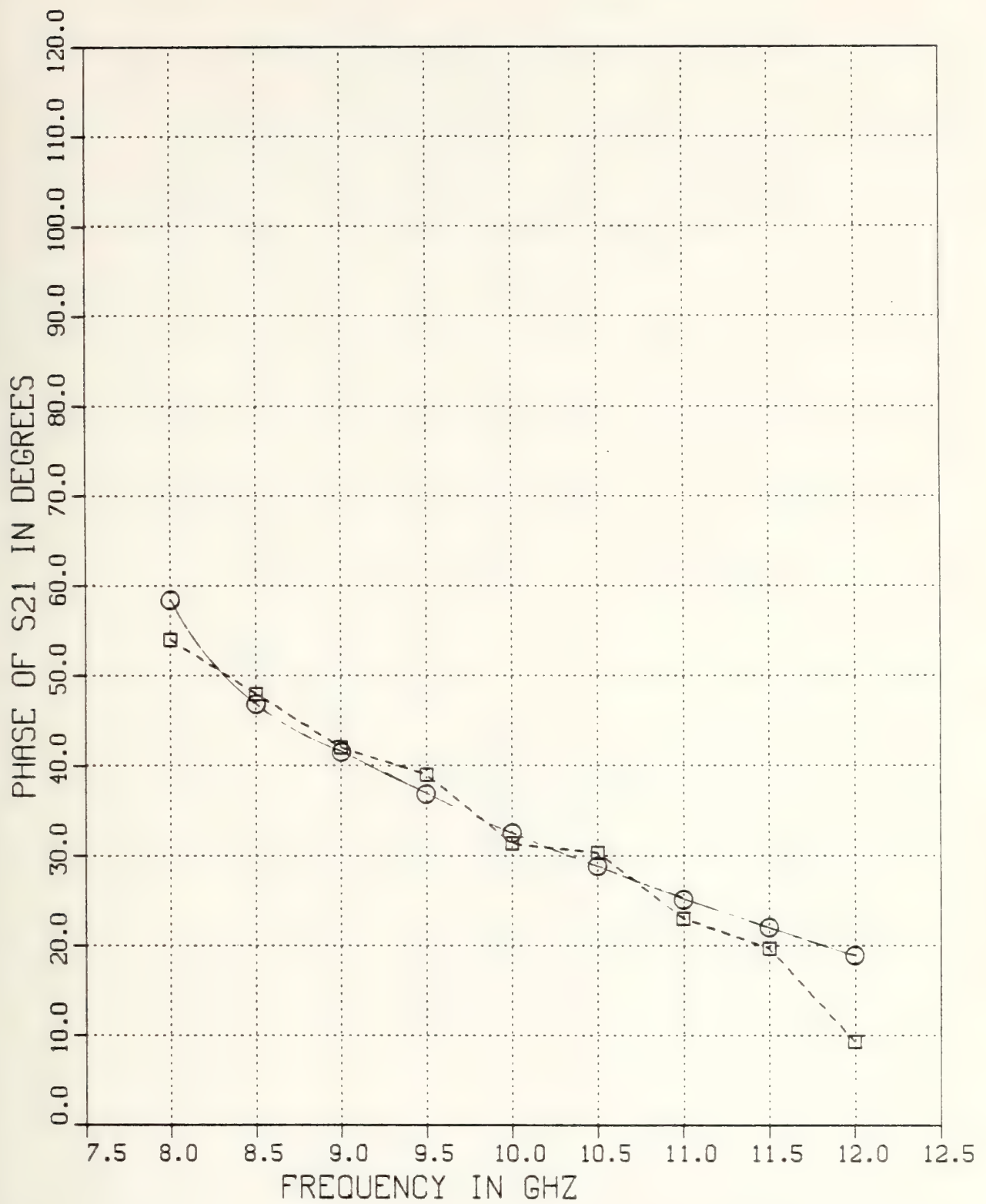


Figure F-20 θ_{21} v.s. Frequency for $T=.05$ inch Inductive Strip,
 $w/b=1.0$, and $\epsilon_{r_2}=1.0$

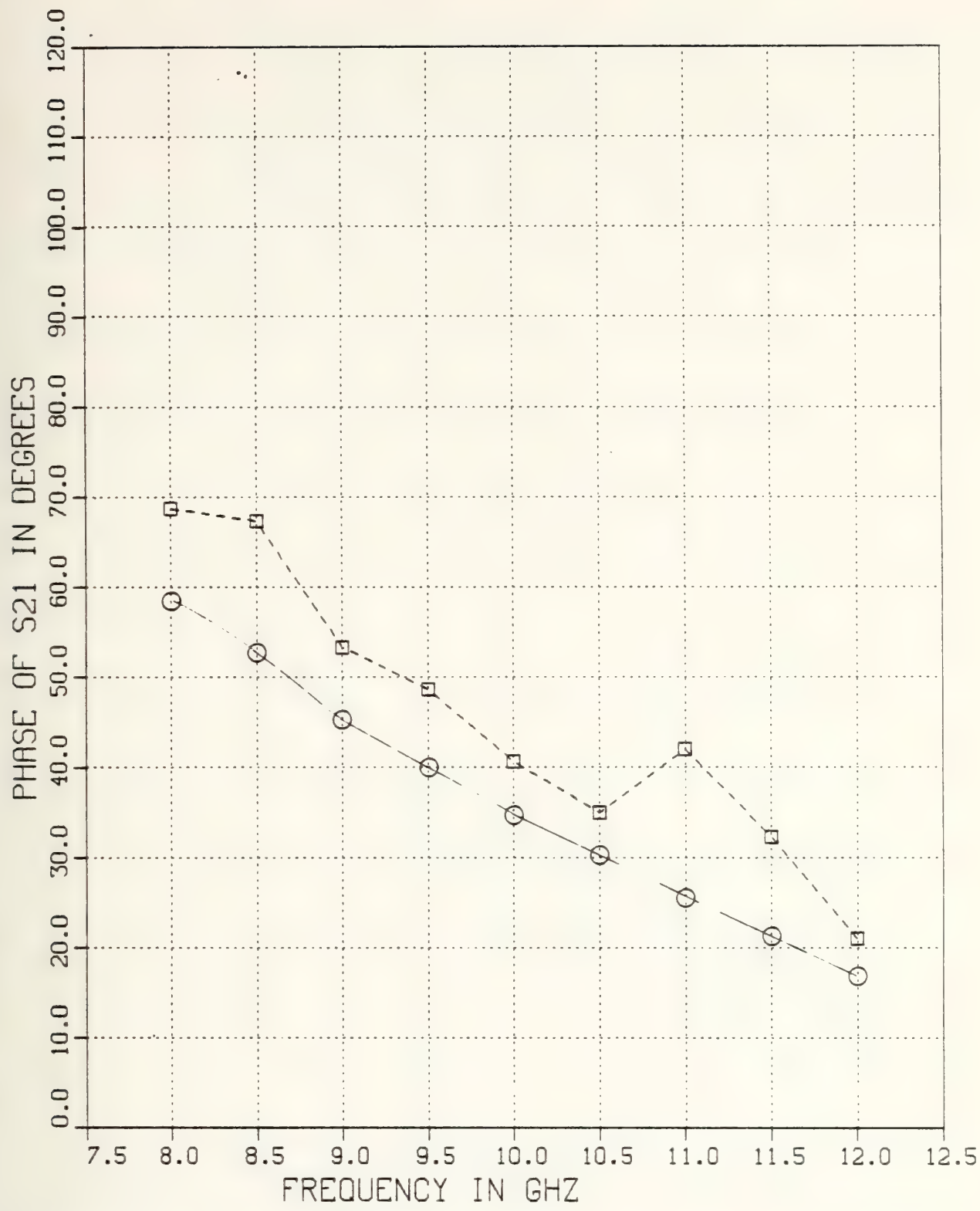


Figure F-21 θ_{21} v.s. Frequency for $T=0.1$ inch Inductive Strip, $w/b=1.0$, and $\epsilon_{r2}=1.0$

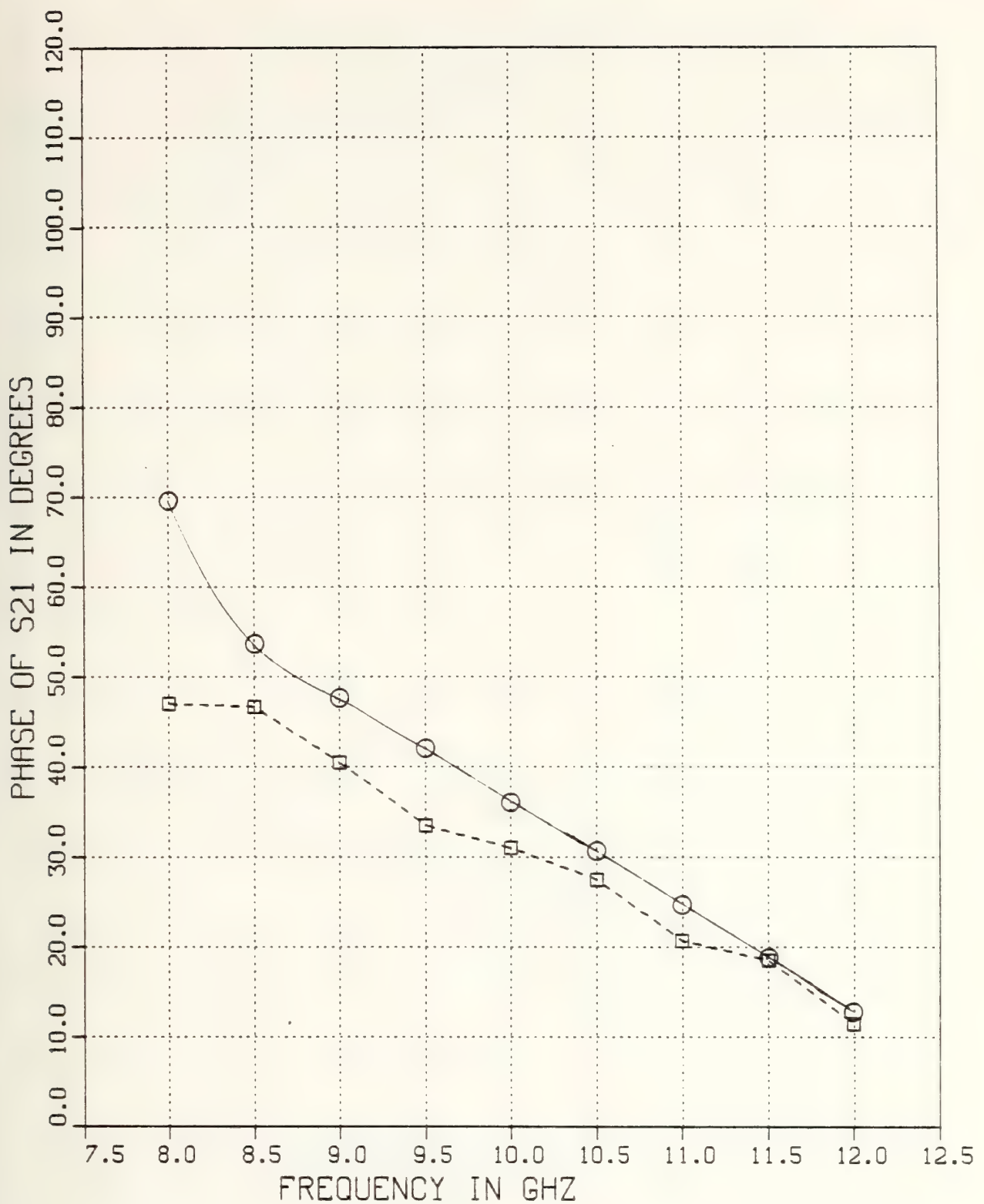


Figure F-22 θ_{21} v.s. Frequency for $T=0.2$ inch Inductive Strip, $w/b=1.0$, and $\epsilon_{r_2}=1.0$

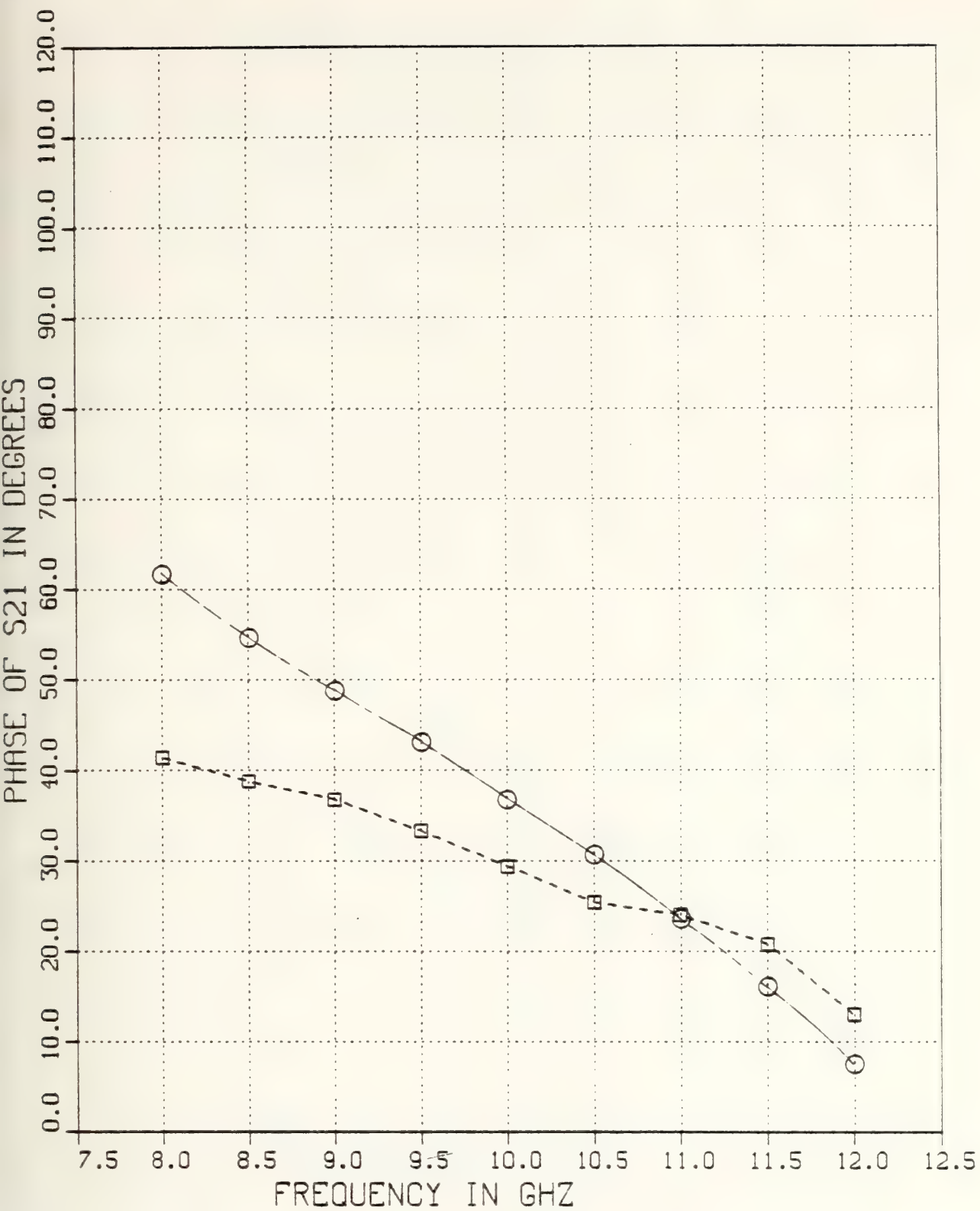


Figure F-23 θ_{21} v.s. Frequency for $T=0.5$ inch Inductive Strip, $w/b=1.0$, and $\epsilon_{r_2}=1.0$

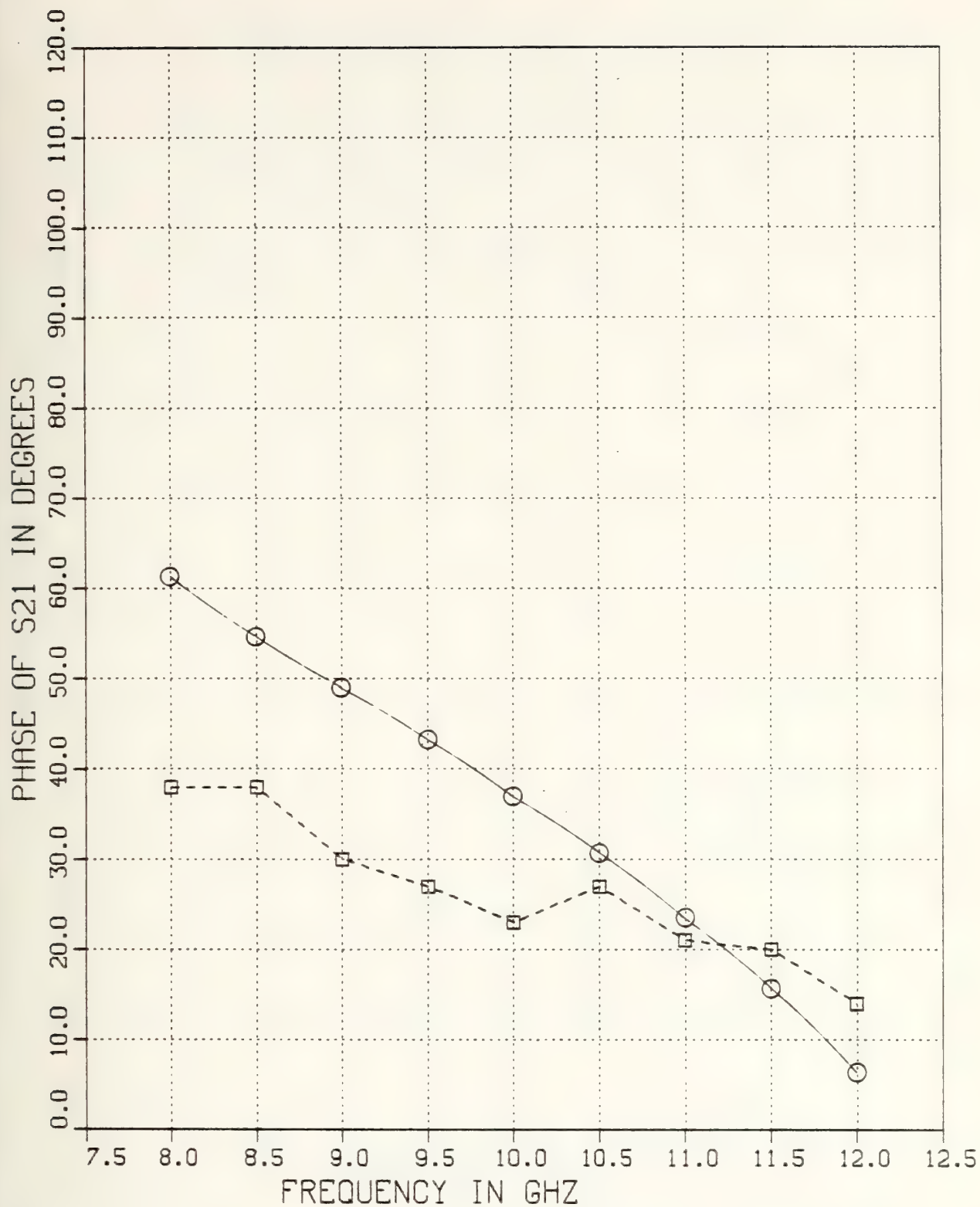


Figure F-24 θ_{21} v.s. Frequency for $T=1.0$ inch Inductive Strip, $w/b=1.0$, and $\epsilon_{r_2}=1.0$

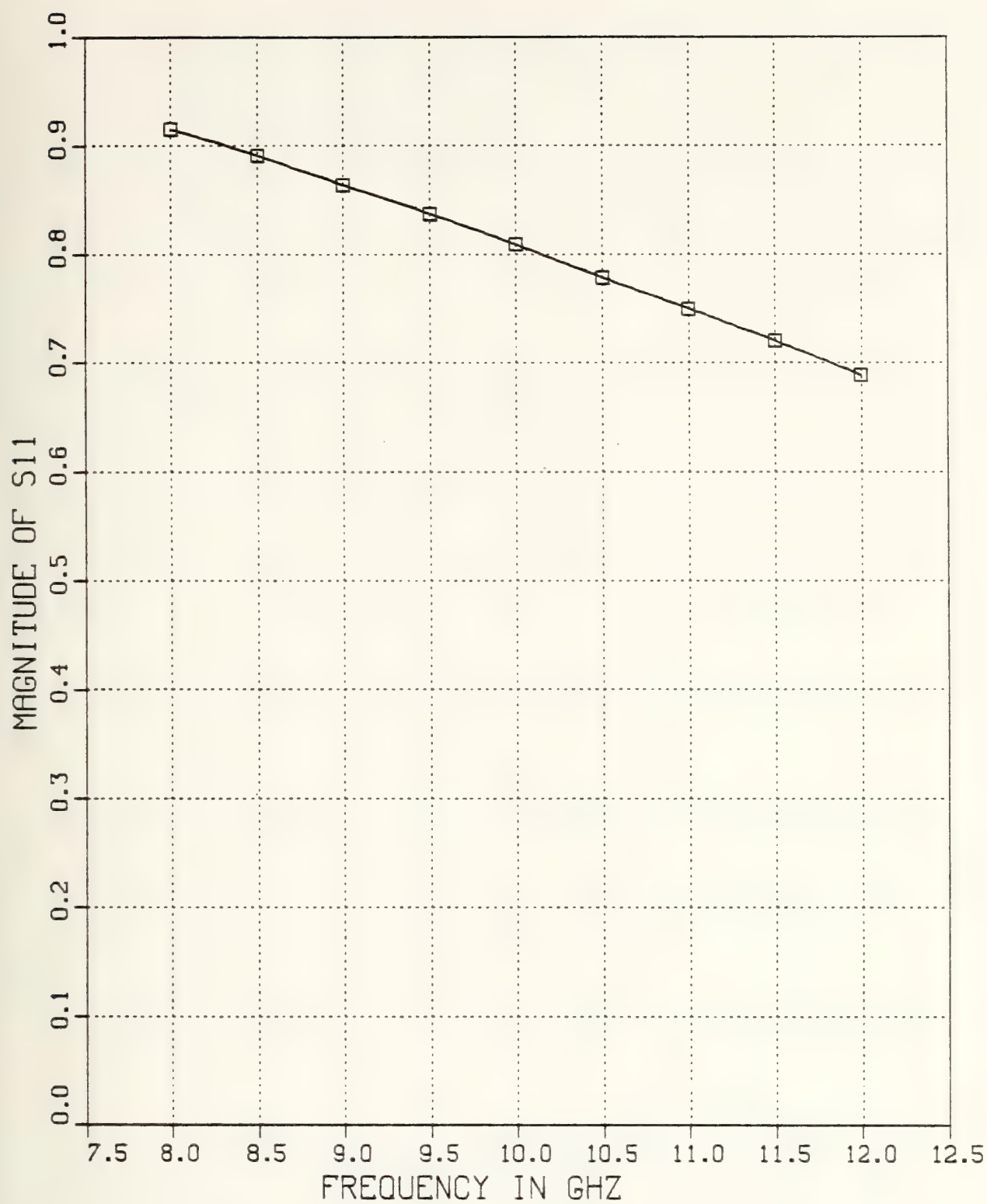


Figure F-25 $|S_{11}|$ v.s. Frequency for $T=.05$ inch Inductive Strip, $w/b=0.5$, and $\epsilon_{r_2}=1.0$

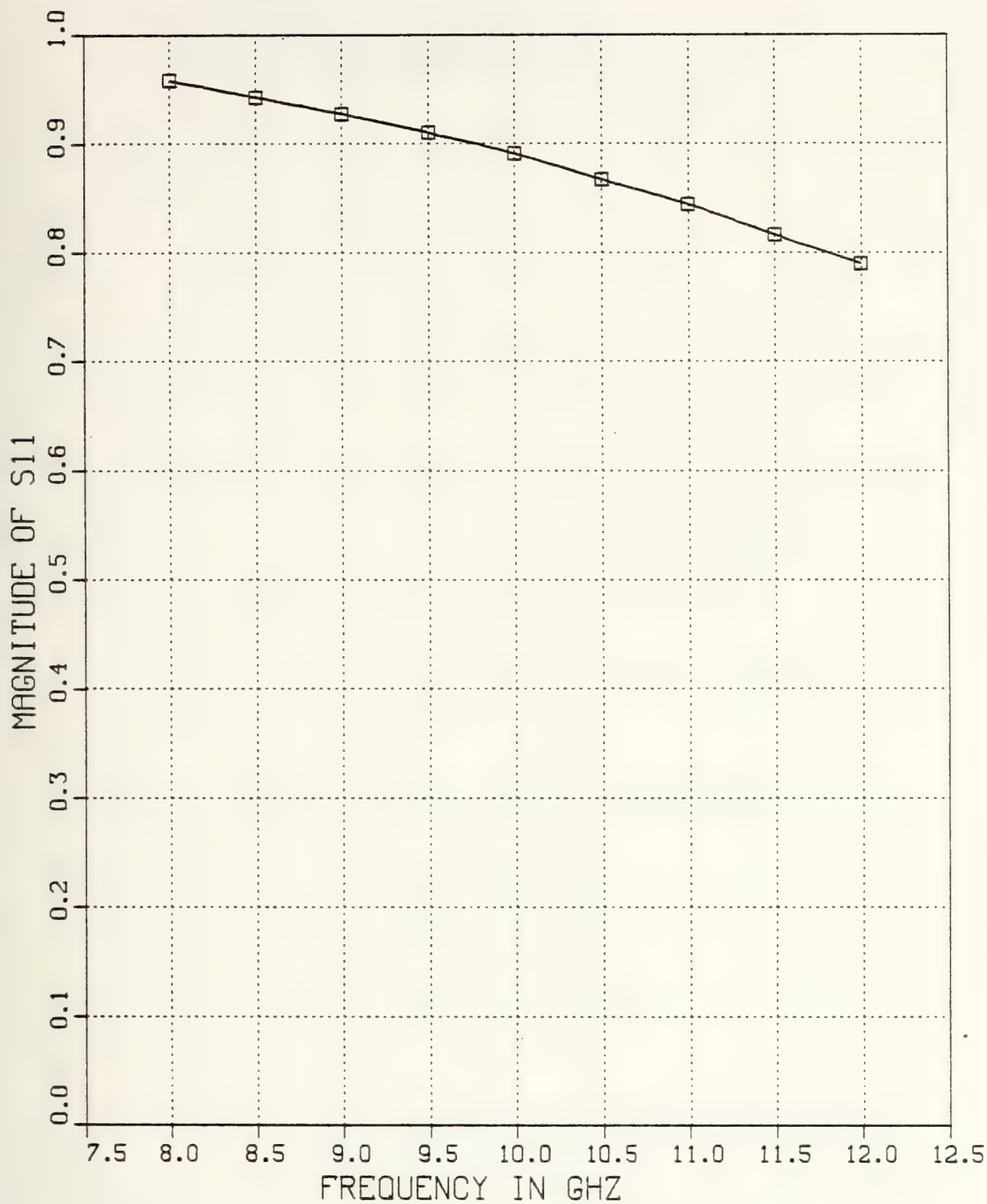


Figure F-26 $|S_{11}|$ v.s. Frequency for $T=0.1$ inch Inductive Strip, $w/b=0.5$, and $\epsilon_{r2}=1.0$

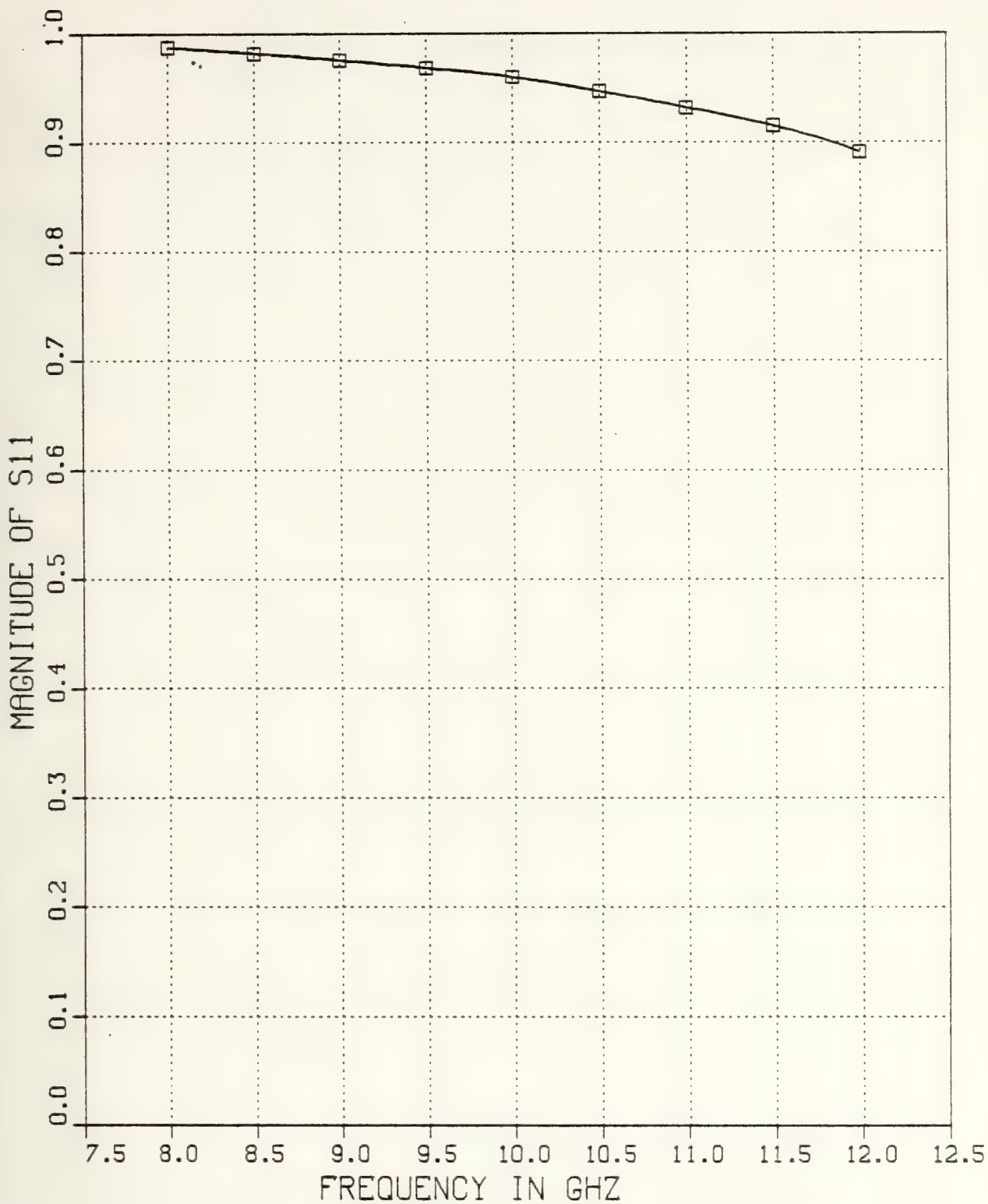


Figure F-27 $|S_{11}|$ v.s. Frequency for $T=0.2$ inch Inductive Strip, $w/b=0.5$, and $\epsilon_{r_2}=1.0$

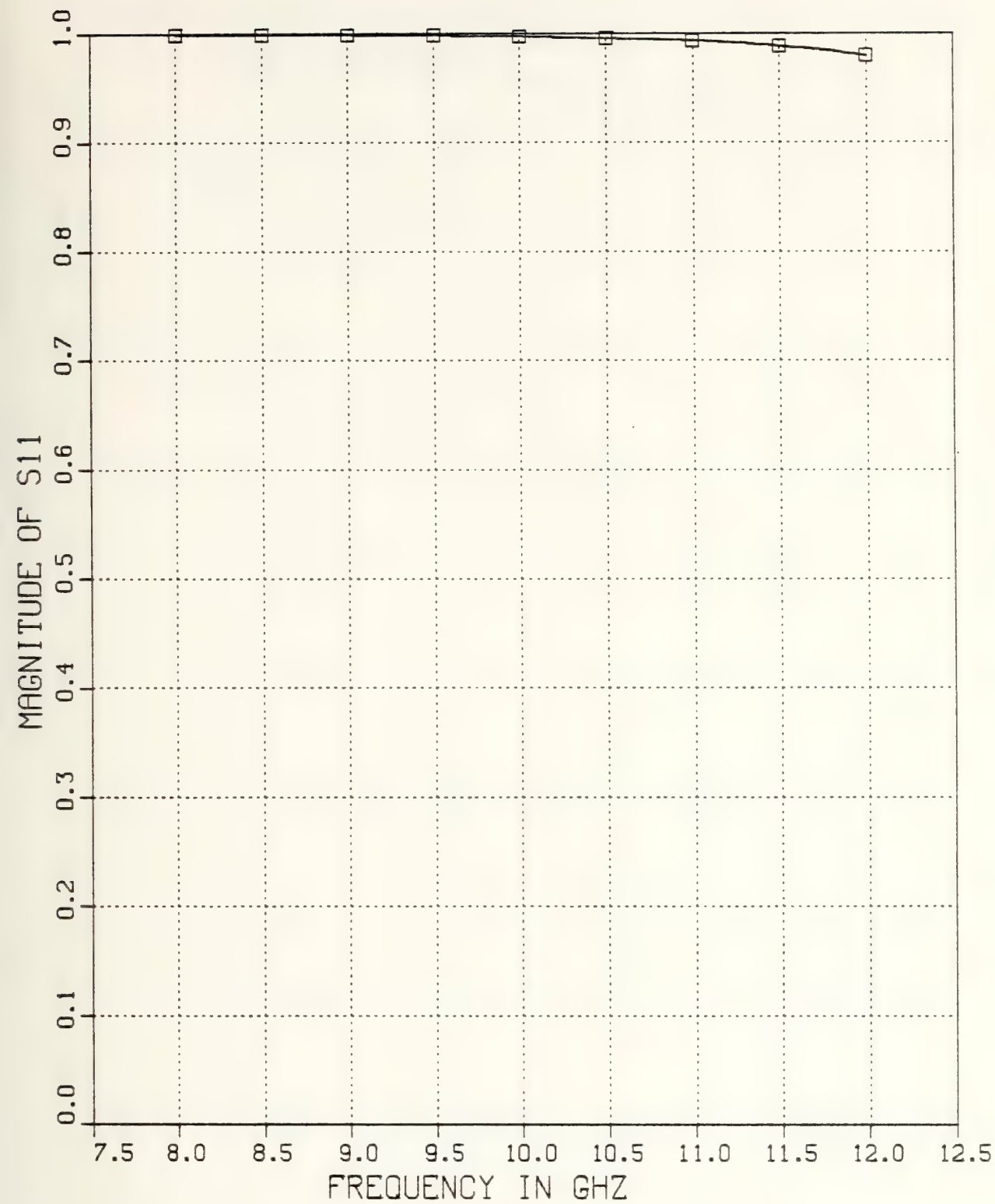


Figure F-28 $|S_{11}|$ v.s. Frequency for $T=0.5$ inch Inductive Strip, $w/b=0.5$, and $\epsilon_{r_2}=1.0$

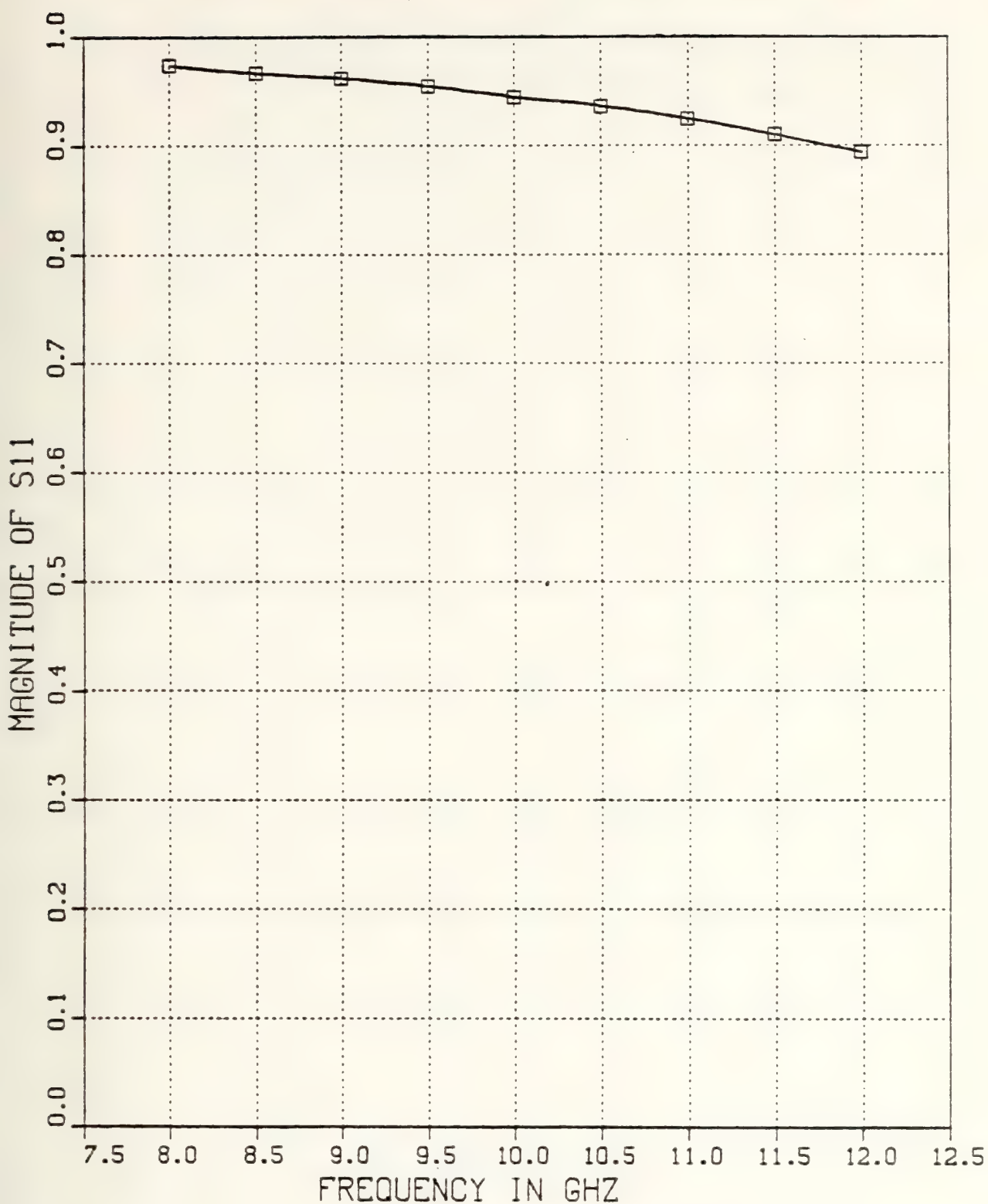


Figure F-29 $|S_{11}|$ v.s. Frequency for $T=.05$ inch Inductive Strip, $w/b=.25$, and $\epsilon_{r2}=1.0$

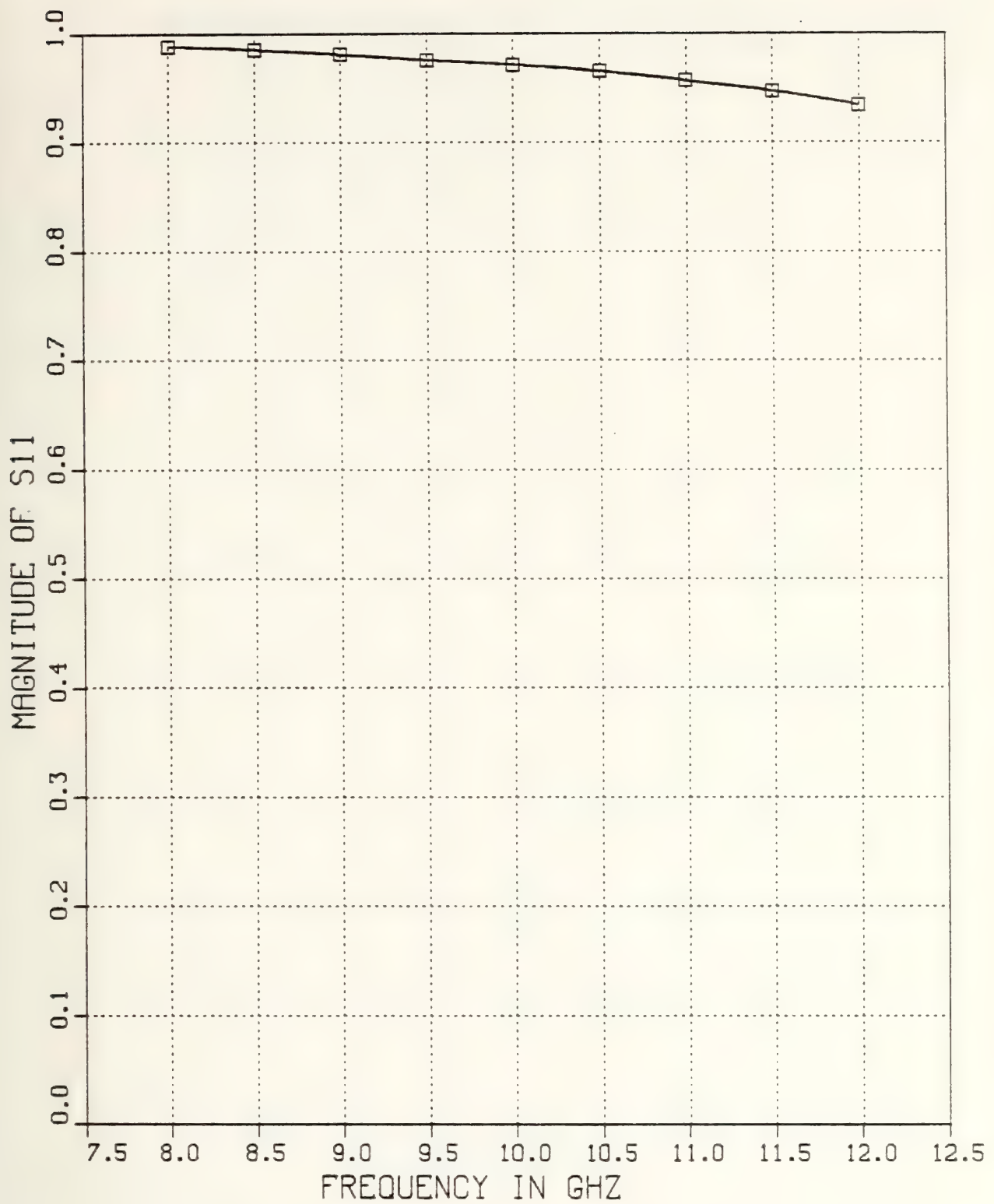


Figure F-30 $|S_{11}|$ v.s. Frequency for $T=0.1$ inch Inductive Strip, $w/b=.25$, and $\epsilon_{r_2}=1.0$

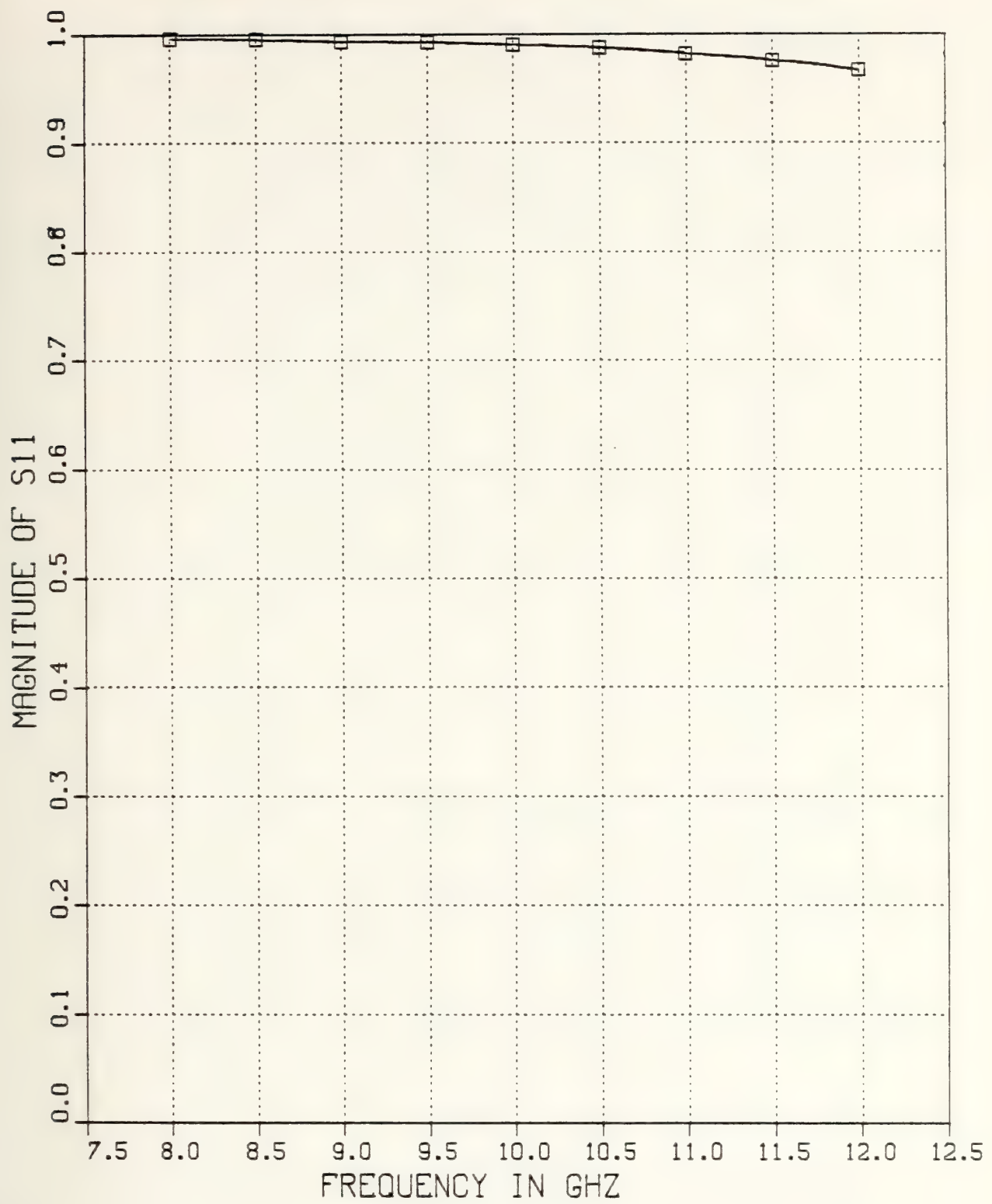


Figure F-31 $|S_{11}|$ v.s. Frequency for $T=0.2$ inch Inductive Strip, $w/b=.25$, and $\epsilon_{r2}=1.0$

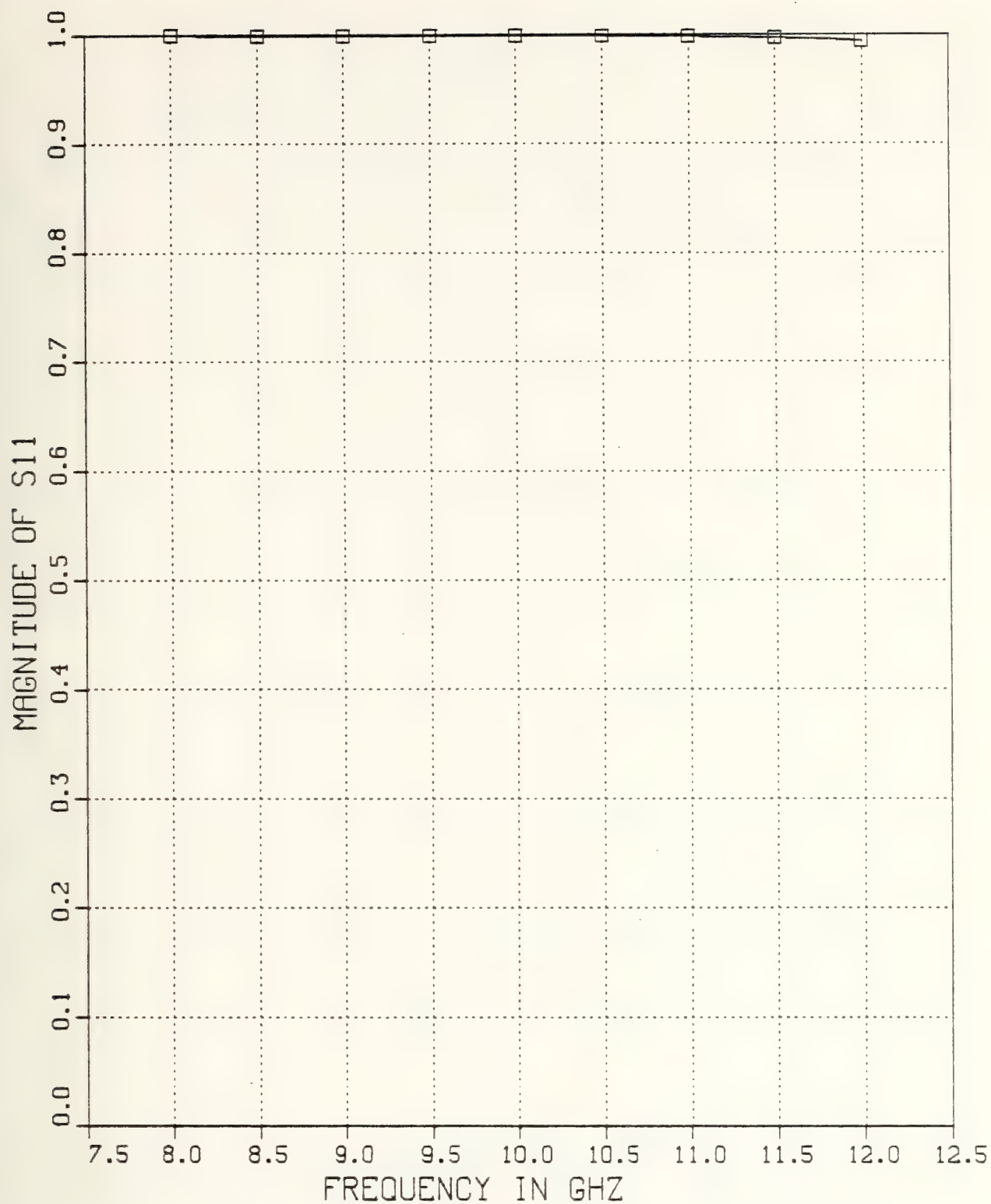


Figure F-32 $|S_{11}|$ v.s. Frequency for $T=0.5$ inch Inductive Strip, $w/b=.25$, and $\epsilon_{r_2}=1.0$

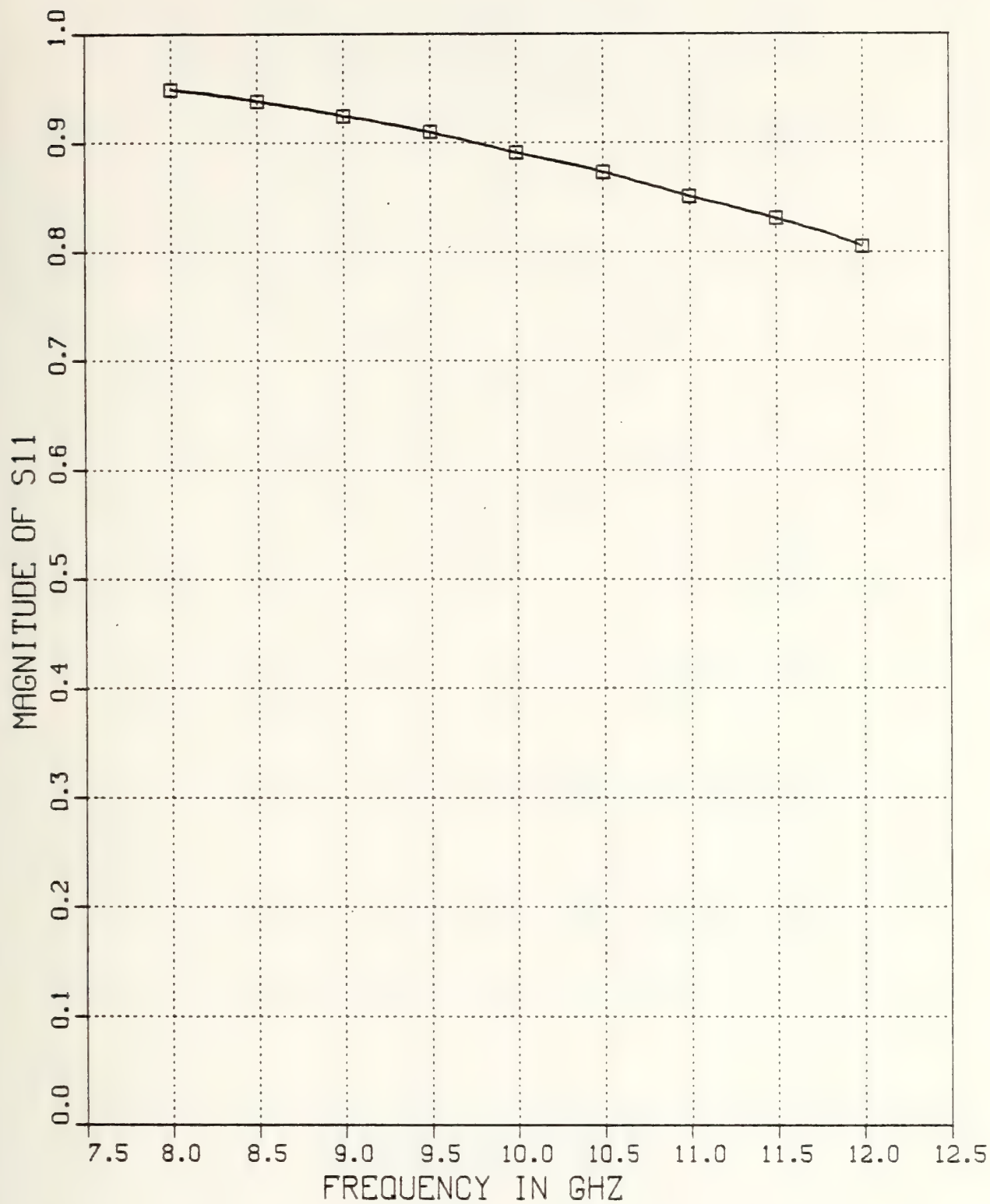


Figure F-33 $|S_{11}|$ v.s. Frequency for $T=.05$ inch Inductive Strip, $w/b=.2$, and $\epsilon_{r_2}=1.0$

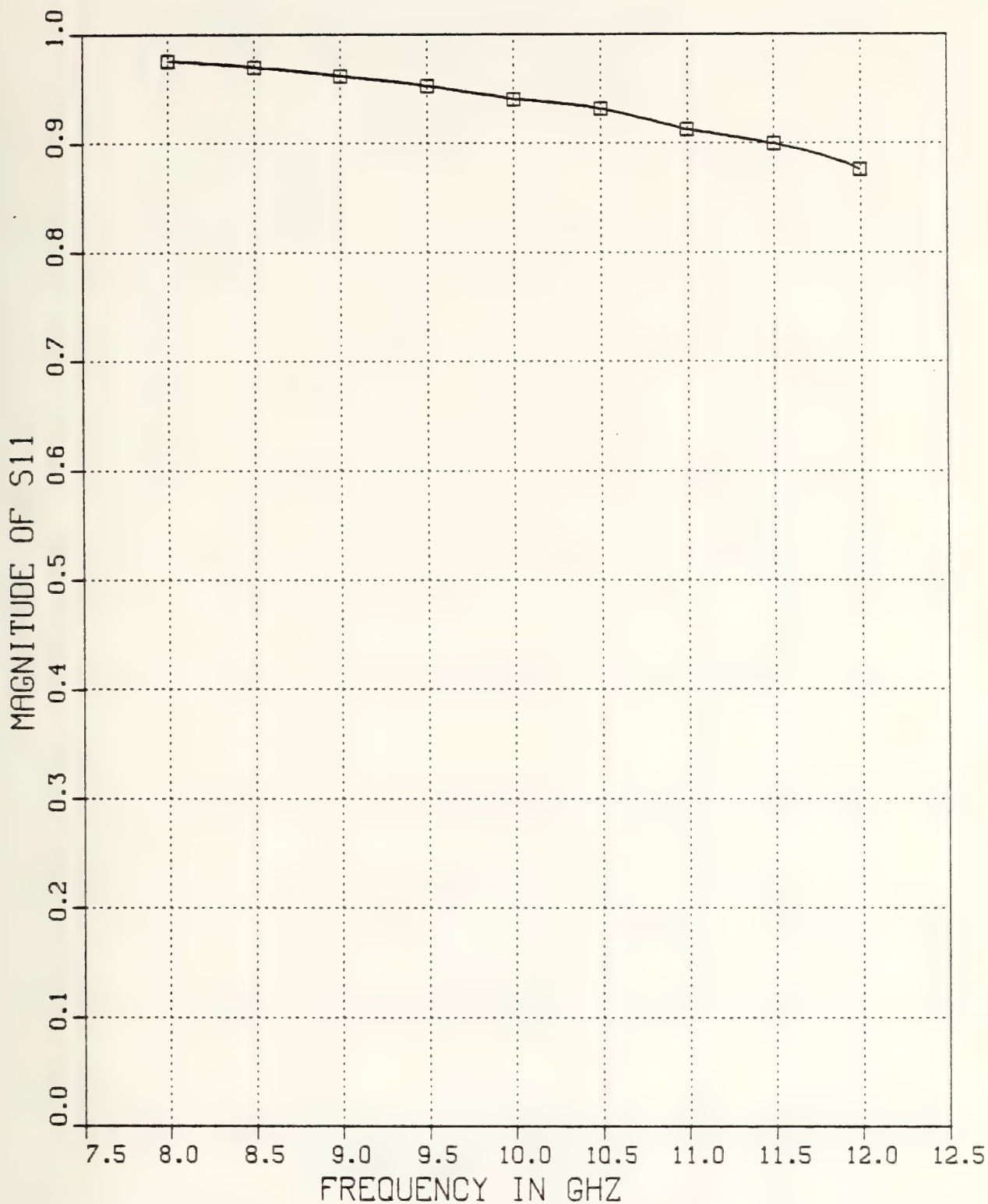


Figure F-34 $|S_{11}|$ v.s. Frequency for $T=0.1$ inch Inductive Strip, $w/b=.2$, and $\epsilon_{r_2}=1.0$

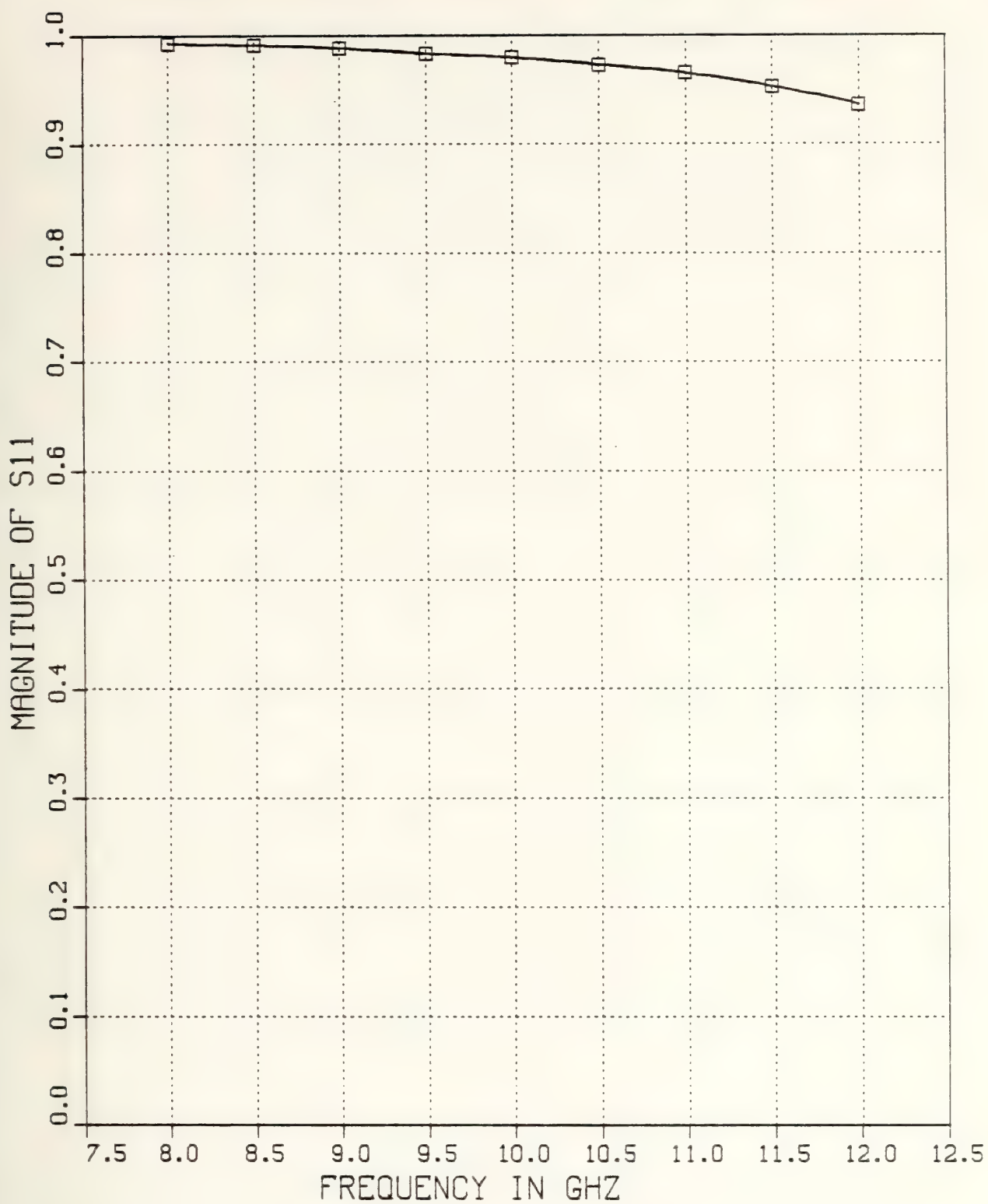


Figure F-35 $|S_{11}|$ v.s. Frequency for $T=0.2$ inch Inductive Strip, $w/b=.2$, and $\epsilon_{r_2}=1.0$

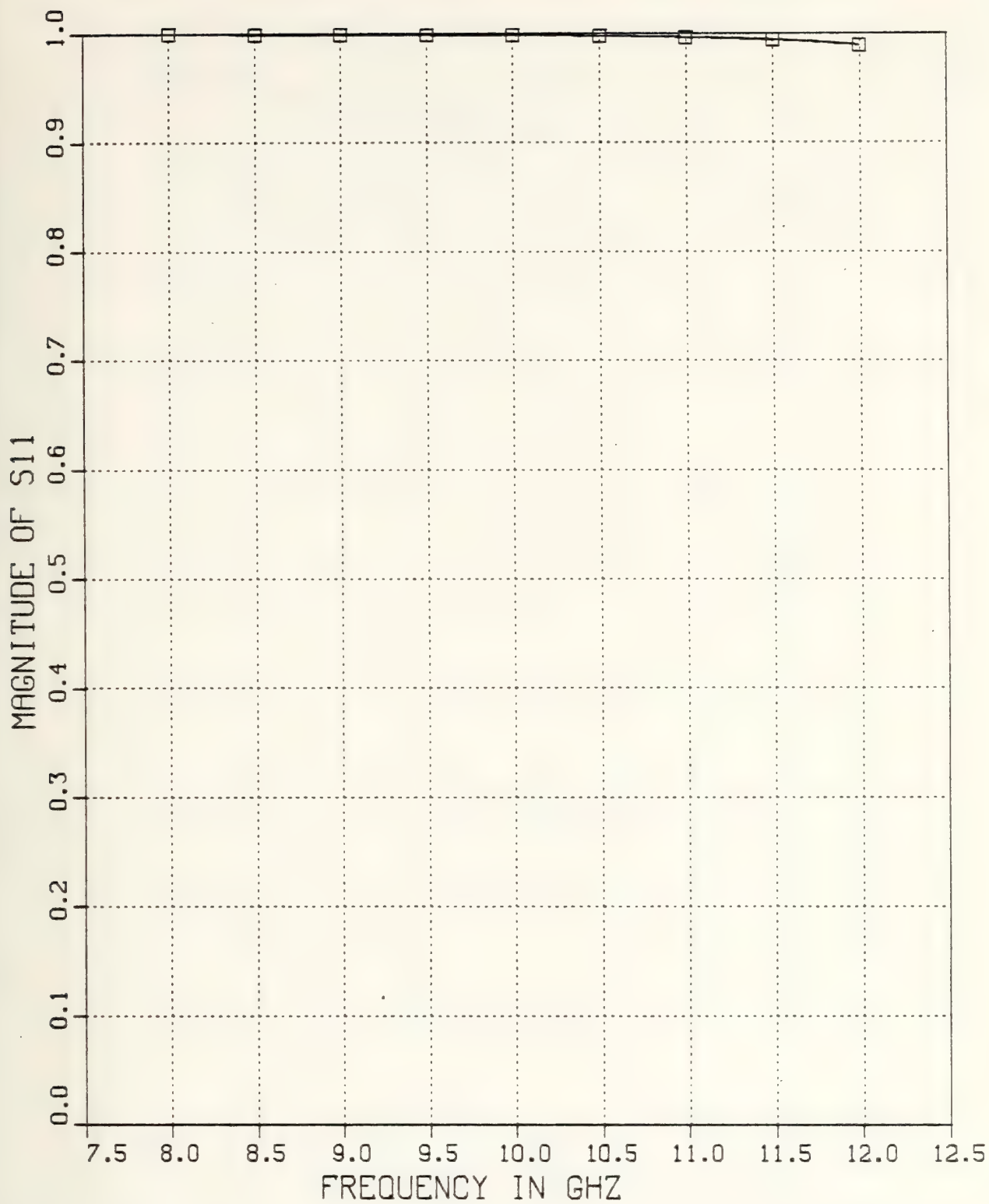


Figure F-36 $|S_{11}|$ v.s. Frequency for $T=0.5$ inch Inductive Strip, $w/b=.2$, and $\epsilon_{r_2}=1.0$

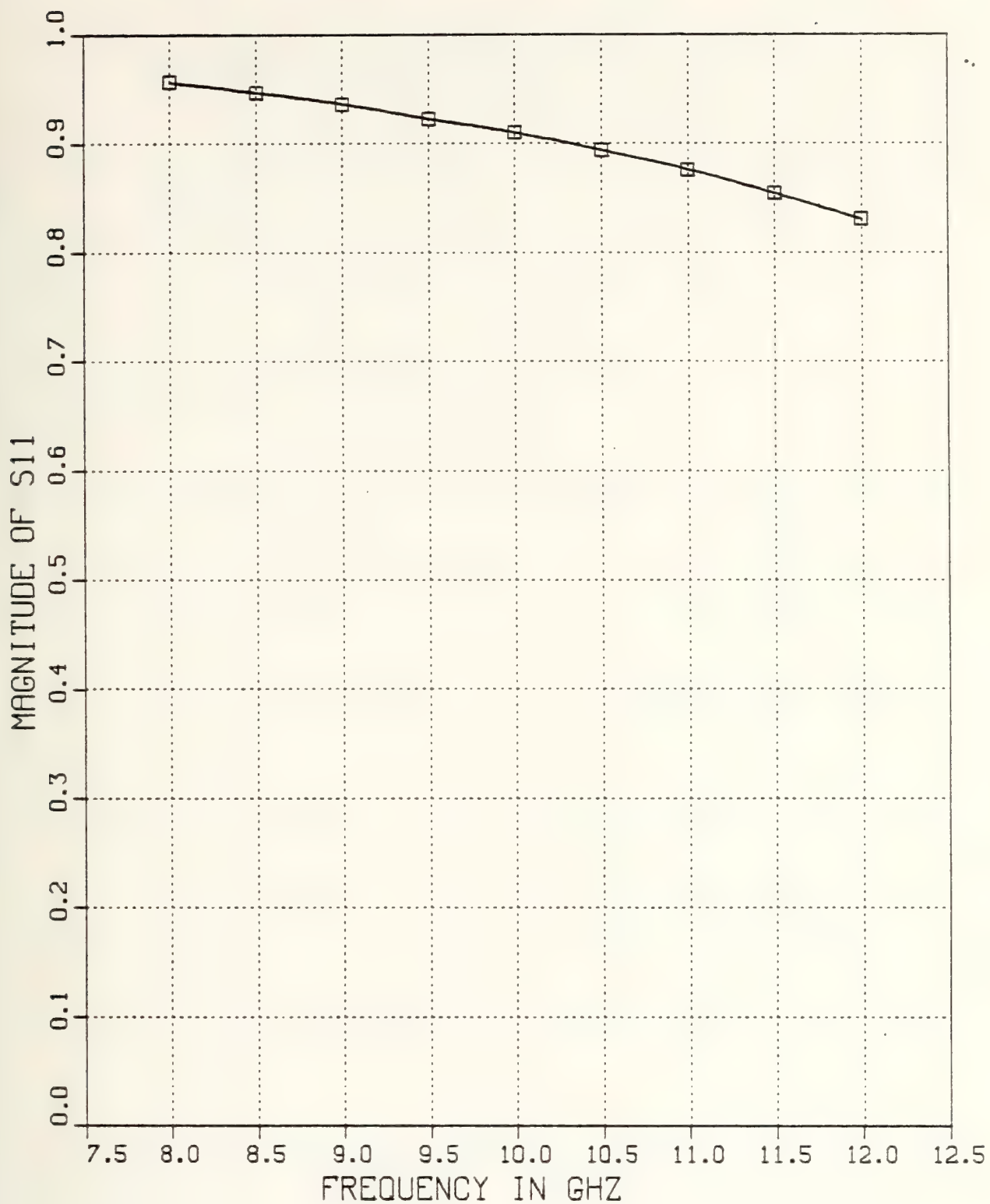


Figure F-37 $|S_{11}|$ v.s. Frequency for $T=.05$ inch Inductive Strip, $w/b=.1$, and $\epsilon_{r_2}=1.0$

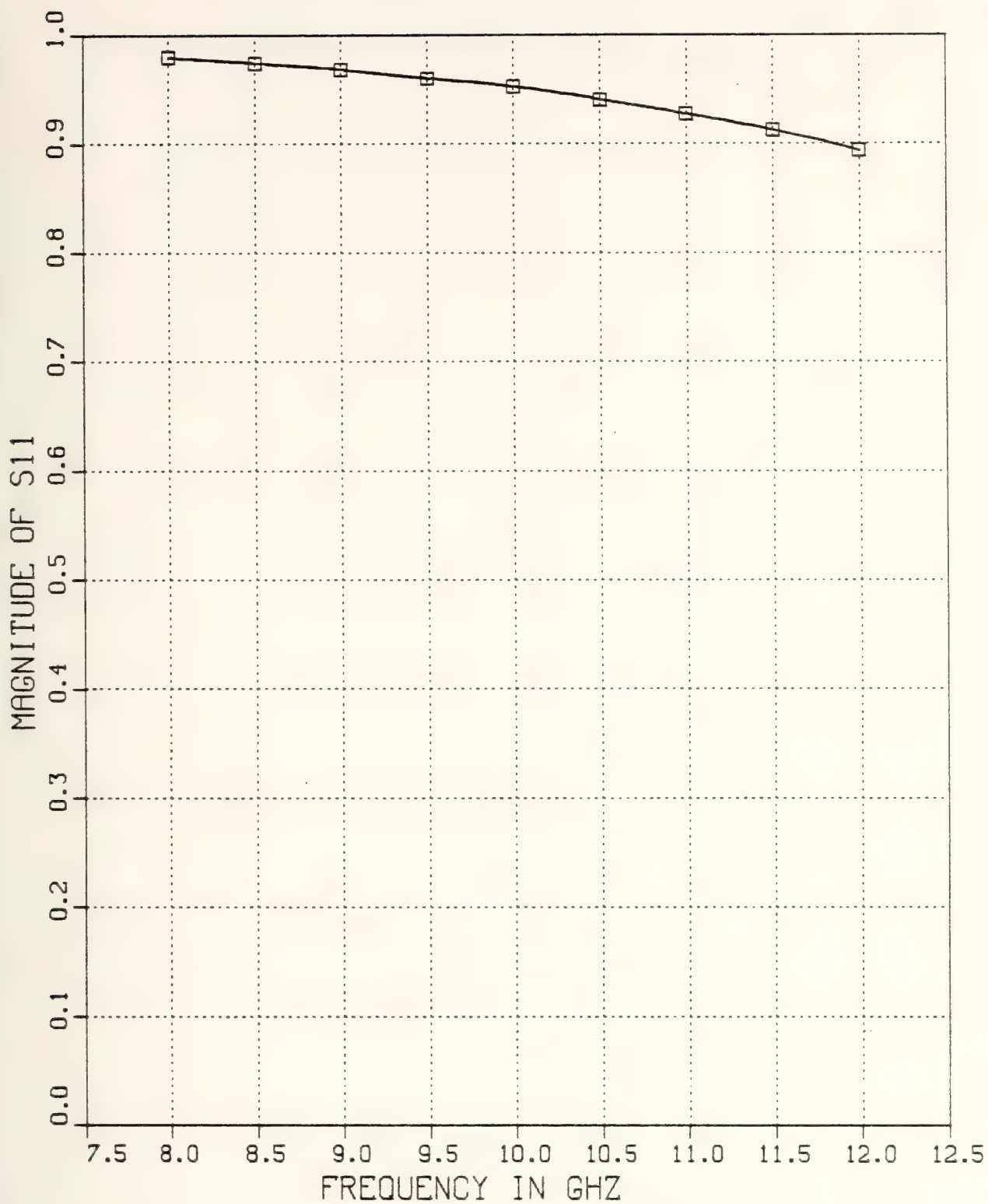


Figure F-38 $|S_{11}|$ v.s. Frequency for $T=0.1$ inch Inductive Strip, $w/b=.1$, and $\epsilon_{r_2}=1.0$

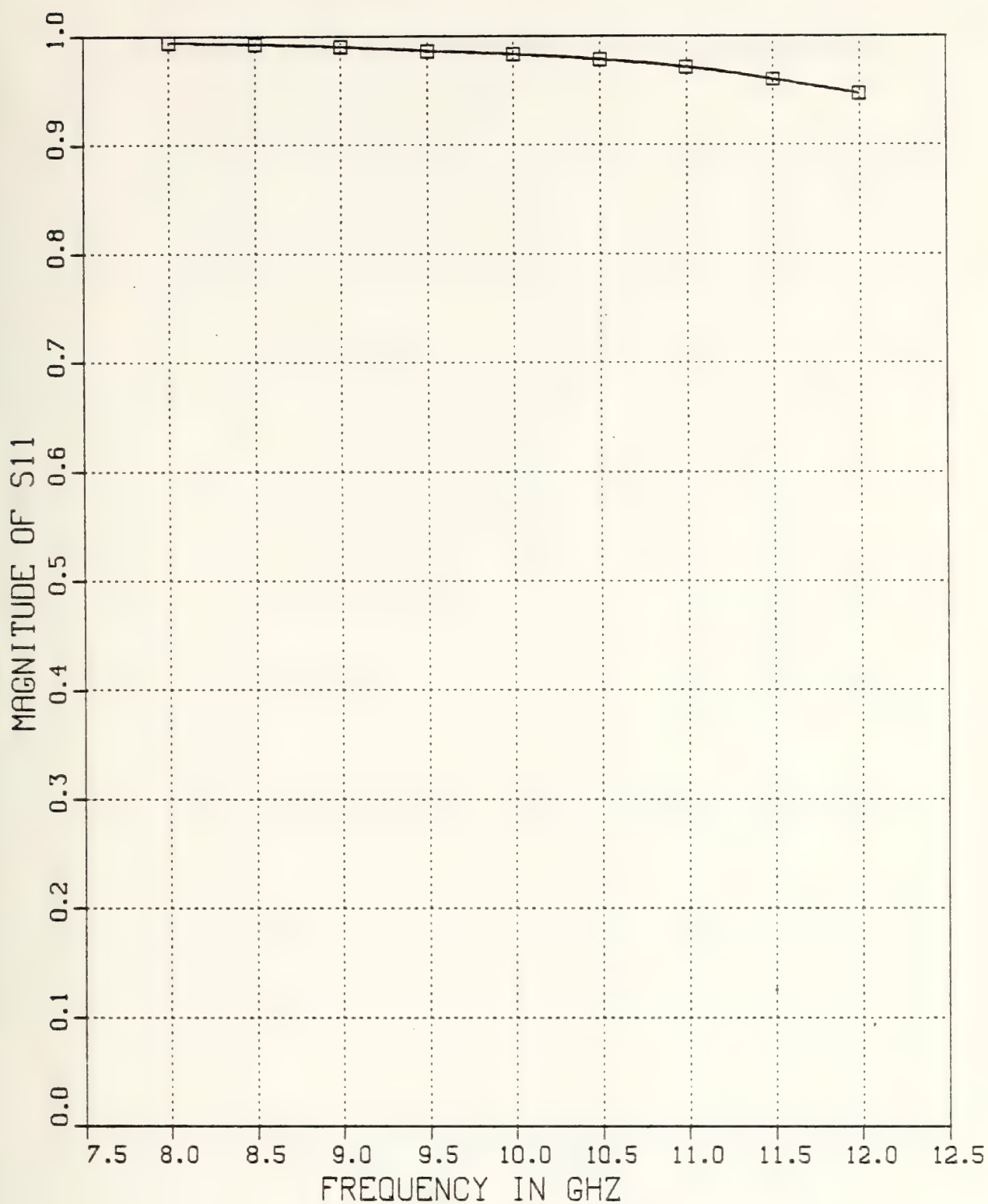


Figure F-39 $|S_{11}|$ v.s. Frequency for $T=0.2$ inch Inductive Strip, $w/b=.1$, and $\epsilon_{r_2}=1.0$

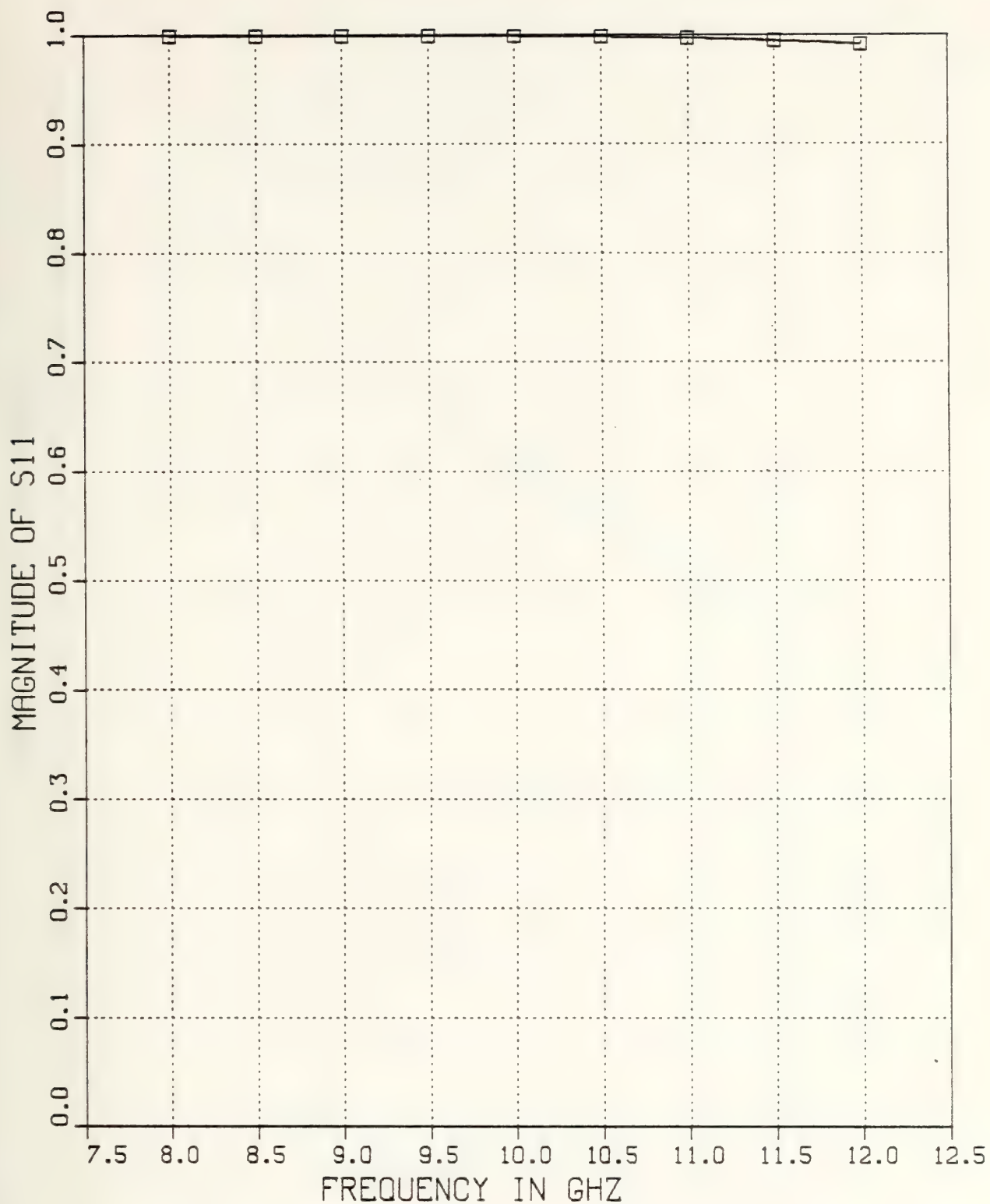


Figure F-40 $|S_{11}|$ v.s. Frequency for $T=0.5$ inch Inductive Strip, $w/b=.1$, and $\epsilon_{r2}=1.0$

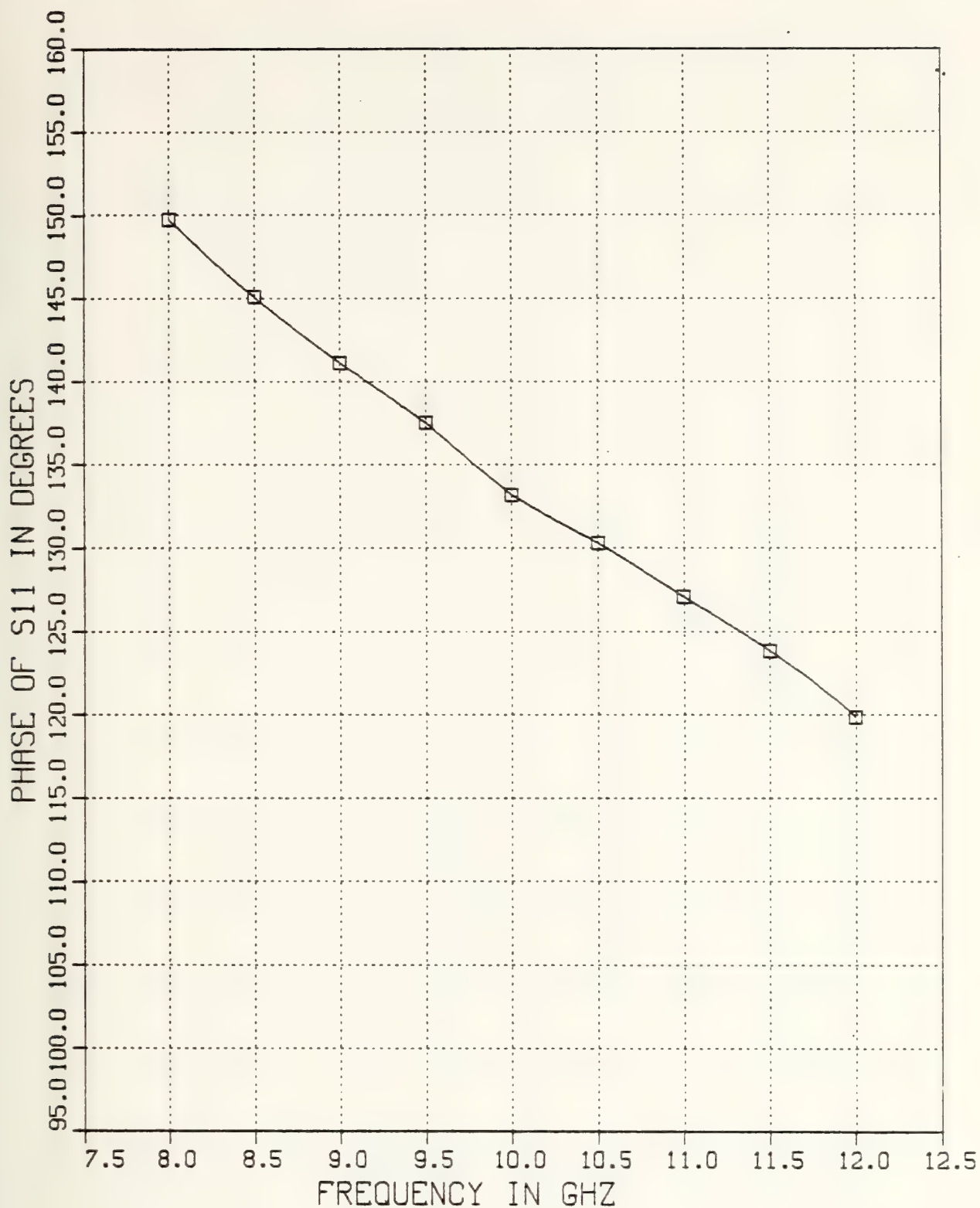


Figure F-41 θ_{11} v.s. Frequency for $T=.05$ inch Inductive Strip, $w/b=.5$, and $\epsilon_{r_2}=1.0$

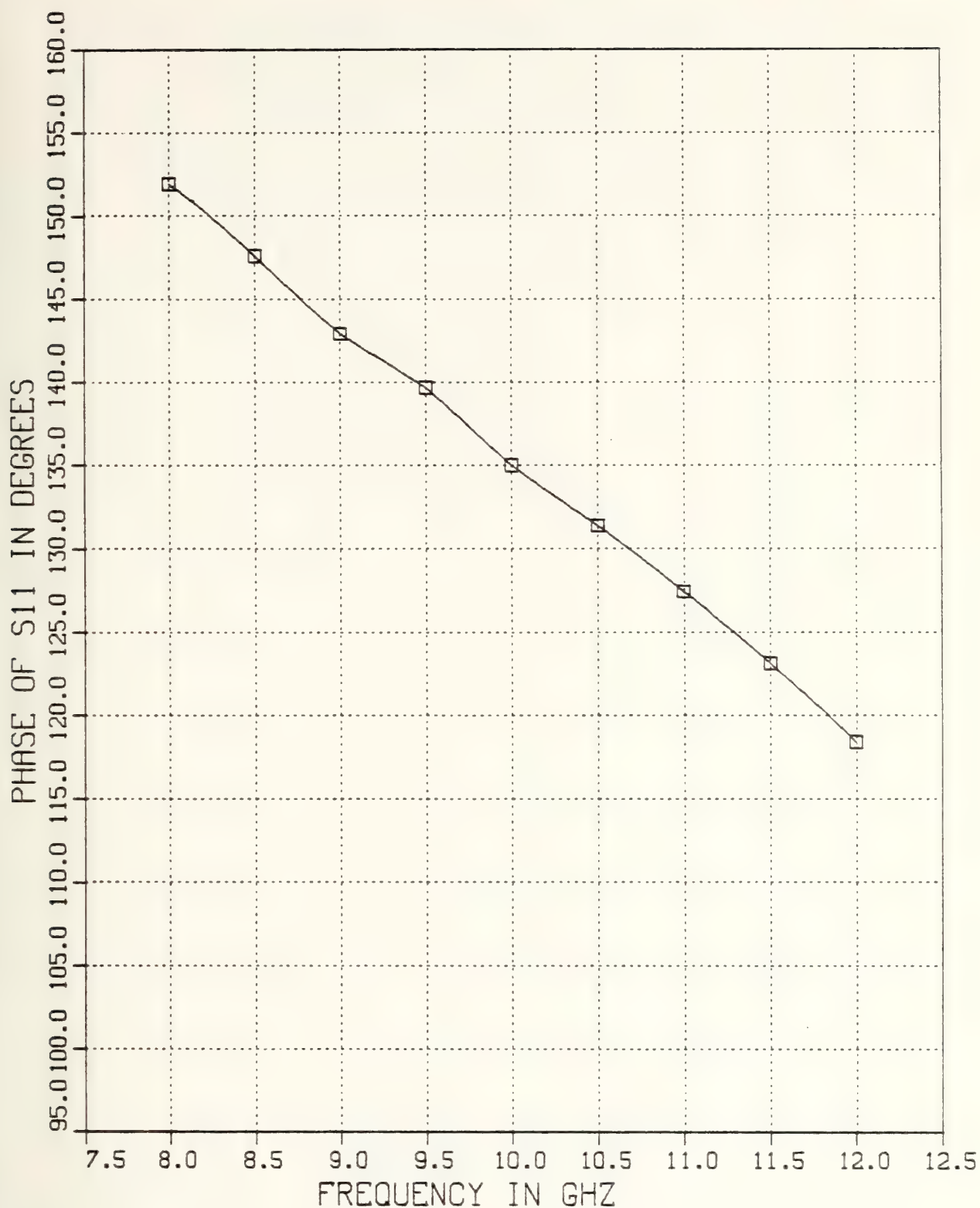


Figure F-42 θ_{11} v.s. Frequency for $T=0.1$ inch Inductive Strip, $w/b=.5$, and $\epsilon_{r_2}=1.0$

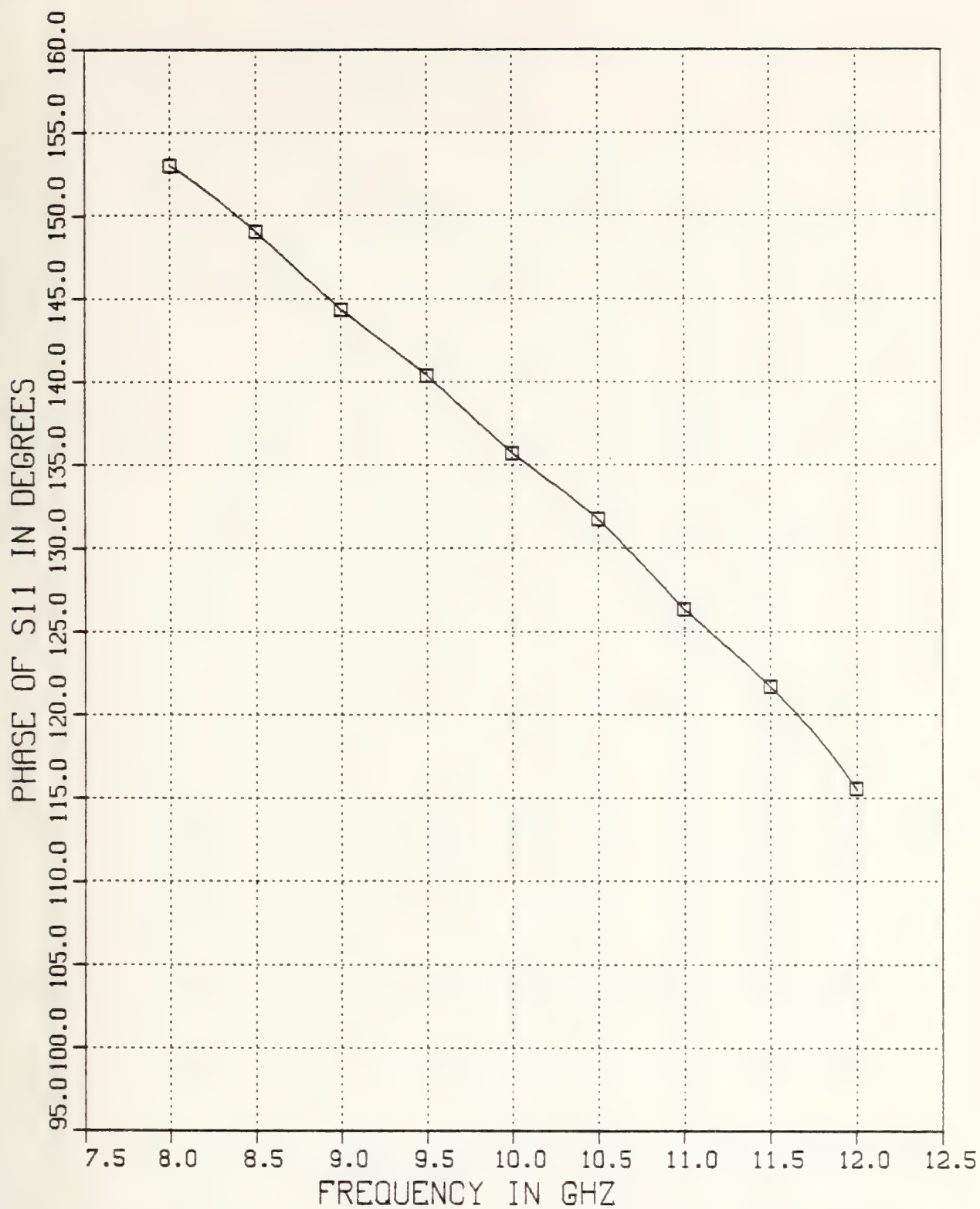


Figure F-43 θ_{11} v.s. Frequency for $T=0.2$ inch Inductive Strip,
 $w/b=.5$, and $\epsilon_{r_2}=1.0$

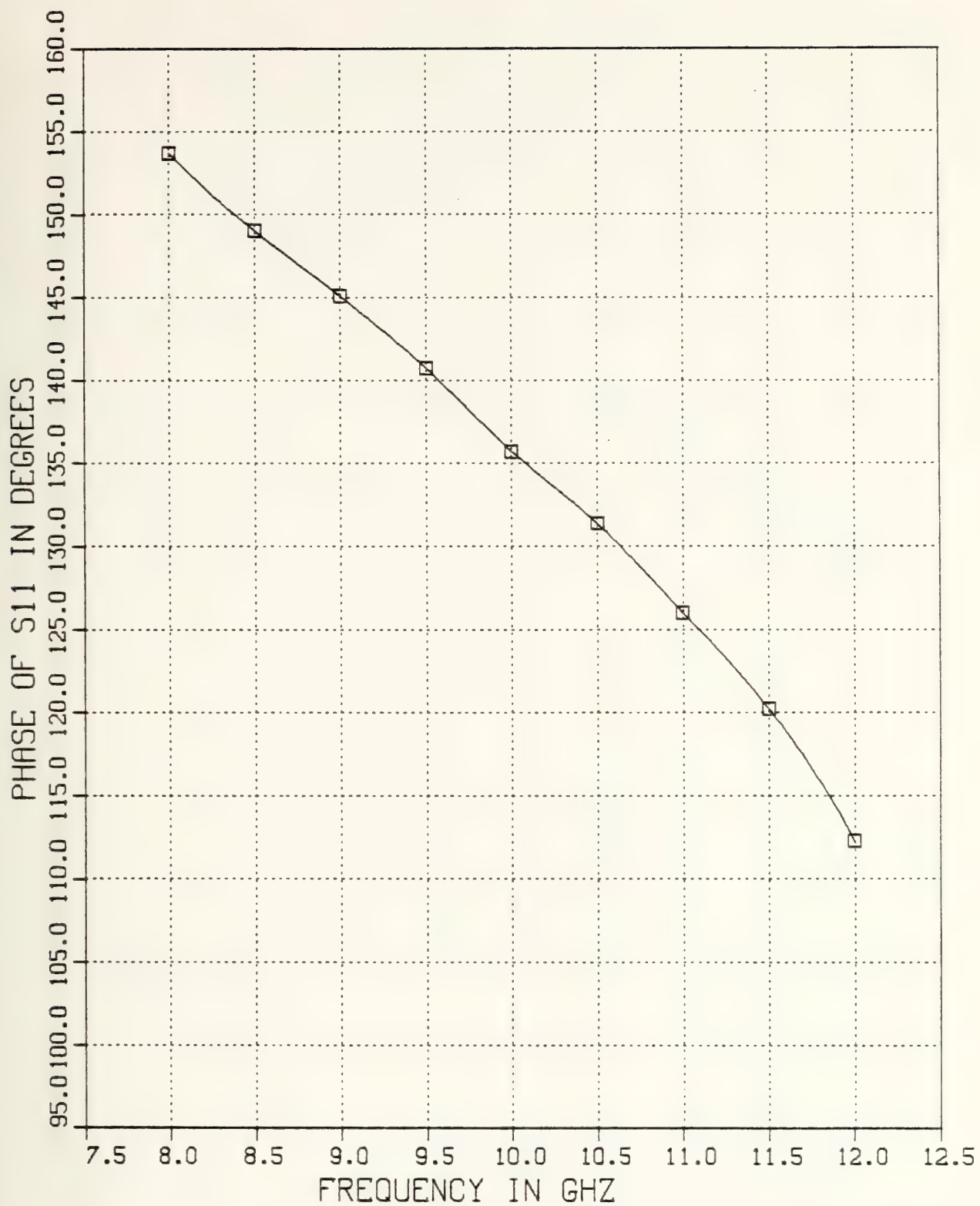


Figure F-44 θ_{11} v.s. Frequency for $T=0.5$ inch Inductive Strip,
 $w/b=.5$, and $\epsilon_{r_2}=1.0$

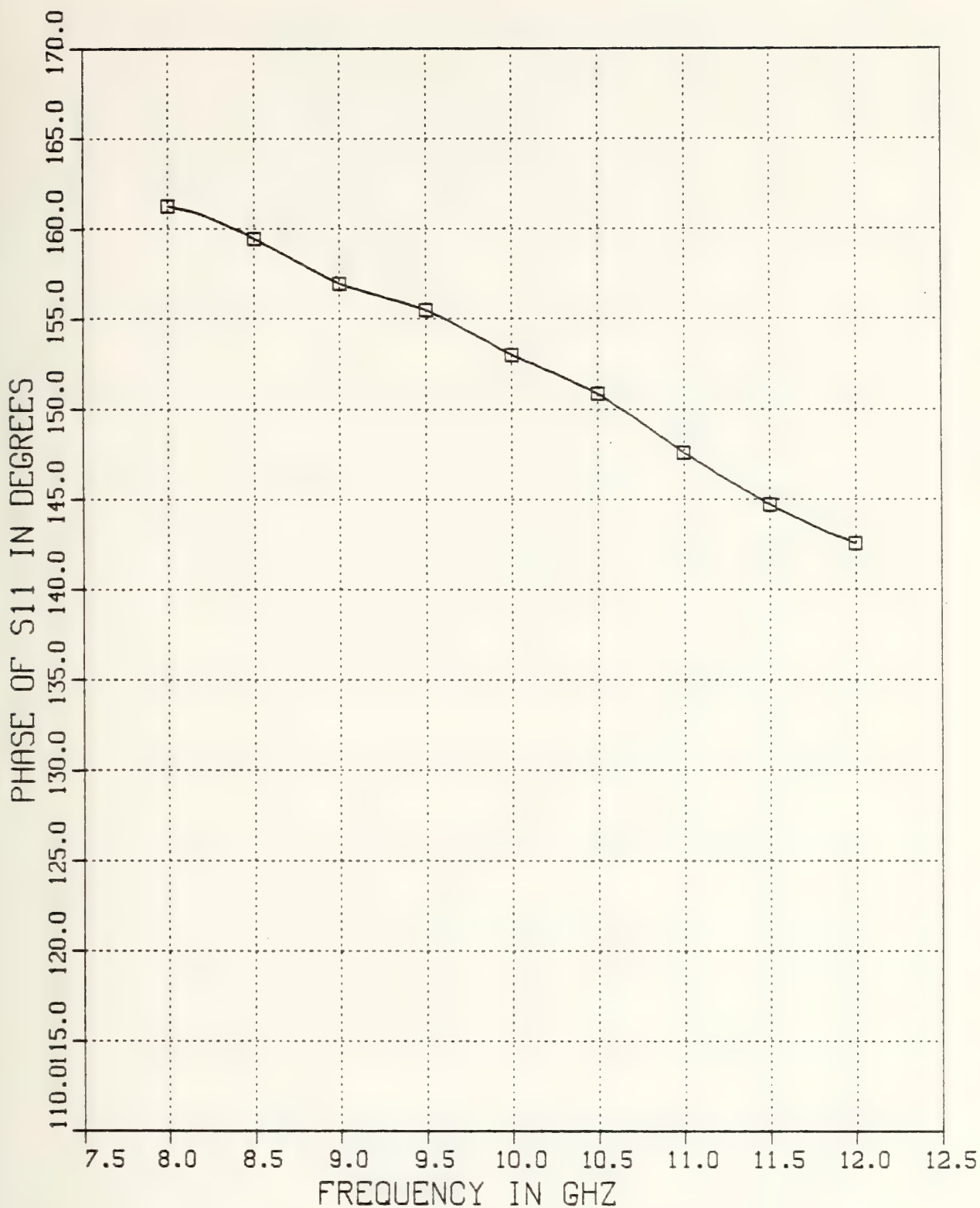


Figure F-45 θ_{11} v.s. Frequency for $T=.05$ inch Inductive Strip, $w/b=.25$, and $\epsilon_{r_2}=1.0$

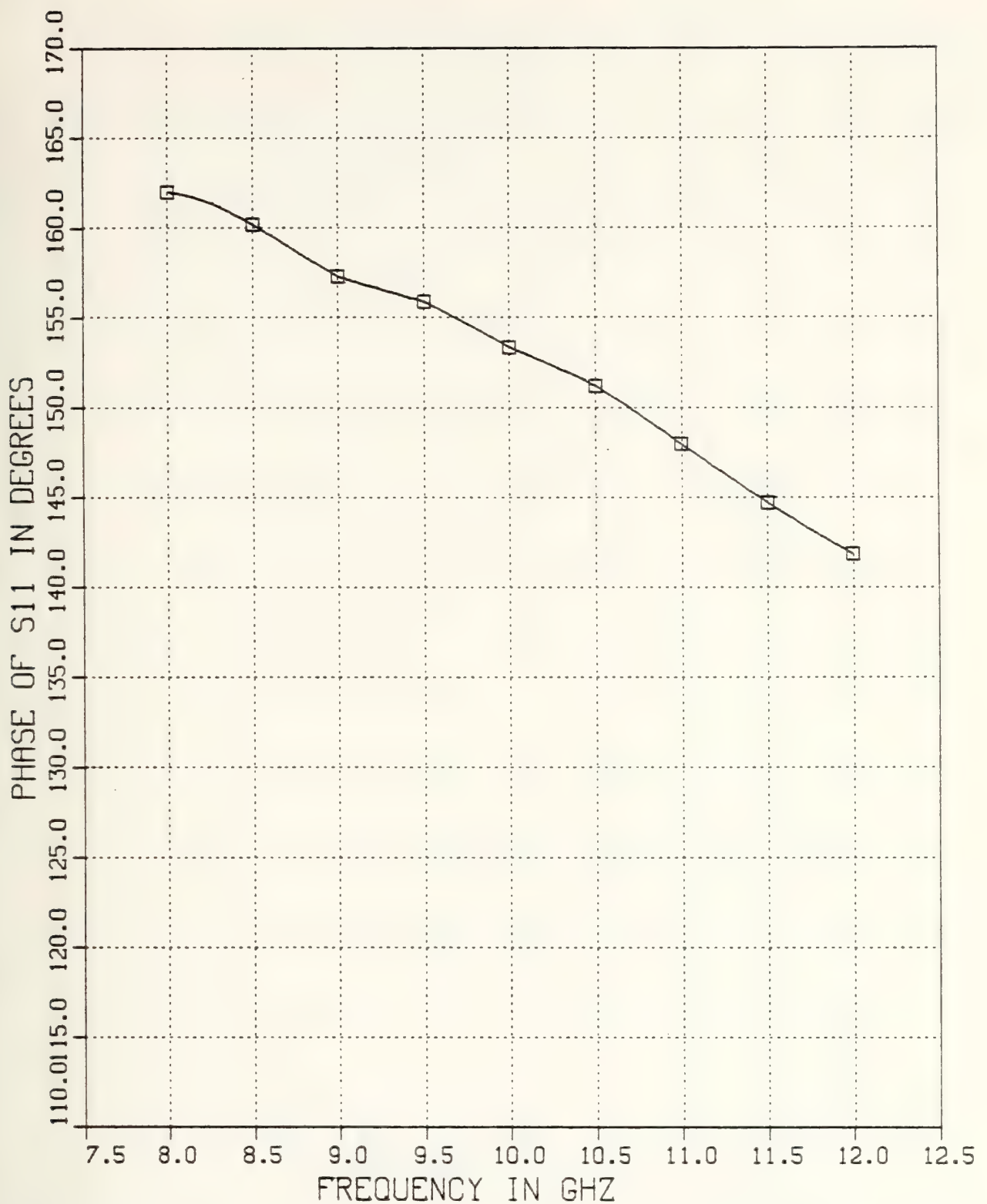


Figure F-46 θ_{11} v.s. Frequency for $T=0.1$ inch Inductive Strip, $w/b=.25$, and $\epsilon_{r_2}=1.0$

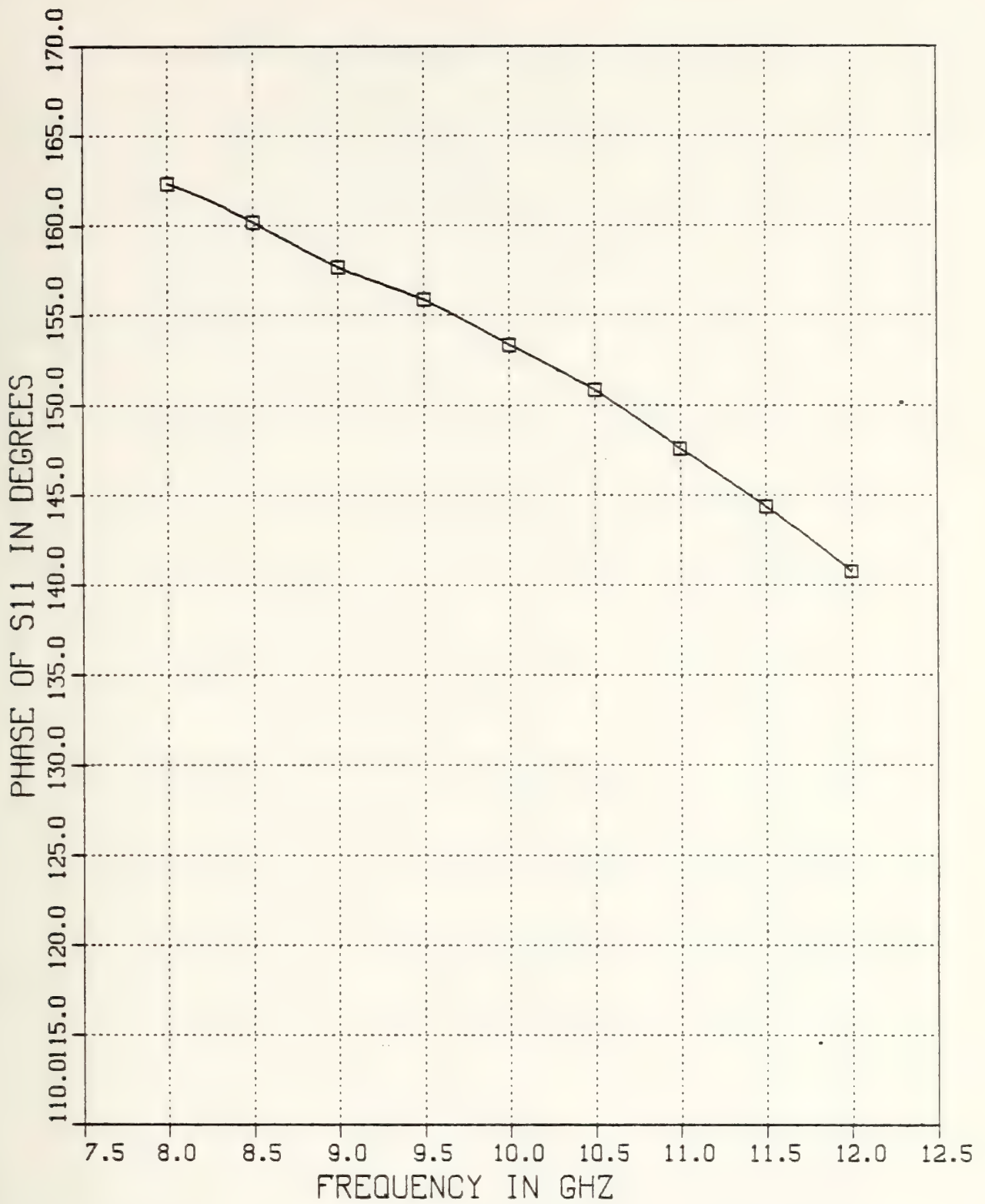


Figure F-47 θ_{11} v.s. Frequency for $T=0.2$ inch Inductive Strip,
 $w/b=.25$, and $\epsilon_{r2}=1.0$

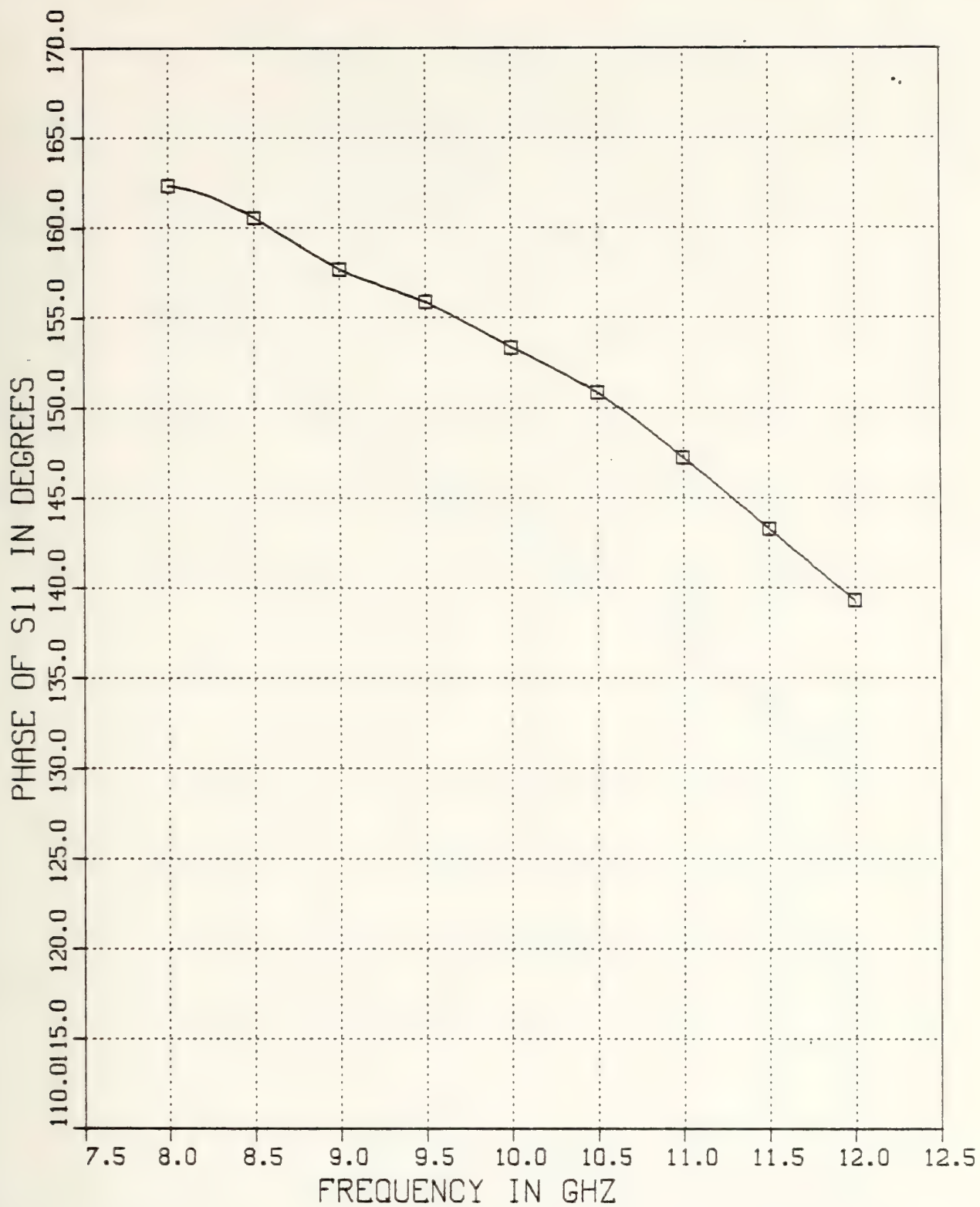


Figure F-48 θ_{11} v.s. Frequency for $T=0.5$ inch Inductive Strip,
 $w/b=.25$, and $\epsilon_{r_2}=1.0$

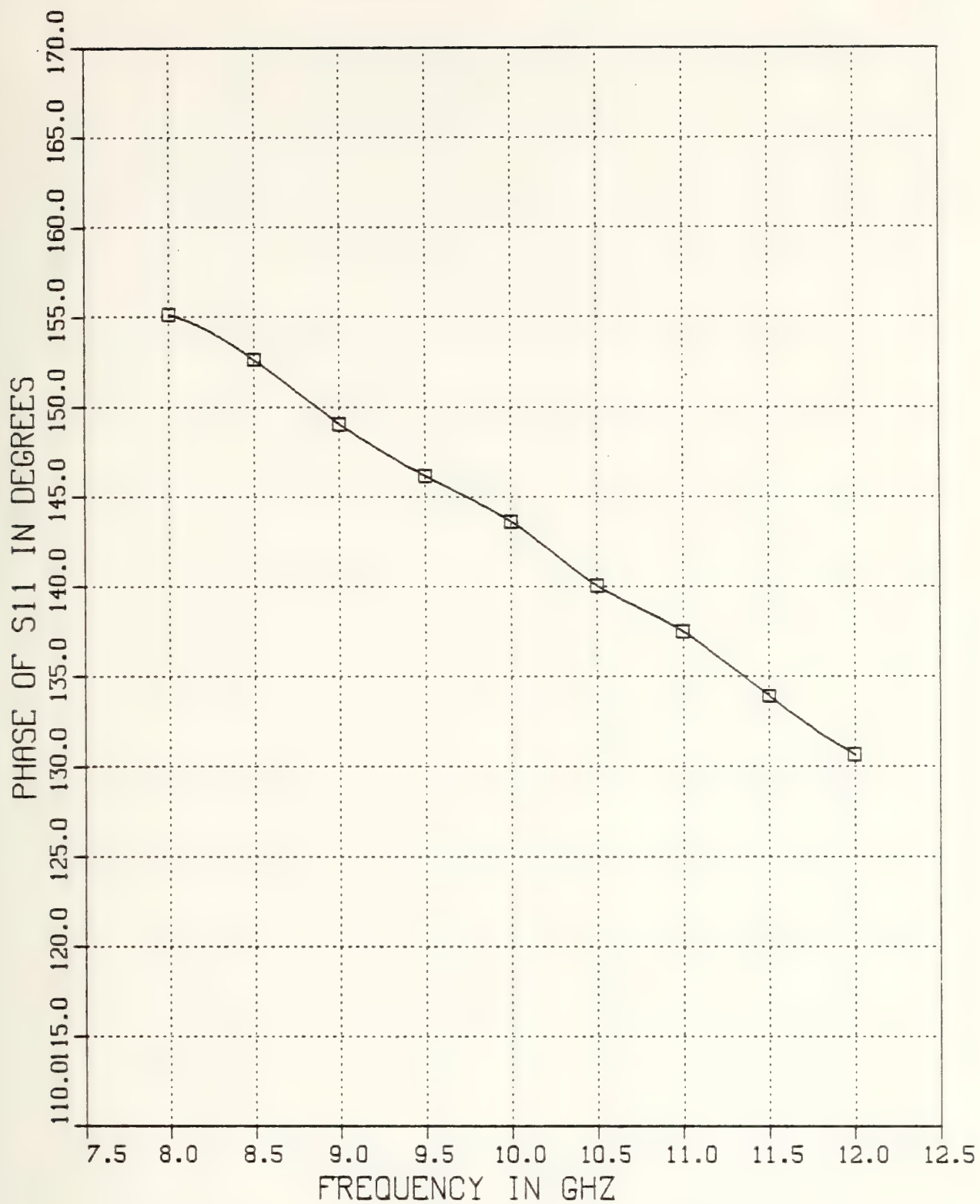


Figure F-49 θ_{11} v.s. Frequency for $T=.05$ inch Inductive Strip,
 $w/b=.2$, and $\epsilon_{r2}=1.0$

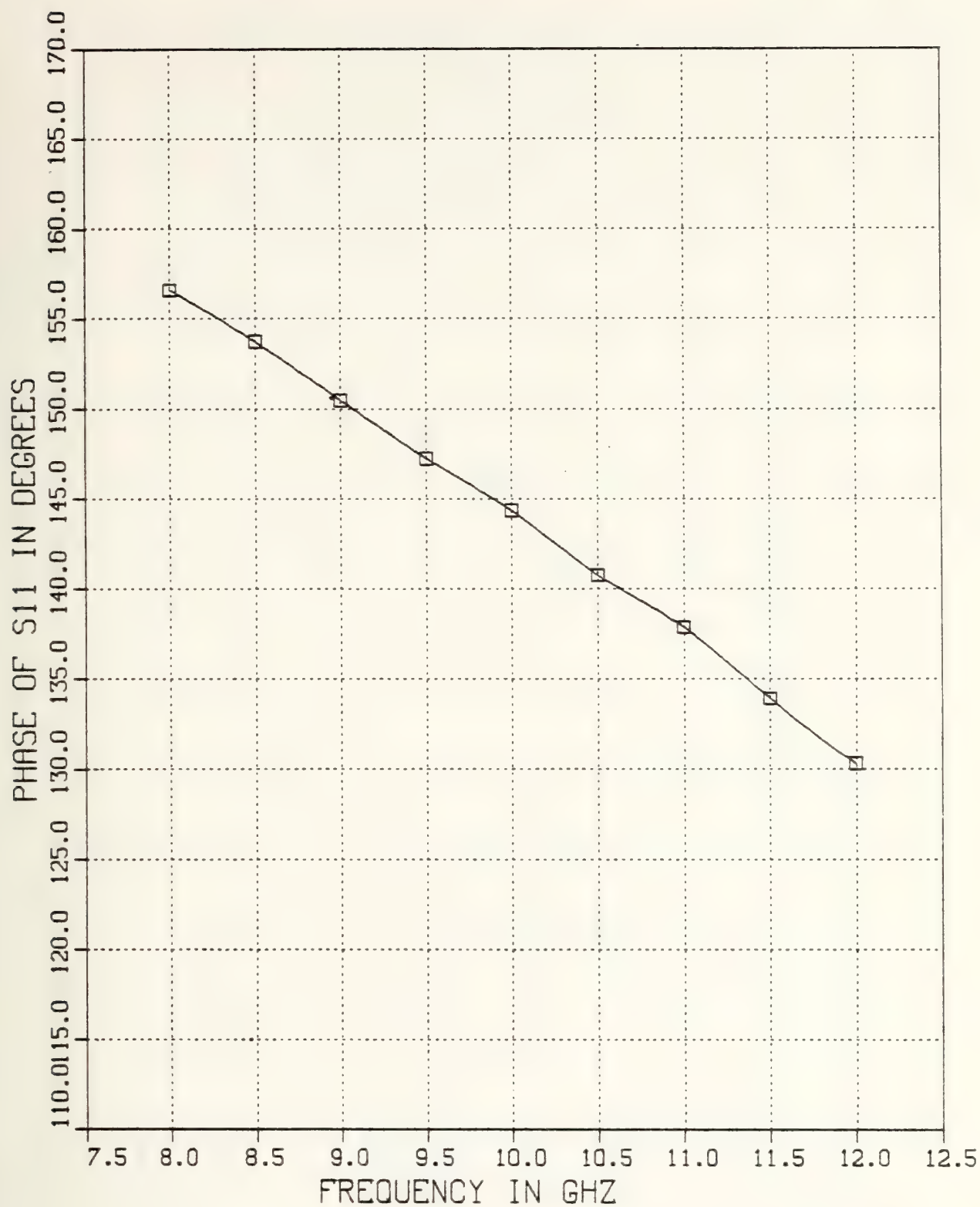


Figure F-50 θ_{11} v.s. Frequency for $T=0.1$ inch Inductive Strip,
 $w/b=.2$, and $\epsilon_{r_2}=1.0$

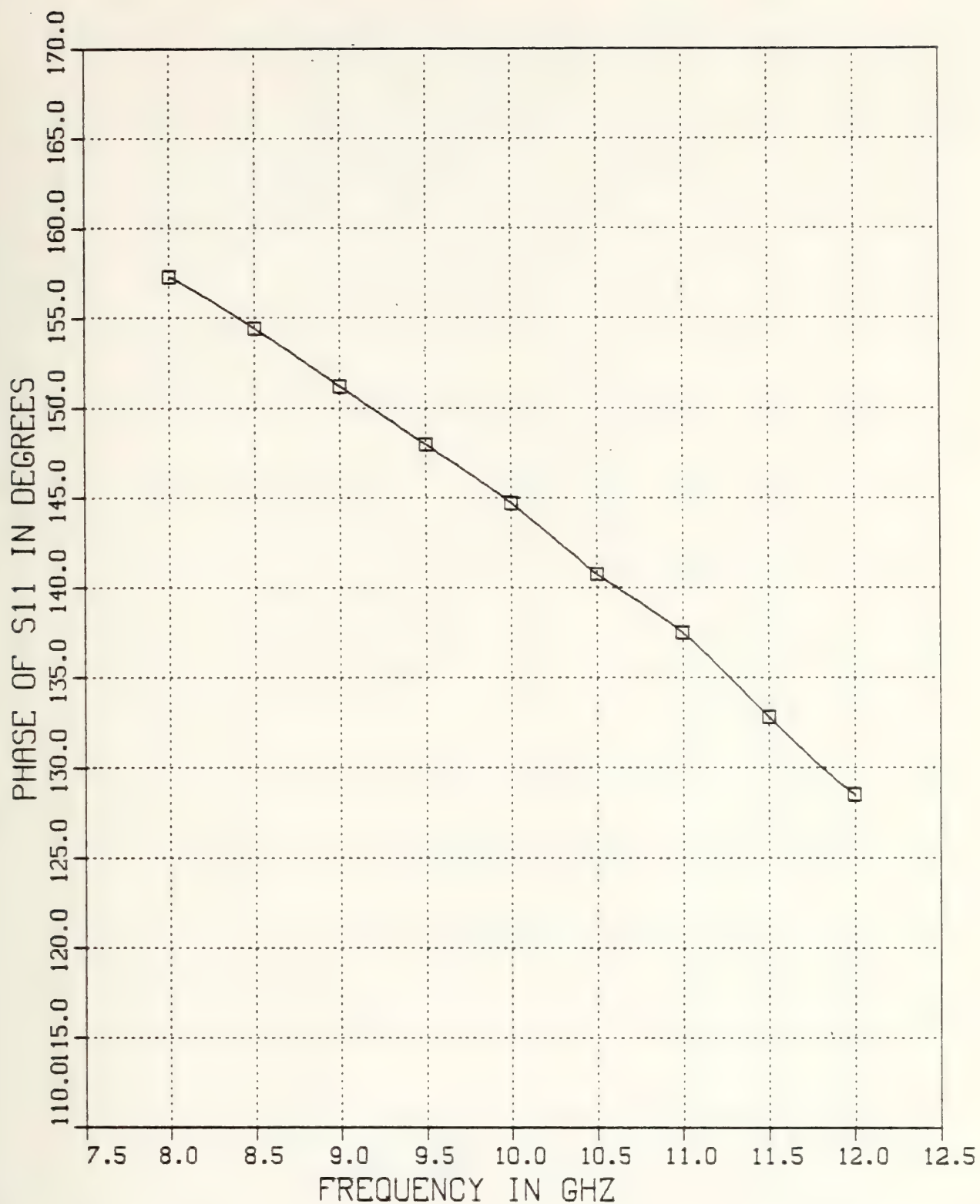


Figure F-51 θ_{11} v.s. Frequency for $T=0.2$ inch Inductive Strip, $w/b=.2$, and $\epsilon_{r_2}=1.0$

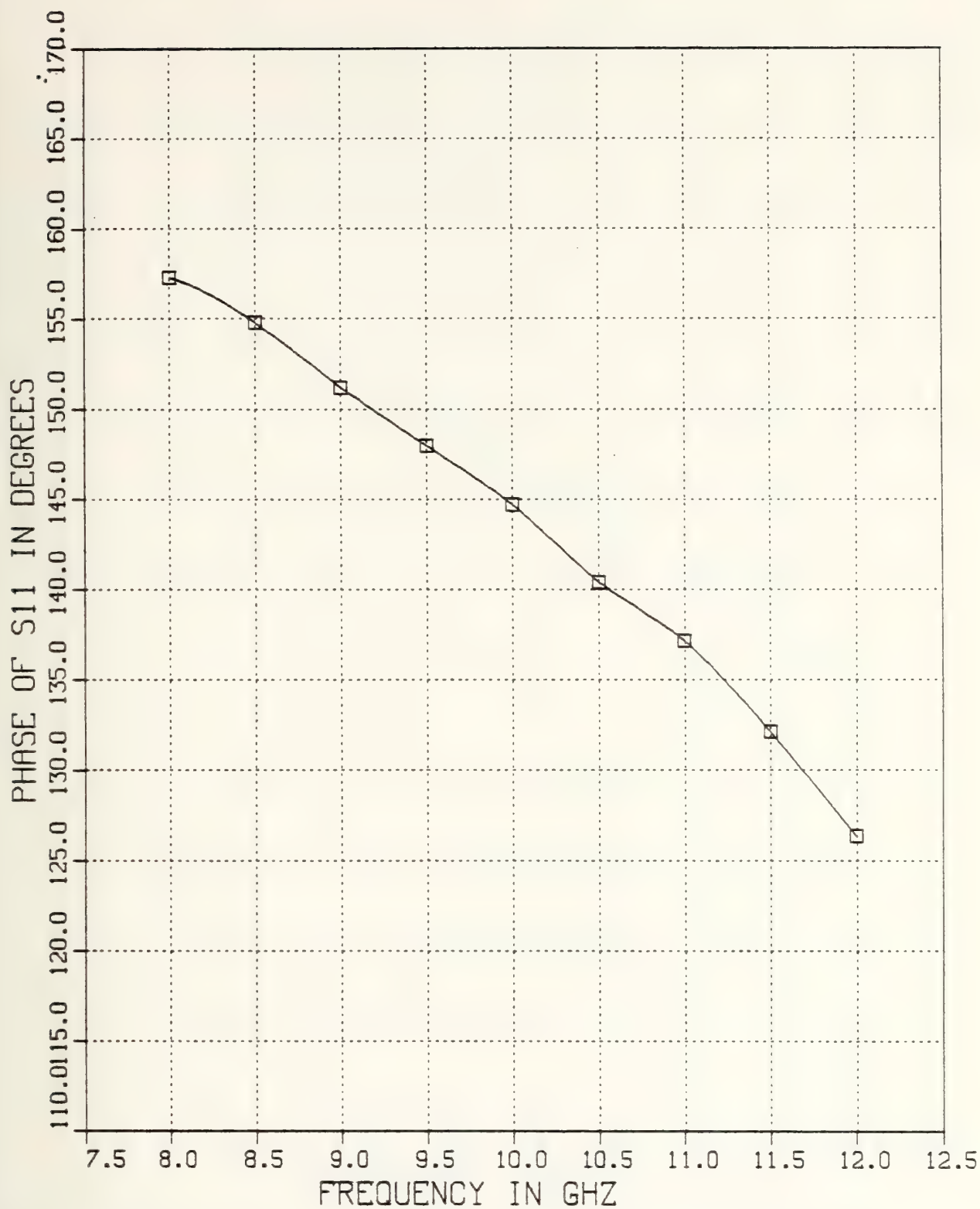


Figure F-52 θ_{11} v.s. Frequency for $T=0.5$ inch Inductive Strip,
 $w/b=.2$, and $\epsilon_{r_2}=1.0$

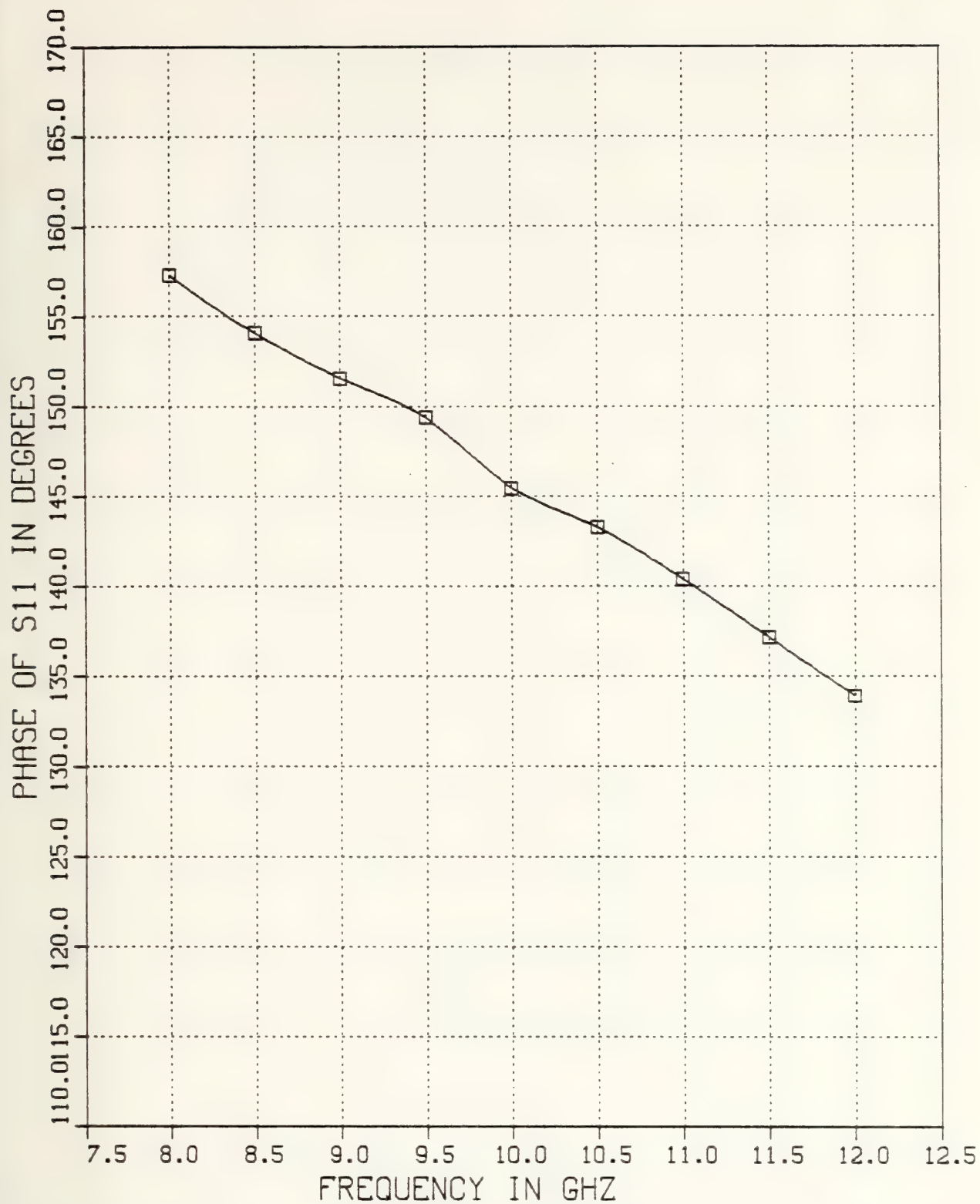


Figure F-53 θ_{11} v.s. Frequency for $T=.05$ inch Inductive Strip,
 $w/b=.1$, and $\epsilon_{r_b}=1.0$

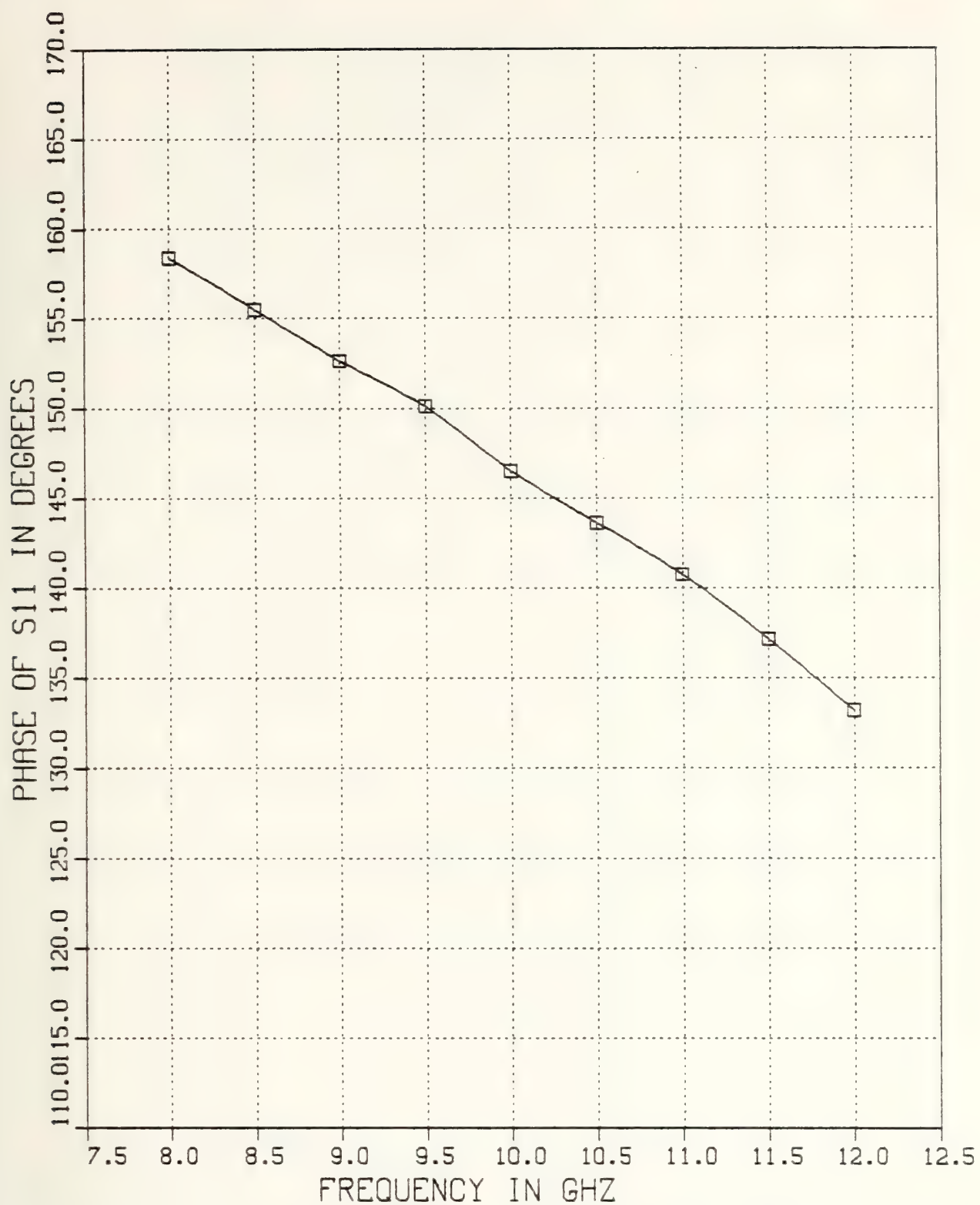


Figure F-54 θ_{11} v.s. Frequency for $T=0.1$ inch Inductive Strip,
 $w/b=.1$, and $\epsilon_{r2}=1.0$

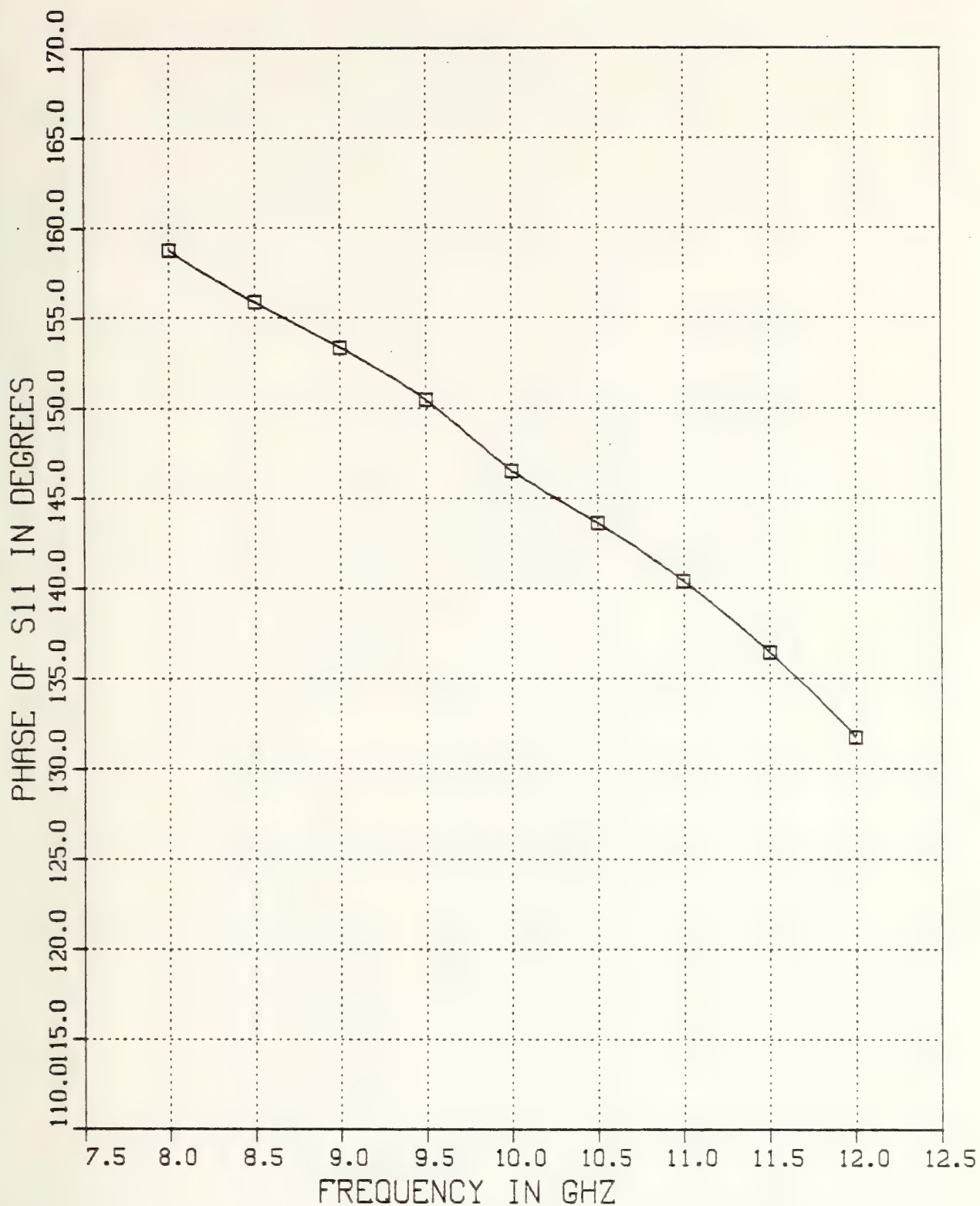


Figure F-55 θ_{11} v.s. Frequency for $T=0.2$ inch Inductive Strip,
 $w/b=.1$, and $\epsilon_{r2}=1.0$

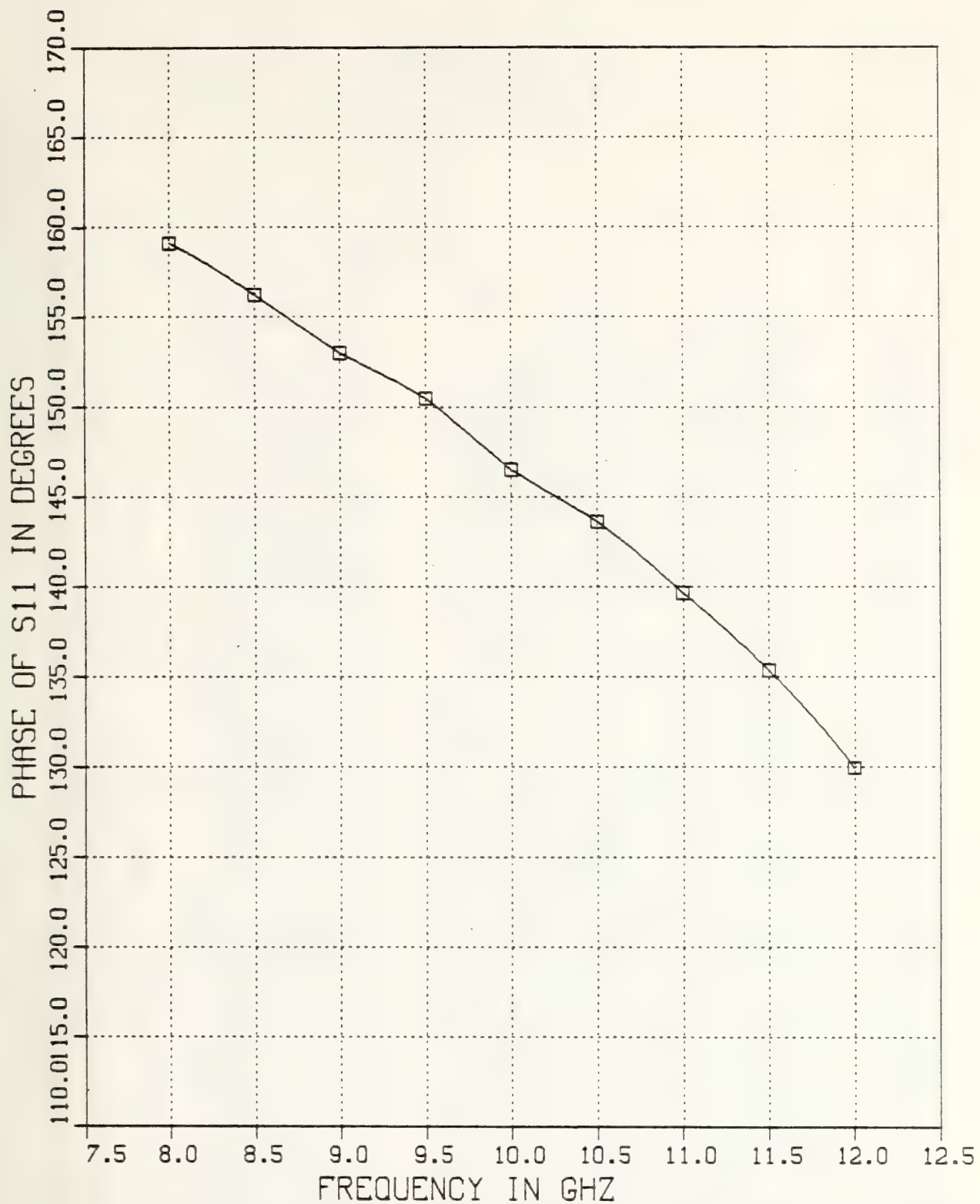


Figure F-56 θ_{11} v.s. Frequency for $T=.5$ inch Inductive Strip,
 $w/b=.1$, and $\epsilon_{r_2}=1.0$

APPENDIX G

FINCAV: PROGRAM LISTING FOR THE SINGLE RESONANT CAVITY

```

** ID,XREF,EXT
** *****
** FIN-LINE TRANSMISSION STRUCTURE
** *****
** SINGLE CAVITY RESONANCE LENGTH AND EQUIVALENT REACTANCE
** *****
**
** AUTHORS: PROF. JEFFERY B. KNORR AND CPT. JOHN C. DEAL
** DATE: 30 MARCH 1984
**
** THIS ROUTINE IS DESIGNED TO CALCULATE THE FIN-LINE GUIDE WAVE-
** LENGTH, RESONANT LENGTH OF A SINGLE RESONANT CAVITY, AND THE CORR-
** ESPONDING EQUIVALENT REACTANCE OF THE SHORTING SEPTUM (INDUCTIVE
** DISCONTINUITY). IT USES THIS ROUTINE, SELECT THE FIN-LINE GEOMETRIC
** PARAMETERS AND FREQUENCIES OF INTEREST AND LOAD THE DATA FILE AS
** SHOWN BELOW. SELECT THE NUMBER OF BASIS FUNCTIONS DESIRED BY SET-
** TING THE MATRIX ORDER EQUAL TO THE NUMBER OF BASIS FUNCTIONS. FOR
** MATICES LARGER THAN 10X10 (ORDER = 10), SET XCONST = 40.0 AND
** ZCONST = 1000.0, AT LEAST. CHANGE THE ARRAY DIMENSIONS OF LL AND LT
** AND THE ROWDIM VARIABLE IF THE ORDER IS SELECTED TO BE GREATER THAN
** 20.
**
** THE PROGRAM CONSISTS OF THREE NESTED
** ALGORITHMIC STRUCTURE 'DC' LOOPS WITH TWO
** EMBEDDED SEARCH ROUTINES AND SEVEN GAP WIDTHS OF INTERFERENCES. THE FIRST (OUTER)
** LOOP IS AN ITERATION OVER THE FIN GAP WIDTHS OF INTERFERENCES. THE FIRST (OUTER)
** SECOND (MIDDLE) LOOP IS AN ITERATION OVER THE FIN GAP WIDTHS OF INTERFERENCES. THE FIRST (OUTER)
** INTEREST, D/LAMBDA. WITHIN THIS LOOP IS A MODIFIED BISECTIONAL
** SEARCH FOR THE NORMALIZED GUIDE WAVELENGTH, LAMBDA PRIMS/LAMBDA,
** WHICH CAUSES THE INNER X-COMPONENT OF THE G11 DYADIC GREEN'S FUNCTION,
** AND THE SQUARE OF THE INNER X-COMPONENT OF THE THERD (INNER) LOOP WHICH
** TO GO TO ZERO. AFTER THIS SEARCH IS SEPTUM WIDTHS OF INTEREST, T/D.
** IS AN ITERATION OVER THE NORMALIZED SEPTUM WIDTHS OF INTEREST, T/D.
** A SIMPLIFIED BISECTIONAL SEARCH, L/LAMBDA PRODUCT TO FIND THE VALUE OF THE
** DETERMINANT OF A MATRIX CONSIST OF THE INNER PRODUCT OF THE
** THE ELEMENTS OF THIS MATRIX, THE SQUARE OF THE X-COMPONENT OF THE
** G11 DYADIC GREEN'S FUNCTION, THE SQUARE OF THE X-COMPONENT OF THE
** X-DIRECTED ELECTRIC FIELD, THE MTH Z-COMPONENT OF THE X-DIRECTED ELECTRIC
** FIELD. THEREFORE, WITHIN THIS SEARCH THE MATRIX OF X OF <M,N> INNER AND
** PRODUCT TERMS IS GENERATED FOR EACH ESTIMATE OF THE SOLUTION AND
** CORRESPONDINGLY EACH SEARCH ITERATION.
**
** INPUT PARAMETER DATA FILE
** THE INPUT DATA CONSISTS OF THE FIN-LINE GEOMETRIES, RELATIVE
** DIELECTRIC CONSTANTS, AND FREQUENCIES OF INTEREST IN NORMALIZED FILE
** FORM AS DESCRIBED IN THE VARIABLE DEFINITIONS. THE INPUT DATA FILE
** (FIELDS) IS FOUND AT THE END OF THE PROGRAM AND IS ORGANIZED AS
** FOLLOWS:

```



```

DIMENSION DOVLI(9)
DIMENSION WOVBI(8)
DIMENSION TOVDI(8)
COMMON/C1/EP SR1,EP SR2,EP SR3,H1OVD,H2OVD,BOVD
COMMON/C2/C2PI,C2PISQ,PI
COMMON/C3/DOVL,WQVB
COMMON/C4/TOVD
COMMON/C5/XCONST,ZCONST
SPECIFY L(M,N) ORDER AND ROW DIMENSION
ORDER = 3
C
ROWDIM = 20
SPECIFY LIMIT OF SUMMATION CONSTANTS FOR THE X AND Z FIELDS
XCONST = 22.0
ZCONST = 100.0
SPECIFY MIN AND MAX SEARCH INTERVAL LIMITS,(LEFT AND RIGHT)
XLMIN = 0.1
XRMAX = 0.5
SPECIFY SEARCH ACCURACY RESIDUE
ACCUR = 0.0001
C
READ INPUT DATA
READ(5,101)(DOVLI(I),I=1,7)
READ(5,102)(DOVLI(I),I=8,9)
READ(5,100) EP SR1,EP SR2,EP SR3
READ(5,100) H1OVD,H2OVD,BOVD
READ(5,100) WQVBI
READ(5,100) TOVDI
C
WRITE STRUCTURE PARAMETERS
WRITE(6,110)
WRITE(6,120) ORDER
WRITE(6,200) EP SR1,EP SR2,EP SR3
WRITE(6,300) H1OVD,H2OVD,BOVD
WRITE(6,400)
WRITE(6,100)
WRITE(6,100)
WRITE(6,100)
WRITE(6,499)
WRITE(6,100)
WRITE(6,100)
C
DEFINE CONSTANTS
PI = ARCCOS(-1.0)
C2PI = 6.283185307
C2PISQ = C2PI**2
SPECIFY FIN GEOMETRY
DO 12 IW=1,8
WQVB = WQVBI(IW)
WQVD = WQVB#BOVD
IF(WQVB.EQ.0.) GO TO 13
SPECIFY DO 11 ID=1,9

```



```

DCVL=DOVLI(10)
IF(DOVL.EQ.0.1) GO TO 12
WRITE(6,500) WOVB,WOVD,DOVL
C SEARCH FOR ZERO OF IPRD1
C REF: GOTTFREID, PROGRAMMING WITH FORTRAN IV, PG. 157
C SEARCH INTERVAL IS XL=.1 TO XR=3
XL=.1
XR=.3
EPSLN=.0013579
ITER=1
C CALCULATE INTERIOR POINTS
1 XL=XL+.5*(XR-XL-EPSLN)
C SUBROUTINE IPRD USES COMMON BLOCKS /C1/C2/C3/
CALL IPRD1(XL1,YL1)
CALL IPRD1(XR1,YR1)
IF(YL1*2-YR1*2) 2,5,3
C YR1*2 GREATER THAN YL1*2
2 XR=XR1
GO TO 4
C YL1*2 GREATER THAN YR1*2
3 XL=XL1
C TEST FOR END OF SEARCH
4 IF(ITER.GE.100) GO TO 6
ITER=ITER+1
IF(XR-XL.GT.3.*EPSLN) GO TO 1
C WRITE SOLUTION
LPROVL=.5*(XL1+XR1)
WRITE(6,600) LPROVL
GO TO 8
C WRITE OUTPUT - SEARCH FAILED TO CONVERGE
6 WRITE(6,610)
GO TO 11
C CONTINUE
C SEARCH FOR RESONANT LENGTH OF FINLINE CAVITY
CC 28 IT=1,8
TOVD=TOVD I(1T)
IF(TOVD.EQ.0.) GO TO 11
C SEARCH INTERVAL IS XLMIN TO XRMAX
XL = XLMIN
XR = XRMAX
EPSLN = .5*ABS(XL-XR)
DUM = 0.0
ITER=1
C CALCULATE INTERIOR POINTS
21 IF(.NOT.(EPSLN.LE.ACCUR).AND.(ITER.LT.100)) GO TO 22
C TEST FOR END OF SEARCH LINE 21 ABOVE
XEST = .5*(XL+XR)

```



```

C  CALCULATE L(M,N) MATRIX ELEMENTS:  L(M,N) * ALFA(N) = G(M)
DO 31 MTH = 1,ORDER
DO 32 NTH = MTH,ORDER
CALL IPROD2(MTH,NTH,LPROVL,XL,YLEL)
LL(MTH,NTH) = YLEL
IF(.NOT.(MTH.NE.NTH)) GO TO 33
LL(NTH,MTH) = LL(MTH,NTH)
CONTINUE
33 CALL IPROD2(MTH,NTH,LPROVL,XEST,YREL)
LR(MTH,NTH) = YREL
IF(.NOT.(MTH.NE.NTH)) GO TO 34
LR(NTH,MTH) = LR(MTH,NTH)
CONTINUE
34 CONTINUE
32 CONTINUE
31 DO 35 MTH = 1,ORDER
WRITE(6,130) (LL(MTH,NTH),NTH=1,ORDER)
CONTINUE
35 DO 36 MTH = 1,ORDER
WRITE(6,130) (LR(MTH,NTH),NTH=1,ORDER)
CONTINUE
36 CALCULATE THE DETERMINANT OF THE L(M,N) MATRIX:
CALL DTERM(ORDER,LL,DETL,RCWDIM)
YL = DETL
YR = DETR
DUM = YL*YR
IF(.NOT.(DUM.LT.0.0)) GO TO 23
XR = XEST
GO TO 24
CONTINUE
23 XL = XEST
CONTINUE
24 EPSLN = 5*ABS(XL-XR)
ITER = ITER+1
GO TO 21
CONTINUE
22 IF(.NOT.(ITER.LT.100)) GO TO 25
LRES = 5*(XL+XR)
X = TAN(C2PI*.5*(.5-LRES))
WRITE SOLUTION FOR SHORT CIRCUIT REACTANCE
WRITE(6,800) TOVD,LRES,X
GO TO 26
CONTINUE
25 WRITE OUTPUT - SEARCH FAILED TO CONVERGE
WRITE(6,805) TOVD
CONTINUE
26 CONTINUE
28

```



```

REAL LPROVL
COMMON/C1/EP SR1,EP SR2,EP SR3,H1OVD,H2OVD,BOVC
COMMON/C2/C2PI,C2PISQ,P1
COMMON/C3/DOVL,W0VB
COMMON/C5/XCONST,ZCONST
BETAD = C2PI*DOVL/LPROVL
BOVW = 1./W0VB
SPECIFY LIMIT FOR SUMMATION ON N
IF(W0VB.EQ.1.) MMA X=1
IF(W0VB.LT.1.) MMA X=INT((XCONST*BOVW)/C2PI)
IF(MMAX.GT.40) MMA X=40
SUM1 = 0.0
DO 11 M=1,MMAX
N=M-1
ALFD=N*C2PI/BOVD
CALL GRN11(ALFD,BETAD,DOVL,G11)
CALL EXSQ1(ALFD,W0VB,BOVD,EXXSQ)
SUM1=SUM1+2.*G11*EXXSQ
IF(N.EQ.0) SUM1=G11
11 CONTINUE
RETURN
END
SUBROUTINE IPKOD2(MTH,NTH,LPROVL,LRES,SUM2)
*****
***** THIS SUBROUTINE IS DESIGNED TO CALCULATE THE INNER PRODUCT OF
***** THE GL1 DYADIC GREEN'S FUNCTION, THE FOURIER TRANSFORM OF THE MTH
***** Z-COMPONENT OF THE X-DIRECTED ELECTRIC FIELD, AND THE FOURIER
***** TRANSFORM OF THE X-DIRECTED ELECTRIC FIELD.
*****
***** VARIABLE DEFINITIONS*****
***** EXXSQ = SQUARE OF THE FOURIER TRANSFORM OF THE X-COMPONENT OF THE
***** G11 = THE GL1 DYADIC GREEN'S FUNCTION
***** EXZM = THE FOURIER TRANSFORM OF THE MTH Z-COMPONENT OF THE
***** EXZN = THE FOURIER TRANSFORM OF THE NTH Z-COMPONENT OF THE
***** MTH = ROW INDEX
***** NTH = COLUMN INDEX
***** NMAX = THE LIMIT OF SUMMATION OVER ALFD
***** KMAX = THE LIMIT OF SUMMATION OVER ZETAD
***** SUM2 = THE RETURNED VALUE OF THE INNER
***** VARIABLE DECLARATION*****
REAL LPROVL,LRES,L0VD
COMMON/C1/EP SR1,EP SR2,EP SR3,H1OVD,H2OVD,BOVD
COMMON/C2/C2PI,C2PISQ,P1
COMMON/C3/DOVL,W0VB

```



```

COMMON/C4/TOVD
COMMON/C5/XCONST,ZCONST
LOVD=LRES*LPROVL/DOVL
TOVL=TCVD/LOVD
BOVW = 1./WOVB
SPECIFY LIMIT FOR SUMMATION ON N
IF(WOVB.EQ.1.) NMAX=0
IF(WOVB.LT.1.) NMAX=INT((XCONST*BOVW)/C2PI)
IF(NMAX.GT.40) NMAX=40
SPECIFY LIMIT FOR SUMMATION ON K
CONST = ZCONST
RMN = AMAX(MTH,NTH)
KMAX=INT(1.5 + (1.+TOVL)*SQRT(CONST+((2.*RMN-1.)/2.)*2))
SUM2=0.0
N=0
DO 10 K=1,KMAX
ALFD=N*C2PI/BOVD
ZETAC=((K-.5)*C2PI)/((1.+TOVL)*LOVD)
BETAC=ZETAD
CALL GRN11(ALFD,BETAD,DOVL,G11)
CALL EXSQ1(ALFD,WOVB,BOVD,EXXSQ)
CALL EXZ(MTH,ZETAD,LRES,LPROVL,EXZFM)
EXZM = EXZFM
CALL EXZ(MTH,ZETAD,LRES,LPROVL,EXZFN)
EXZN = EXZFN
SUM2=SUM2+2.*G11*EXXSQ*EXZM*EXZN
10 CONTINUE
IF(NMAX.EQ.0) GO TO 14
DO 13 N=1,NMAX
12 K=1,KMAX
ALFD=N*C2PI/BOVD
ZETAD=((K-.5)*C2PI)/((1.+TOVL)*LOVD)
BETAD=ZETAD
CALL GRN11(ALFD,BETAD,DOVL,G11)
CALL EXSQ1(ALFD,WOVB,BOVD,EXXSQ)
CALL EXZ(MTH,ZETAD,LRES,LPROVL,EXZFM)
EXZM = EXZFM
CALL EXZ(MTH,ZETAD,LRES,LPROVL,EXZFN)
EXZN = EXZFN
SUM2=SUM2+4.*G11*EXXSQ*EXZM*EXZN
12 CONTINUE
13 CONTINUE
14 RETURN
END
C SUBR
$EJECT
SUBROUTINE GRN11(ALFD,BETAD,DOVL,G11)

```



```

C** THIS SUBROUTINE IS DESIGNED TO CALCULATE THE G11 DYADIC GREEN'S
C** FUNCTION
C** VARIABLE DEFINITIONS**S FUNCTION, RETURNED VALUE
C** G11 = THE G11 DYADIC GREEN'S FUNCTION, RETURNED VALUE
C**
C** G1DSQ
C** G2DSQ
C** G3DSQ
C** KC1DSQ
C** KC2DSQ
C** KC3DSQ
C** WEPS1D
C** WEPS2D
C** WEPS3D
C** WMUD
C**
C** VARIABLE DECLARATION**H10VD, H20VD, BOVD
C** COMMON/C1/EP SR1, EP SR2, EP SR3, H10VD, H20VD, BOVD
C** COMMON/C2/C2PI, C2PISQ, PI
C** REAL KC1DSQ, KC2DSQ, KC3DSQ, LPROVL, LOVLPR
C** CALCULATE VARIABLES DEPENDENT ON FREQUENCY
C** WMUD=60.*C2PISQ*DOVL
C** WEPS1D=EP SR1*DOVL/60.
C** WEPS2D=EP SR2*DOVL/60.
C** WEPS3D=EP SR3*DOVL/60.
C** CALCULATE VARIABLES DEPENDENT ON FRRQUENCY AND BETAD
C** BETADSQ=BETAD**2
C** KC1DSQ=C2PISQ*EP SR1*DOVL**2-BETADSQ
C** KC2DSQ=C2PISQ*EP SR2*DOVL**2-BETADSQ
C** KC3DSQ=C2PISQ*EP SR3*DOVL**2-BETADSQ
C** CALCULATE VARIABLES DEPENDENT ON FREQUENCY, BETAD AND ALFD
C** ALFDSQ=ALFD**2
C** G1DSQ=ALFDSQ-KC1DSQ
C** G2DSQ=ALFDSQ-KC2DSQ
C** G3DSQ=ALFDSQ-KC3DSQ
C** CALL TFN(G1DSQ, H10VD, TFN1)
C** CALL TFN(G2DSQ, 1., TFN2)
C** CALL TFN(G3DSQ, H20VD, TFN3)
C** D11=-KC2DSQ*(1.+(WEPS3D*G3DSQ*KC2DSQ*TFN2)/(WEPS2D*G2DSQ*KC3DSQ*
C** 1TFN3))
C** D12=((ALFD*BETAD)/(WEPS2D*G2DSQ))*((KC2DSQ/KC1DSQ)-1.)*KC2DSQ
C** D21=-ALFD*BETAD*((KC2DSQ/KC1DSQ)+(WEPS3D*KC2DSQ*G3DSQ*TFN2)/
C** 1(WEPS2D*KC3DSQ*G2DSQ*TFN3))
C** D22=WMUD*(1.+(KC2DSQ*TFN3)/(KC3DSQ*TFN2))+((ALFDSQ*BETADSQ)/(G2DSQ
C** 1*WMUD*WEPS2D))*((KC2DSQ/KC3DSQ)-1.)
C** DET=D11*U22-D21*D12
C** CALCULATE G11
C** G11A=-KC1DSQ/(WMUD*TFN1)
C** G11B=- (KC2DSQ*D12*ALFD*BETAD*KC2DSQ*TFN2)/(DET*WMUD*G2DSQ*KC3DSQ)

```



```

$EJECT SUBROUTINE EXZ (MNT H,ZETAD,LRES,LPROVL,EXZFMN)
C***** THIS SUBROUTINE IS DESIGNED TO CALCULATE THE FOURIER TRANSFORM
C OF THE Z-COMPONENT OF THE X-DIRECTED ELECTRIC FIELD.
C***** VARIABLE DEFINITION*****
C EXZFMN = THE FOURIER TRANSFORM OF THE MNTH Z-COMPONENT OF THE
C X-DIRECTED ELECTRIC FIELD, THE RETURNED VALUE.
C MNTH = ROW OR COLUMN INDEX
C***** VARIABLE DECLARATION*****
COMMON/C2/C2PI,C2PISQ,PI
REAL LRES,LPROVL,LOVD,NUMBER,DENOM,DIM
LOVD=LRES*LPROVL/DOVL
THETA=ZETAD*.5*LOVD
ATHETA=ABS(THETA)
DIM=FLOAT(MNTH)
RESID=ABS(ATHETA)-((2.*DIM-1.)*PI/2.)
SIGN=(-1.0)**MNTH
NUMBER=COS(ATHETA)
DENOM=((THETA)**2)-(((2.*DIM)-1.)*PI/2.)**2)
IF(.NOT.(RESID.LT.0.000001)) GO TO 35
EXZFMN=1./PI
GO TO 36
35 CONTINUE
EXZFMN=(SIGN)**((2.*DIM)-1.0)**(NUMBER/DENOM)
36 CONTINUE
RETURN
END

```

```

C***** IDENTIFICATION: DETERMINANT OF A REAL MATRIX
C TITLE: DETERMINANTS
C CATEGORY: JEAN BOW
C PROGRAMMER: FEBRUARY 1965, CONVERTED TO SYSTEM/360, JANUARY 1967
C DATE: UPDATED BY P.J. COLLINS JANUARY 1984
C*****
B. PURPOSE: SUBROUTINE COMPUTES THE DETERMINANT OF A MATRIX OF REAL
NUMBERS BY GAUSS' METHOD OF ELIMINATION WITH ROW PIVOTING.
C. USAGE:
1. CALLING SEQUENCE:
CALL DTERM(N,A,DET,M)
2. PARAMETERS:
N - ORDER OF MATRIX A. (INTEGER)
A - MATRIX, THE DETERMINANT OF WHICH IS TO BE COMPUTED. (REAL*8)
DET - DETERMINANT OF MATRIX A. (REAL*8)
M - ROW DIMENSION OF MATRIX A. (THE INTEGER APPEARING IN USER'S
DIMENSION STATEMENT.)
C*****

```


APPENDIX H

FINSTRP: PROGRAM LISTING FOR THE COUPLED RESONANT CAVITIES

```

$JOB *****
ID,XREF,EXT *****
*****
FIN-STRIP *****
*****
ODD AND EVEN MODE RESONANT LENGTHS OF TWO UNILATERALLY
COUPLED CAVITIES AND EQUIVALENT CIRCUIT REACTANCES AND
SCATTERING PARAMETERS FOR THE INDUCTIVE POST, (STRIP).
*****
AUTHORS: PROF. JEFFERY B. KNORR AND CPT. JOHN C. DEAL
DATE: 30 MARCH 1984
*****
THIS ROUTINE IS DESIGNED TO CALCULATE THE FIN-LINE GUIDE WAVE-
LENGTH, THE ODD AND EVEN MODE RESONANT LENGTHS OF TWO UNILATERALLY
COUPLED FIN-LINE RESONANT CAVITIES AND THE CORRESPONDING AND THE
CIRCUIT REACTANCES OF THE INDUCTIVE STRIP AS FUNCTIONS OF THE
SCATTERING PARAMETERS OF THE INDUCTIVE STRIP AS A LOSS
ODD AND EVEN MODE NETWORK. TO USE THIS ROUTINE, SELECT THE FINLINE
GEOMETRIC PARAMETERS AND THE FREQUENCIES OF INTEREST AND LOAD THE
DATA FILE AS SHOWN BELOW. SELECT THE NUMBER OF BASIS FUNCTIONS
DESIRED BY SETTING THE MATRIX DIMENSION OF LRE, LLE, LRO, AND LLO
FUNCTIONS. CHANGE THE ARRAY DIMENSION IS SELECTED TO BE GREATER THAN
AND THE ROUTINE WILL OBTAIN THE ODD AND EVEN MODE RESONANT LENGTHS AND SCATTERING
20. TO OBTAIN THE SCATTERING PARAMETERS AND ASSOCIATED AS
COMMENT OUT THE SCATTERING PARAMETERS AND ASSOCIATED AS
WRITE AND FORMAT THE STATEMENTS. TO OBTAIN THE SCATTERING PARAMETERS AS
OUTPUT, COMMENT OUT THE EQUIVALENT CIRCUIT REACTANCE CALCULATIONS
AND ASSOCIATED WRITE AND FORMAT STATEMENTS.
*****
ALGORITHMIC STRUCTURE
*****
THE PROGRAM CONSISTS OF THREE NESTED 'DO' LOOPS WITH TWO
EMBEDDED SEARCH ROUTINES AND SEVEN SUBROUTINES. THE FIRST (OUTER)
LOOP IS AN ITERATION OVER THE FIN GAP WIDTHS OF INTEREST, W/B. THE
SECOND (MIDDLE) LOOP IS AN ITERATION OVER THE FREQUENCIES OF
INTEREST, D/LAMBDA. WITHIN THIS LOOP IS A MODIFIED BISECTIONAL
SEARCH FOR THE INNER GUIDE WAVELENGTH, LAMBDA GREEN'S FUNCTION
WHICH CAUSES THE INNER PRODUCT OF THE X-DIRECTED ELECTRIC FIELD
AND THE SQUARE OF THE X-COMPONENT IS THE THIRD (INNER) LOOP WHICH
IS AN ITERATION OVER THE SEARCHED SEPTUM WIDTHS OF INTEREST, D.
TO GO TO ZERO. AFTER THE SEARCH IS NORMALIZED SUCCESSFULLY FOR THE ODD CASES
WITHIN THE RESONANT LENGTHS, TWO SUCCESSIVE FIND THE VALUE OF THE EVEN/
ODD MODE BISECTIONAL SEARCH IS USED TO FIND THE VALUE OF THE EVEN/
A SIMPLE BISECTIONAL SEARCH IS USED TO FIND THE VALUE OF THE EVEN/
ODD NORMALIZED REACTANCE LENGTH, LEO/LAMBDA CT PRIME, WHICH CAUSES THE
DETERMINANT OF A MATRIX OF THE INNER PRODUCT OF THE
THE ELEMENTS OF THIS MATRIX, THE SQUARE OF THE X-COMPONENT OF THE
GIL DIRECTED ELECTRIC FIELD, THE MTH Z-COMPONENT OF THE X-DIRECTED

```



```

ELECTRIC FIELD, THE NTH Z-COMPONENT OF THE X-DIRECTED ELECTRIC, AND
THE MTH AND NTH SPATIAL SHIFT FUNCTIONS FOR THE Z-COMPONENT FUNCT-
IONS. THEREFORE, WITHIN THIS SEARCH THE MATRIX OF <M,N> INNER
PRODUCT TERMS IS GENERATED FOR EACH ESTIMATE OF THE SOLUTION AND
CORRESPONDINGLY EACH SEARCH ITERATION. THE EQUIVALENT CIRCUIT REACT-
ANCES AND SCATTERING PARAMETERS ARE THEN CALCULATED FROM THE EVEN
ODD MODE RESONANT LENGTHS.

      INPUT PARAMETER DATA FILE
      THE INPUT DATA CONSISTS OF THE FIN-LINE GEOMETRIES, RELATIVE
      DIELECTRIC CONSTANTS, AND FREQUENCIES OF INTEREST IN NORMALIZED FILE
      FORM AS DESCRIBED IN THE VARIABLE DEFINITIONS. THE INPUT DATA FILE
      (FIELDS) IS FOUND AT THE END OF THE PROGRAM AND IS ORGANIZED AS
      FOLLOWS:

      INPUT DATA FILE

      D/LAMBDA      NORMALIZED FREQUENCIES
      D/LAMBDA      NORMALIZED FREQUENCIES
      EPSR1,2,3     RELATIVE DIELECTRIC CONSTANTS FOR REGIONS 1,2,3
      H1/D, H2/D, B/D  NORMALIZED FIN POSITION COORDS AND WG HEIGHT
      W/B           NORMALIZED FIN GAP WIDTHS
      T/D           NORMALIZED SEPTUM WIDTHS

      HERE W = FIN GAP WIDTH
            B = HEIGHT OF RECTANGULAR WAVEGUIDE
            D = DIELECTRIC THICKNESS
            LAMBDA = FREE SPACE WAVELENGTH
            T = WIDTH OF THE INDUCTIVE STRIP (SEPTUM)

      ***VARIABLE DEFINITIONS***
      ACCUR = ACCURACY OF THE RESULTING NUMERICAL DETERMINATION OF THE
              ODD AND EVEN MODE RESONANT LENGTHS
      ALFD = NORMALIZED 'X' TRANSFORM VARIABLE
      BETA D = NORMALIZED HEIGHT/D
      BOVD = WAVEGUIDE HEIGHT/D
      DOVL = D/FREE SPACE WAVELENGTH
      EPSR1,2,3 = RELATIVE DIELECTRIC CONSTANTS FO REGIONS 1,2,3 RESP.
      H1/D = FIN POSITION COORDINATE/D
      H2/D = FIN POSITION COORDINATE/D
      LLE = MATRIX OF INNER PRODUCT TERMS FOR THE LEFT EST OF LERES
      LRE = MATRIX OF INNER PRODUCT TERMS FOR THE LEFT EST OF LERES
      LRO = MATRIX OF INNER PRODUCT TERMS FOR THE RIGHT EST OF LERES
      LROVD = RESONANT LENGTH/D
      LPOVL = RESONANT WAVELENGTH/
      LPOVL = EST OF THE EVEN MODE RESONANCE LENGTH/GUIDE WAVELENGTH

```



```

C READ INPLT DATA
  READ(5,101)(DOVLI(I),I=1,7)
  READ(5,102)(DOVLI(I),I=8,9)
  READ(5,100) EPSR1, EPSR2, EPSR3
  READ(5,100) H1QVD, H2QVD, BOVD
  READ(5,100) WOVBI
  READ(5,100) TOVDI
C WRITE STRUCTURE PARAMETERS
  WRITE(6,110) ORDER
  WRITE(6,120) EPSR1, EPSR2, EPSR3
  WRITE(6,200) H1QVD, H2QVD, BOVD
  WRITE(6,300)
  WRITE(6,400)
  WRITE(6,100)
  WRITE(6,100)
  WRITE(6,100)
  WRITE(6,489)
  WRITE(6,100)
C DEFINE CONSTANTS
  PI = DARCOS(-1.000)
  C2PI = 6.283185307
  C2PI*2
C SPECIFY FIN GEOMETRY
  DO 12 IW=1,8
    WOVBI=WOVBI(IW)
    WOV=WOVB*8QVD
    IF(WCVB.EQ.0.) GO TO 13
  SPECIFY 11 ID = 1,9
    DOVL = DOVLI(ID)
    IF(DOVL.EQ.0.) GO TO 12
    WRITE(6,500) WOVBI, WOV, DOVL
  SEARCH FOR ZERO OF IPRDI
  REF: GOTTFREID, PROGRAMMING WITH FORTRAN IV, PG. 157
C SEARCH INTERVAL IS XL=.1 TO XR=3
  XL=.1
  XR=.3
  EPSLN = 1.3579D-3
  ITER=1
C CALCULATE INTERIOR POINTS
  XL1=XL+.5*(XR-XL-EPSLN)
  XR1=XL1+EPSLN
C SUBROUTINE IPROD USES COMMON BLOCKS /C1/C2/C3/
  CALL IPROD1(XL1,YL1)
  CALL IPROD1(XR1,YR1)
  IF(YL1*2-YR1**2) 2,5,3
C YR1*2 GREATER THAN YL1**2
  XR=XR1
  2

```



```

C      YL1*2 GREATER THAN YR1*2
3      XL=XL1
C      TEST FOR END OF SEARCH
4      IF(ITER.GE.100) GO TO 6
        ITER=ITER+1
        IF(XR-XL.GT.3.*EPSLN) GO TO 1
5      LPROVL=.5*(XL1+XR1)
C      WRITE SOLUTION
        WRITE(6,600) LPROVL
        GC TO 8
C      WRITE OUTPUT - SEARCH FAILED TO CONVERGE
6      WRITE(6,610)
        GC TO 11
8      CONTINUE
C      SEARCH FOR EVEN MODE RESONANT LENGTH OF INDUCTIVELY COUPLED FINLINE
C      CAVITY.
        WRITE(6,499)
        DO 28 I=1,8
            TOVD=TOVD1(I,T)
            TOVW=TOVD/WOVD
            IF(TOVD.EQ.0.0) GO TO 11
C      SEARCH INTERVAL IS XLEMIN TO XREMAX
            XLE=XLEMIN
            XRE=XREMAX
            EPSLNE=.5*DABS(XLE-XRE)
            SIGNE=0.0
            ITER=1
C      CALCULATE INTERIOR POINTS
C      AND TEST FOR END OF SEARCH
31      IF(.NOT.((EPSLNE.GE.ACCUR).AND.(ITERE.LT.100))) GO TO 32
C      CALCULATE L(M,N) MATRIX ELEMENTS; L(M,N) * ALFA(N) = G(M)
        DO 51 MTH=1,ORDER
            DO 52 NTH=1,ORDER
                CALL IPROD3(MTH,NTH,LPROVL,XLE,YLELE)
                LLE(MTH,NTH)=YLELE
                IF(.NOT.(MTH.NE.NTH)) GO TO 53
                LLE(NTH,MTH)=LLE(MTH,NTH)
            CONTINUE
53      CALL IPROD3(MTH,NTH,LPROVL,XRESTE,YRELE)
                LRE(MTH,NTH)=YRELE
                IF(.NOT.(MTH.NE.NTH)) GO TO 54
                LRE(NTH,MTH)=LRE(MTH,NTH)
            CONTINUE
54      CONTINUE
52      CONTINUE
51      DO 55 MTH=1,ORDER
C

```



```

C
C
C
C
C
55 WRITE(6,130) (LLE(MTH,NTH),NTH=1,ORDER)
CONTINUE
DO 56 MTH = 1,ORDER
WRITE(6,130) (LRE(MTH,NTH),NTH=1,ORDER)
CONTINUE
56 CALCULATE THE DETERMINANT OF THE L(M,N) MATRIX:
CALL DTERM(ORDER,LLE,DETLE,ROWDIM)
YLE = DETLE
CALL DTERM(ORDER,LRE,DETRE,ROWDIM)
YRE = DETRE
SIGNE = YLE*YRE
IF(.NOT.(SIGNE.LT.0.0)) GO TO 33
XRE = XRESTE
GO TO 34
33 CONTINUE
XLE = XRESTE
34 CONTINUE
EPSLNE = .5*DABS(XLE-XRE)
ITERE = ITERE + 1
PRINT,XLE,XRE,ITERE
GO TO 31
32 CONTINUE
IF(.NOT.(ITERE.LT.100)) GO TO 35
LERES = .5*(XLE+XRE)
XE = DTAN(C2PI*(.5-LERES))
GO TO 36
35 CONTINUE
WRITE OUTPUT - SEARCH FAILED TO CONVERGE
WRITE(6,810)
36 CONTINUE
SEARCH FOR ODD MODE RESONANT LENGTH OF INDUCTIVELY COUPLED FINLINE
CAVITY. INTERVAL IS XLOMIN TO XROMAX
XLO = XLOMIN
XRO = XROMAX
EPSLNO = .5*DABS(XLO-XRO)
SIGNO = 0.0
ITERO = 1
41 CALCULATE INTERIOR POINTS
AND TEST FOR END OF SEARCH
IF(.NOT.(EPSLNO.GE.ACCUR).AND.(ITERO.LT.100)) GO TO 42
41 CONTINUE
XRESTO = .5*(XLO+XRO)
42 CALCULATE L(M,N) MATRIX ELEMENTS: L(M,N) * ALFA(N) = G(M)
DO 61 MTH = 1,ORDER
DO 62 NTH = MTH,ORDER
IPWR = MTH + NTH + 1
SIGN = (-1.0)**IPWR
CALL IPRD4(MTH,NTH,LPROVL,XLO,YLELO)

```


63

```

LLO(MTH,NTH) = YLELO*SIGN
IF(.NOT.(MTH.NE.NTH)) GO TO 63
LLO(NTH,MTH) = LLO(MTH,NTH)
CONTINUE
CALL IPROD4(MTH,NTH,LPROVL,XRESTO,YRELU)
LRO(MTH,NTH) = YRELO*SIGN
IF(.NOT.(MTH.NE.NTH)) GO TO 64
LRO(NTH,MTH) = LRO(MTH,NTH)
CONTINUE

```

64
62
61

```

CONTINUE
DO 65 MTH = 1,ORDER
WRITE(6,130) (LLO(MTH,NTH),NTH=1,ORDER)
CONTINUE
DO 66 MTH = 1,ORDER
WRITE(6,130) (LRO(MTH,NTH),NTH=1,ORDER)

```

65

```

CONTINUE
CALCULATE THE DETERMINANT OF THE L(M,N) MATRIX:
CALL DTERM(ORDER,LLO,DETLO,ROWDIM)
YLO = DETLO
CALL DTERM(ORDER,LRO,DETRO,ROWDIM)
YRO = DETRO

```

66

```

SIGNO = YLO*YRO
IF(.NOT.(SIGNO.LT.0.0)) GO TO 43
XRO = XRESTO

```

43

```

GO TO 44
CONTINUE

```

44

```

XLO = XRESTO
CONTINUE
EPSLNO = 5*DABS(XLO-XRO)
ITERO = ITERO + 1
PRINT,XLO,XRO,ITERO
GO TO 41

```

42

```

CONTINUE
IF(.NOT.(ITERO.LT.100)) GO TO 45
LORES = .5*(XLO+XRO)
XO = DTAN(C2PI*(.5-LORES))

```

45

```

GO TO 46
CONTINUE
WRITE OUTPUT - SEARCH FAILED TO CONVERGE
WRITE(6,820)

```

46

```

CALCULATE EQUIVALENT CIRCUIT REACTANCES XS AND XM FOR INDUCTIVE POST
XS=.5*(XE+XO)
XM=.5*(XE-XO)
CLWRITE SOLUTIONS FOR LE/LPR, LO/LPR, XS AND XM
WRITE(6,800) LOVD,TOVM,LERES,LORES,XS,XM
CSCALCULATE THE SCATTERING PARAMETERS FOR INDUCTIVE POST

```



```

C MSG3: SEARCH FOR ZERO OF IPROD2 FAILED TO CONVERGE
C MSG4: SEARCH FOR ZERO OF IPROD3 FAILED TO CONVERGE
C MSG5: SEARCH FOR ZERO OF IPROD4 FAILED TO CONVERGE
C SUBR *****
$EJECT *****
C SUBROUTINE IPROD1(LPROVL,SUM1) *****
C ***** THIS SUBROUTINE IS DESIGNED TO CALCULATE THE INNER PRODUCT OF *****
C THE GL DYADIC GREEN'S FUNCTION AND THE SQUARE OF THE FOURIER TRANS *****
C -FORM OF THE X-COMPONENT OF THE X-DIRECTED ELECTRIC FIELD *****
C ***** VARIABLE DEFINITIONS ***** TRANSFORM OF THE X-COMPONENT OF THE *****
C EXXSQ = SQUARE OF THE FOURIER TRANSFORM OF THE X-COMPONENT OF THE *****
C ***** X-DIRECTED ELECTRIC FIELD *****
C G11 = THE GL DYADIC GREEN'S FUNCTION *****
C MMAX = THE LIMIT OF SUMMATION OVER ALFD *****
C SUM1 = THE RETURNED VALUE OF THE INNER PRODUCT *****
C ***** VARIABLE DECLARATION ***** *****
C ***** IMPLICIT REAL*8 (A-H), REAL*8 (O-Z) *****
C ***** REAL*8 LPROVL *****
COMMON/C1/EP SR1,EP SR2,EP SR3,H1OVD,H2OVD,BOVD
COMMON/C2/C2PI,C2PISQ,P1
COMMON/C3/DOVL,W0VB
COMMON/C5/XCONST,ZCONST
BETAD = C2PI*DOVL/LPROVL
BOVW = 1./W0VB
C SPECIFY LIMIT FOR SUMMATION ON N *****
IF(W0VB.EQ.1.) MMAX=1
IF(W0VB.LT.1.) MMAX=IDINT((XCONST*BOVW)/C2PI)
IF(MMAX.GT.40) MMAX=40
SUM1 = 0.0
DO 11 M=1,MMAX
N=M-1
ALFD=N*C2PI/BOVD
CALL GRN11(ALFD,BETAD,DOVL,G11)
CALL EXSQ1(ALFD,W0VB,BOVD,EXXSQ)
SUM1=SUM1+2.*G11*EXXSQ
IF(N.EQ.0) SUM1=G11
11 CONTINUE
RETURN
END
C SUBR *****
$EJECT *****
C SUBROUTINE IPROD3(MTH,NTH,LPROVL,LERS,SUM3) *****
C ***** THIS SUBROUTINE IS DESIGNED TO CALCULATE THE INNER PRODUCT OF *****
C THE GL DYADIC GREEN'S FUNCTION, THE FOURIER TRANSFORM OF THE MTH *****
C Z-COMPONENT OF THE X-DIRECTED ELECTRIC FIELD, THE FOURIER TRANSFORM *****

```



```

16 CONTINUE
C DETERMINE IF NTH IS EVEN OR ODD
REMAIN = MOD(NTH,2)
IF(.NOT.(REMAIN.EQ.0)) GO TO 17
NA = NTH/2
CALL EXZSH5(NN,ZETAD,LERES,LPROVL,EXZSN)
EXZN = EXZSN
CALL EXZSH5(ZETAD,LERES,LPROVL,TOVD,EXZE5N)
SHIFTN = EXZE5N
GO TO 18
17 CONTINUE
NN = (NTH+1)/2
CALL EXZCOS(NN,ZETAD,LERES,LPROVL,EXZCN)
EXZN = EXZCN
CALL EXZSH3(ZETAD,LERES,LPROVL,TOVD,EXZE3N)
SHIFTN = EXZE3N
18 CONTINUE
SUM3 = SUM3+2.*G11*EXXSQ*EXZM*EXZN*SHIFTM*SHIFTN
10 CONTINUE
IF(NMAX.EQ.0) GO TO 14
DO 13 N = 1,NMAX
DO 12 K = 1,KMAX
RN = DFL0AT(N)
RK = DFL0AT(K)
ALFD = RN#C2PI/BOVD
ZETAD = ((RK-.5)*C2PI)/(2.*LEOVD+TOVD)
BETAD = ZETAD
CALL GRN11(ALFD,BETAD,DOVL,G11)
CALL EXSQ1(ALFD,W0VB,BOVD,EXXSQ)
IF NTH IS EVEN OR ODD
REMAIN = MOD(NTH,2)
IF(.NOT.(REMAIN.EQ.0)) GO TO 25
MM = NTH/2
CALL EXZSH5(MM,ZETAD,LERES,LPROVL,EXZSM)
EXZM = EXZSM
CALL EXZSH5(ZETAD,LERES,LPROVL,TOVD,EXZE5M)
SHIFTM = EXZE5M
GO TO 26
25 CONTINUE
MM = (NTH+1)/2
CALL EXZCOS(MM,ZETAD,LERES,LPROVL,EXZCM)
EXZM = EXZCM
CALL EXZSH3(ZETAD,LERES,LPROVL,TOVD,EXZE3M)
SHIFTM = EXZE3M
26 CONTINUE
C DETERMINE IF NTH IS EVEN OR ODD
REMAIN = MOD(NTH,2)
IF(.NOT.(REMAIN.EQ.0)) GO TO 27

```



```

NN = NTH/2
CALL EXZSIN(NN,ZETAD,LERES,LPROVL,EXZSN)
EXZN = EXZSN
CALL EXZSH5(ZETAD,LERES,LPROVL,TOVD,EXZE5N)
SHIFTN = EXZE5N
GO TO 28
CONTINUE
27 NN = (NTH+1)/2
CALL EXZCOS(NN,ZETAD,LERES,LPROVL,EXZCN)
EXZN = EXZCN
CALL EXZSH3(ZETAD,LERES,LPROVL,TOVC,EXZE3N)
SHIFTN = EXZE3N
CONTINUE
28 CCN = SUM3+4. *G11*EXXSQ*EXZM*EXZN*SHIFTM*SHIFTN
CONTINUE
12 CONTINUE
13 CONTINUE
14 RETURN
END
C SUBROUTINE IPR0D4(MTH,NTH,LPROVL,LRES,SUM4)
$EJECT *****
C ***** THIS SUBROUTINE IS DESIGNED TO CALCULATE THE INNER PRODUCT OF
C ***** THE GL1 DYADIC GREEN'S FUNCTION, THE FOURIER TRANSFORM OF THE MTH
C ***** Z-COMPONENT OF THE X-DIRECTED ELECTRIC FIELD, THE FOURIER TRANSFORM
C ***** OF THE NTH Z-COMPONENT OF THE X-DIRECTED ELECTRIC FIELD, AND THE
C ***** MTH AND NTH SPATIAL SHIFT FUNCTIONS FOR THE Z-COMPONENT FUNCTION.
C ***** WITH AN ESTIMATE OF THE ODD MODE RESONANT LENGTH AS AN ARGUMENT.
C ***** IF M OR N IS EVEN, THE FOURIER TRANSFORM OF THE Z-COMPONENT IS A
C ***** SIN FUNCTION WITH AN INDEX VALUE OF MTH/2 OR NTH/2.
C ***** IF M OR N IS ODD, THE FOURIER TRANSFORM OF THE Z-COMPONENT IS A
C ***** COS FUNCTION WITH AN INDEX VALUE OF (MTH+1)/2 OR (NTH+1)/2.
C ***** EXXSQ = SQUARE OF THE FOURIER TRANSFORM OF THE X-COMPONENT OF THE
C ***** X-DIRECTED ELECTRIC FIELD
C ***** G11 = THE GL1 DYADIC GREEN'S FUNCTION
C ***** EXZM = THE FOURIER TRANSFORM OF THE MTH Z-COMPONENT OF THE
C ***** EXZN = THE FOURIER TRANSFORM OF THE NTH Z-COMPONENT OF THE
C ***** EXZCM = THE FOURIER TRANSFORM OF THE MTH Z-COMPONENT OF THE
C ***** ELECTRIC FIELD WHERE M IS ODD AND THE SPATIAL FUNCTION IS A
C ***** COSINE FUNCTION.
C ***** EXZCN = THE FOURIER TRANSFORM OF THE NTH Z-COMPONENT OF THE
C ***** ELECTRIC FIELD WHERE N IS ODD AND THE SPATIAL FUNCTION IS A
C ***** COSINE FUNCTION.
C ***** EXZ04M = THE FOURIER TRANSFORM OF THE SPATIAL SHIFT OF THE MTH Z-

```



```

SUM4 = 0.0
N=0
K=0
RN = DFLOAT(N)
RK = DFLOAT(K)
ALFD=RN*C2PI/BOVD
ZETAD = (RK*C2PI)/(2.*LOOVD+TOVD)
BETAD = ZETAD
CALL GRN11(ALFD,BETAD,DOVL,G11)
CALL EXSC1(ALFD,W0VB,BOVD,EXXSQ)
C DETERMINE IF MTH IS EVEN OR ODD
REMAIN = MOD(MTH,2)
IF (.NOT. (REMAIN.EQ.0)) GO TO 5
MM = MTH/2
CALL EXZSIN(MM,ZETAD,LORES,LPROVL,EXZSM)
EXZM = EXZSM
CALL EXZSH6(ZETAD,LORES,LPROVL,TOVD,EXZO6M)
SHIFTM = EXZO6M
GO TO 6
5 CONTINUE
MM = (MTH+1)/2
CALL EXZCOS(MM,ZETAD,LORES,LPROVL,EXZCM)
EXZM = EXZCM
CALL EXZSH4(ZETAD,LORES,LPROVL,TOVD,EXZO4M)
SHIFTM = EXZO4M
6 CONTINUE
NTH IS EVEN OR ODD
REMAIN = MOD(NTH,2)
IF (.NOT. (REMAIN.EQ.0)) GO TO 7
NN = NTH/2
CALL EXZSIN(NN,ZETAD,LORES,LPROVL,EXZSN)
EXZN = EXZSN
CALL EXZSH6(ZETAD,LORES,LPROVL,TOVD,EXZO6N)
SHIFTN = EXZO6N
GO TO 8
7 CONTINUE
NN = (NTH+1)/2
CALL EXZCOS(NN,ZETAD,LORES,LPROVL,EXZCN)
EXZN = EXZCN
CALL EXZSH4(ZETAD,LORES,LPROVL,TOVD,EXZO4N)
SHIFTN = EXZO4N
8 CONTINUE
SUM4=G11*EXXSQ*EXZM*EXZN*SHIFTM*SHIFTN
N=0
DO 10 K = 1,KMAX
RN = DFLOAT(N)
RK = DFLOAT(K)
ALFD = RN*C2PI/BOVD

```



```

ZETAL = (RK*CC2PI)/(2.*LOOVD+TOVD)
BETAD = ZETAD
CALL GRN11(ALFD,BETAD,DOVL,G11)
CALL EXSQ1(ALFD,W0VB,BOVD,EXXSQ)
C DETERMINE IF MTH IS EVEN OR ODD
REMAIN = MOD(MTH,2)
IF(.NOT.(REMAIN.EQ.0)) GO TO 15
MM = MTH/2
CALL EXZSIN(MM,ZETAD,LORES,LPROVL,EXZSM)
EXZM = EXZSM
CALL EXZSH6(ZETAD,LORES,LPROVL,TOVD,EXZO6M)
SHIFTM = EXZO6M
GO TO 16
15 CONTINUE
MM = (MTH+1)/2
CALL EXZCOS(MM,ZETAD,LORES,LPROVL,EXZCM)
EXZM = EXZCM
CALL EXZSH4(ZETAD,LORES,LPROVL,TOVD,EXZO4M)
SHIFTM = EXZO4M
16 CONTINUE
C DETERMINE IF NTH IS EVEN OR ODD
REMAIN = MOD(NTH,2)
IF(.NOT.(REMAIN.EQ.0)) GO TO 17
NN = NTH/2
CALL EXZSIN(NN,ZETAD,LORES,LPROVL,EXZSN)
EXZN = EXZSN
CALL EXZSH6(ZETAD,LORES,LPROVL,TOVD,EXZO6N)
SHIFTN = EXZO6N
GO TO 18
17 CONTINUE
NN = (NTH+1)/2
CALL EXZCOS(NN,ZETAD,LORES,LPROVL,EXZCN)
EXZN = EXZCN
CALL EXZSH4(ZETAD,LORES,LPROVL,TOVD,EXZO4N)
SHIFTN = EXZO4N
18 CONTINUE
SUM4 = SUM4+2.*G11*EXXSQ*EXZN*SHIFTM*SHIFTN
10 CONTINUE
IF(NMAX.EQ.0) GO TO 14
K=0
DO
11 N = 1,NMAX
RN = DFLOAT(N)
RK = DFLOAT(K)
ALFD = RN*CC2PI/BOVD
ZETAD = (RK*CC2PI)/(2.*LOOVD+TOVD)
BETAD = ZETAD
CALL GRN11(ALFD,BETAD,DOVL,G11)
CALL EXSQ1(ALFD,W0VB,BOVD,EXXSQ)

```



```

C DETERMINE IF MTH IS EVEN OR ODD
REMAIN = MOD(MTH,2)
IF(.NOT.(REMAIN.EQ.0)) GO TO 25
MM = MTH/2
CALL EXZSIN(MM,ZETAD,LORES,LPROVL,EXZSM)
EXZM = EXZSM
CALL EXZSH6(ZETAD,LORES,LPROVL,TOVD,EXZO6M)
SHIFTM = EXZO6M
GO TO 26
25 CONTINUE
MM = (MTH+1)/2
CALL EXZCOS(MM,ZETAD,LORES,LPROVL,EXZCM)
EXZM = EXZCM
CALL EXZSH4(ZETAD,LORES,LPROVL,TOVD,EXZO4M)
SHIFTM = EXZO4M
26 CONTINUE
C DETERMINE IF NTH IS EVEN OR ODD
REMAIN = MOD(NTH,2)
IF(.NOT.(REMAIN.EQ.0)) GO TO 27
NN = NTH/2
CALL EXZSIN(NN,ZETAD,LORES,LPROVL,EXZSN)
EXZN = EXZSN
CALL EXZSH6(ZETAD,LORES,LPROVL,TOVD,EXZO6N)
SHIFTN = EXZO6N
GO TO 28
27 CONTINUE
NN = (NTH+1)/2
CALL EXZCOS(NN,ZETAD,LORES,LPROVL,EXZCN)
EXZN = EXZCN
CALL EXZSH4(ZETAD,LORES,LPROVL,TOVD,EXZO4N)
SHIFTN = EXZO4N
28 CONTINUE
SUM4 = SUM4+2.*G11*EXXSQ*EXZM*EXZN*SHIFTM*SHIFTN
11 CONTINUE
DO 13 N = 1,NMAX
12 K = 1,KMAX
RN = DFL0AT(N)
RK = DFL0AT(K)
ALFD = RN*C2PI/BOVD
ZETAD = (RK*C2PI)/(2.*LOOVD+TOVD)
BETAD = ZETAD
CALL GRN11(ALFD,BETAD,DOVL,G11)
CALL EXSQ1(ALFD,W0V8,BOVD,EXXSQ)
IF MTH IS EVEN OR ODD
REMAIN = MOD(MTH,2)
IF(.NOT.(REMAIN.EQ.0)) GO TO 35
MM = MTH/2
CALL EXZSIN(MM,ZETAD,LORES,LPROVL,EXZSM)

```



```

35      EXZM = EXZSM
      CALL EXZSH6(ZETAD, LORES, LPROVL, TOVC, EXZO6M)
      SHIFTM = EXZO6M
      GC TO 36
      CCNTINUE
      MM = (MTH+1)/2
      CALL EXZCOS(MM, ZETAD, LORES, LPROVL, EXZCM)
      EXZM = EXZCM
      CALL EXZSH4(ZETAD, LORES, LPROVL, TOVD, EXZO4M)
      SHIFTM = EXZO4M
      CCNTINUE
36  C DETERMINE
      IF NTH IS EVEN OR ODD
      IF NTH = MOD(NTH, 2)
      IF (.NOT. (REMAIN.EQ.0)) GO TO 37
      NN = NTH/2
      CALL EXZSIN(NN, ZETAD, LORES, LPROVL, EXZSN)
      EXZN = EXZSN
      CALL EXZSH6(ZETAD, LORES, LPROVL, TOVC, EXZO6N)
      SHIFTN = EXZO6N
      GC TO 38
      CCNTINUE
37      NN = (NTH+1)/2
      CALL EXZCOS(NN, ZETAD, LORES, LPROVL, EXZCN)
      EXZN = EXZCN
      CALL EXZSH4(ZETAD, LORES, LPROVL, TOVD, EXZO4N)
      SHIFTN = EXZO4N
      CCNTINUE
38      SUM4 = SUM4 + 4. * G11 * EXXSQ * EXZM * EXZN * SHIFTM * SHIF TN
      CCNTINUE
12  CONTINUE
13  CONTINUE
14  CONTINUE
      RETURN
      END
3  SUBR *****
$EJECT *****

```

```

*****
SUBROUTINE GRN11(ALFD, BETAD, DOVL, G11)
*****
C ***** THIS SUBROUTINE IS DESIGNED TO CALCULATE THE G11 DYADIC GREEN'S
C FUNCTION *****
C ***** VARIABLE DEFINITIONS *****
C G11 = THE G11 DYADIC GREEN'S FUNCTION, RETURNED VALUE
C G1DSQ
C G2DSQ
C G3DSQ
C KC1DSQ
C KC2DSQ
C KC3DSQ
C WEPSID
*****

```



```

C WEPS2D
C WEPS3D
C WMUD
C *****
VARIABLE DECLARATION *****
IMPLICIT REAL*8 (A-H), REAL*8 (O-Z)
REAL*8 KC1DSQ, KC2DSQ, KC3DSQ, LPROVL, LOVLPR
COMMON/C1/EP SR1, EP SR2, EP SR3, H1OVD, H2OVD, BOVD
COMMON/C2/C2PI, C2PISQ, PI
C CALCULATE VARIABLES DEPENDENT ON FREQUENCY
WMUD=60.*C2PISQ*DOVL
WEPS1D=EP SR1*DOVL/60.
WEPS2D=EP SR2*DOVL/60.
WEPS3D=EP SR3*DOVL/60.
C CALCULATE VARIABLES DEPENDENT ON FRRQUENCY AND BETAD
BETDSQ=BETAD**2
KC1DSQ=C2PISQ*EP SR1*DOVL**2-BETDSQ
KC2DSQ=C2PISQ*EP SR2*DOVL**2-BETDSQ
KC3DSQ=C2PISQ*EP SR3*DOVL**2-BETDSQ
C CALCULATE VARIABLES DEPENDENT ON FREQUENCY, BETAD AND ALFD
ALFDSQ=ALFD**2
G1DSQ=ALFDSQ-KC1DSQ
G2DSQ=ALFDSQ-KC2DSQ
G3DSQ=ALFDSQ-KC3DSQ
CALL TFN(G1DSQ, H1OVD, TFN1)
CALL TFN(G2DSQ, H1OVD, TFN2)
CALL TFN(G3DSQ, H2OVD, TFN3)
D11=-KC2DSQ*(1.+(WEPS3D*G3DSQ*KC2DSQ*TFN2)/(WEPS2D*G2DSQ*KC3DSQ*
1TFN3))
D12=((ALFD*BETAD)/(WEPS2D*G2DSQ))*((KC2DSQ/KC1DSQ)-1.)*KC2DSQ
D21=-ALFD*BETAD*((KC2DSQ/KC1DSQ)+(WEPS3D*KC2DSQ*G3DSQ*TFN2)/
1(WEPS2D*KC3DSQ*G2DSQ*TFN3))
D22=WMUD*(1.+(KC2DSQ*TFN3)/(KC3DSQ*TFN2))+((ALFDSQ*BETDSQ)/(G2DSQ
1*WMUD*WEPS2D))*((KC2DSQ/KC3DSQ)-1.)
DET=D11*D22-D12
C CALCULATE G11
G11A=-KC1DSQ/(WMUD*TFN1)
G11B=-(KC2DSQ*D12*ALFD*BETAD*KC2DSQ*TFN2)/(DET*WMUD*G2DSQ)
G11C=-(KC2DSQ*D12*ALFD*BETAD*TFN2)/(DET*WMUD*G2DSQ)
G11D=-(KC2DSQ*D11*KC2DSQ*TFN3)/(DET*KC3DSQ*G2DSQ)
G11E=-(KC2DSQ*D11)/(DET*TFN2)
G11=G11A+G11B+G11C+G11D+G11E
RETURN
END
C SUBROUTINE TFN(G1DSQ, H1OVD, TFN1)
$EJECT
C *****
C THIS SUBROUTINE IS DESIGNED TO CALCULATE THE TANGENT AND THE

```



```

C HYPERBOLIC TANGENT FUNCTIONS FOR THE GRN11 SUBROUTINE.
C**VARIABLE DEFINITIONS*****
C GID
C GIDSQ
C HIOVD
C IFNI
C**
      THE RETURNED VALUE
      VARIABLE DECLARATION#8 (A-H); REAL*8 (O-Z)
      IMPLICIT REAL*8 (A-H); REAL*8 (O-Z)
      GID=DSQRT(DABS(GIDSQ))
      ARG=GICD*HIOVD**2
      IF (ARG.LE.0.) GO TO 1
      IF (ARG.GT.0.) AND.(ARG.LT.100.) GO TO 2
      IF (ARG.GE.100.) GO TO 3
      IF NI=-GID*DTAN(GID*HIOVD)
      1 GO TO 4
      2 IF NI=GIC*DTANH(GID*HIOVD)
      3 GO TO 4
      4 IF NI=GID
      5 RETURN
      6 END
C SUBJECT *****
C $EJECT *****
      SUBROUTINE EXXSQ(ALFD,WQVB,BOVD,EXXSQ)
      *****
      THIS SUBROUTINE IS DESIGNED TO CALCULATE THE FOURIER TRANSFORM
      OF THE X-COMPONENT OF THE X-DIRECTED ELECTRIC FIELD AND SQUARE IT.
      *****
      VARIABLE DEFINITIONS*****
      EXXSQ = SQUARE OF THE FOURIER TRANSFORM OF THE X-COMPONENT OF THE
      X-DIRECTED ELECTRIC FIELD, THE RETURNED VALUE
      *****
      VARIABLE DECLARATION*****
      IMPLICIT REAL*8 (A-H), REAL*8 (O-Z)
      COMMON/C2/C2PI,C2PISQ,PI
      WQVD=WQVB*BOVD
      CALCULATE EXXSQ, THE X TRANSFORM OF THE E FIELD BETWEEN THE FINS
      IF (ALFD.EQ.0.) EXXSQ=1.0
      IF (ALFD.GT.0.) EXXSQ=(DSIN(.5*ALFD*WQVD)/(.5*ALFD*WQVD))**2
      RETURN
      END
C SUBJECT *****
C $EJECT *****
      SUBROUTINE EXZCOS(MN,ZETAD,LRES,LPROVL,EXZCMN)
      *****
      THIS SUBROUTINE IS DESIGNED TO CALCULATE THE FOURIER TRANSFORM
      OF THE Z-COMPONENT OF THE X-DIRECTED ELECTRIC FIELD WHERE THE
      SPATIAL FUNCTION IS A COSINE FUNCTION.
      *****
      VARIABLE DEFINITIONS*****
      EXZCMN = THE FOURIER TRANSFORM OF THE MNTH COS Z-COMPONENT OF THE
      X-DIRECTED ELECTRIC FIELD, THE RETURNED VALUE.
      *****

```



```

C MN = ROW OR COLUMN INDEX
C ***
C *** VARIABLE DECLARATION ***
IMPLICIT REAL*8 (A-H), REAL*8 (O-Z)
REAL*8 LRES, LPROVL, LOVD, NUMBER, DENOM, DIM
COMMON /C2/C2PI, C2PISQ, PI
COMMON /C3/DOVL, WOV8
LOVD = LRES * LPROVL / DOVL
THETA = ZETAD * .5 * LOVD
DIM = DFL0AT(MN)
RESID = DABS(THETA - ((2. * DIM - 1.) * PI) / 2.)
SIGN = (-1.0) ** MN
NUMBER = DCOS(THETA)
DENOM = (((THETA) ** 2) - (((2. * DIM) - 1.) * PI) / 2.) ** 2)
IF (.NOT. (RESID .LT. 1.0D-7)) GO TO 35
EXZCMN = 1./PI
GO TO 36
35 CONTINUE
EXZCMN = SIGN*.5*((2.*DIM)-1.0)*(NUMBER/DENOM)
36 CONTINUE
RETURN
END
C SUBROUTINE EXZSIN(MN, ZETAD, LRES, LPROVL, EXZSMN)
C ***
C *** THIS SUBROUTINE IS DESIGNED TO CALCULATE THE FOURIER TRANSFORM
C OF THE Z-COMPONENT OF THE X-DIRECTED ELECTRIC FIELD WHERE THE
C SPATIAL FUNCTION IS A SINE FUNCTION.
C *** VARIABLE DEFINITION ***
C EXZSMN = THE FOURIER TRANSFORM OF THE MNTH SIN Z-COMPONENT OF THE
C X-DIRECTED ELECTRIC FIELD, THE RETURNED VALUE.
C ***
C MN = ROW OR COLUMN INDEX
C ***
C *** VARIABLE DECLARATION ***
IMPLICIT REAL*8 (A-H), REAL*8 (O-Z)
REAL*8 LRES, LPROVL, LOVD, NUMBER, DENOM, DIM
COMMON /C2/C2PI, C2PISQ, PI
COMMON /C3/DOVL, WOV8
LOVD = LRES * LPROVL / DOVL
THETA = ZETAD * .5 * LOVD
DIM = DFL0AT(MN)
RESID = DABS(THETA - (DIM*PI))
SIGN = (-1.0) ** MN
NUMBER = DSIN(THETA)
DENOM = (((THETA) ** 2) - ((DIM*PI) ** 2)
IF (.NOT. (RESID .LT. 1.0D-7)) GO TO 35
EXZSMN = .5/PI
GO TO 36
35 CONTINUE

```



```

      EXZSMN = SIGN*DIM*(NUMER/DENOM)
36 CONTINUE
      RETURN
END
C SUBROUTINE EXZSH3(ZETAD, LERES, LPROVL, TOVD, EXZE3)
$EJECT
C *****
C THIS SUBROUTINE IS DESIGNED TO CALCULATE THE FOURIER TRANSFORM
C OF THE SPATIAL SHIFT OF THE Z-COMPONENT OF THE ELECTRIC FIELD FOR
C THE EVEN MODE WHERE THE SHIFT FUNCTION IS A COSINE FUNCTION.
C *****
C ** VARIABLE DEFINITION TRANSFORM OF THE COS SHIFT FUNCTION OF THE Z-
C EXZE3 = COMPONENT OF THE ELECTRIC FIELD FOR THE EVEN MODE, THE
C ** RETURNED VALUE.
C *****
C ** VARIABLE DECLARATION *****
C IMPLICIT REAL*8 (A-H), REAL*8 (O-Z)
C REAL*8 LERES, LPROVL, LEOVD
C COMMON/C2/C2PI, C2PISQ, PI
C COMMON/C3/DOVL, WOV8
C LEOVD = LERES*LPROVL/DOVL
C CALCULATE EXZESH, THE EVEN MODE Z TRANSFORM FACTOR
C EXZE3 = DCOS(ZETAD*.5*(LEOVD+TOVD))
      RETURN
END
C SUBROUTINE EXZSH4(ZETAD, LORES, LPROVL, TOVD, EXZ04)
$EJECT
C *****
C THIS SUBROUTINE IS DESIGNED TO CALCULATE THE FOURIER TRANSFORM
C OF THE SPATIAL SHIFT OF THE Z-COMPONENT OF THE ELECTRIC FIELD FOR
C THE ODD MODE WHERE THE SHIFT FUNCTION IS A SINE FUNCTION.
C *****
C ** VARIABLE DEFINITION TRANSFORM OF THE SIN SHIFT FUNCTION OF THE Z-
C EXZ04 = COMPONENT OF THE ELECTRIC FIELD FOR THE ODD MODE, THE
C ** RETURNED VALUE.
C *****
C ** VARIABLE DECLARATION *****
C IMPLICIT REAL*8 (A-H), REAL*8 (O-Z)
C REAL*8 LORES, LPROVL, LEOVD
C COMMON/C2/C2PI, C2PISQ, PI
C COMMON/C3/DOVL, WOV8
C LEOVD = LORES*LPROVL/DOVL
C CALCULATE EXZ04, THE ODD MODE Z TRANSFORM FACTOR
C EXZ04 = DSIN(ZETAD*.5*(LEOVD+TOVD))
      RETURN
END
C SUBROUTINE
$EJECT

```



```

C ***** SUBROUTINE EXZSH5(ZETAD, LERES, LPROVL, TCVD, EXZES) *****
C THIS SUBROUTINE IS DESIGNED TO CALCULATE THE FOURIER TRANSFORM
C OF THE SPATIAL SHIFT OF THE Z-COMPONENT OF THE ELECTRIC FIELD FOR
C THE EVEN MODE WHERE THE SHIFT FUNCTION IS A SINE FUNCTION.
C THE VARIABLE DEFINITION TRANSFORM OF THE SINE FUNCTION OF THE Z-
C EXZES = THE COMPONENT OF THE ELECTRIC FIELD FOR THE EVEN MODE, THE
C RETURNED VALUE.
C ***** VARIABLE DECLARATION ***** REAL*8 (O-Z)
C IMPLICIT REAL*8 (A-H), REAL*8 (O-Z)
C REAL*8 LERES, LPROVL, LEOVD
C COMMON/C2/C2PI, C2PISQ, PI
C COMMON/C3/DOVL, WOV B
C LEOVD = LERES*LPROVL/DOVL
C CALCULATE EXZES = DSIN(ZETAD*.5*(LEOVD+TCVD))
C RETURN
C *****
C SUBJECT *****
C ***** SUBROUTINE EXZSH6(ZETAD, LORES, LPROVL, TOVD, EXZ06) *****
C THIS SUBROUTINE IS DESIGNED TO CALCULATE THE FOURIER TRANSFORM
C OF THE SPATIAL SHIFT OF THE Z-COMPONENT OF THE ELECTRIC FIELD FOR
C THE ODD MODE WHERE THE SHIFT FUNCTION IS A COSINE FUNCTION.
C THE VARIABLE DEFINITION TRANSFORM OF THE COS SHIFT FUNCTION OF THE Z-
C EXZ06 = THE COMPONENT OF THE ELECTRIC FIELD FOR THE ODD MODE, THE
C RETURNED VALUE.
C ***** VARIABLE DECLARATION ***** REAL*8 (O-Z)
C IMPLICIT REAL*8 (A-H), REAL*8 (O-Z)
C REAL*8 LORES, LPROVL, LEOVD
C COMMON/C2/C2PI, C2PISQ, PI
C COMMON/C3/DOVL, WOV B
C LEOVD = LORES*LPROVL/DOVL
C CALCULATE EXZ06 = LCOSS(ZETAD*.5*(LEOVD+TOVD))
C RETURN
C *****
C SUBROUTINE IDENTIFICATION:
C A. TITLE: DETERMINANT OF A REAL MATRIX
C CATEGORY: DETERMINANTS
C PROGRAMMER: JEAN BOW
C DATE: FEBRUARY 1965, CONVERTED TO SYSTEM/360, JANUARY 1967
C B. PURPOSE:

```



```

C.  USAGE:  THIS SUBROUTINE COMPUTES THE DETERMINANT OF A MATRIX OF REAL
      1.  CALLING SEQUENCE:  NUMBERS BY GAUSS' METHOD OF ELIMINATION WITH ROW PIVOTING.
      2.  CALL DTERM(N,A,DET,M)
      3.  PARAMETERS:
      4.  N - ORDER OF MATRIX A. (INTEGER) WHICH IS TO BE COMPUTED. (REAL*8)
      5.  A - MATRIX; THE DETERMINANT OF MATRIX A. (REAL*8)
      6.  DET - DETERMINANT OF MATRIX A. (THE INTEGER APPEARING IN USER'S
      7.  M - ROW DIMENSION OF MATRIX A. (THE INTEGER APPEARING IN USER'S
      8.  DIMENSION STATEMENT.)
      9.  CAUTIONS TO USER:
      10. IN THE CALLING PROGRAM, "A" MUST APPEAR IN A DIMENSION STATEMENT.
      11. MATRIX A IS DESTROYED.
      12. REFERENCES:
      13. 1. KUNZ, K. S., "NUMERICAL ANALYSIS", MCGRAW-HILL, NEW YORK, 1957
      14. 2. FADDEEV, V. A., "COMPUTATIONAL METHODS OF LINEAR ALGEBRA",
      15. TRANSLATED BY CURTIS D. BENSTER, DOVER PUBLICATIONS, INC.,
      16. NEW YORK, 1959.
      17. *****
      18. SUBROUTINE DTERM(N,A,D,M)
      19. IMPLICIT REAL*8 (A-H), REAL*8 (O-Z)
      20. DIMENSION A(M,M)
      21. DD=1.0D0
      22. DO 34 L=1,N
      23. KP=C
      24. Z=0.0
      25. DO 12 K=L,N
      26. IF(Z-DABS(A(K,L)))11,12,12
      27. Z=DABS(A(K,L))
      28. KP=K
      29. CONTINUE
      30. IF(L-KP)13,20,20
      31. DO 14 J=L,N
      32. Z=A(L,J)
      33. A(L,J)=A(KP,J)
      34. A(KP,J)=Z
      35. DD=-DD
      36. IF(L-N)31,40,40
      37. LPI=L+1
      38. DO 34 K=LPI,N
      39. IF(A(K,L))32,34,32
      40. RATIO=A(K,L)/A(L,L)
      41. DO 33 J=LPI,N
      42. A(K,J)=A(K,J)-RATIO*A(L,J)
      43. CONTINUE
      44. DO 41 K=L,N

```



```

41 DD=DD*A(K,K)
D=DD
RETURN
END

$ENTRY
.0677333 .0719667 .0762 .0804333 .084667 .0889 .0931533
.0973667 1.016 1.0 1.0 1.0 1.0 1.0
1.5 3.5 0.5 0.5 0.5 0.5 0.5
1.0 1.0 1.0 1.0 1.0 1.0 1.0
0.2 0.2 0.2 0.2 0.2 0.2 0.2
$END

```


LIST OF REFERENCES

1. Tischer, F.J., "Transmission Media for the Design of Millimeter-Wave Circuitry", 8th European Microwave Conference 1978, Workshop on Millimeter Wave Circuits.
2. Meier, P.J., "Integrated Fin-Line Millimeter Components", IEEE Trans. MTT, v. 22, pp. 1209-1216, December 1974.
3. Chang, C., and Itoh, T., "Spectral Domain Analysis of Dominant and Higher Order Modes in Fin-Lines", 1979 IEEE MTT-S Int. Microwave Symp., (Orlando, Florida), pp. 344-346.
4. Knorr, J.B., and Shayda, P.M., "Millimeter-Wave Fin-Line Characteristics", IEEE Trans. MTT, v. 28, pp. 737-743, July 1980.
5. Schmidt, L.P., and Itoh, T., "Spectral Domain Analysis of Dominant and Higher Order Modes in Fin-Lines", IEEE Trans MTT, v. 28, pp. 981-985, September 1980.
6. El-Sherbiny, A.M.A., "Exact Analysis of Shielded Microstrip Lines and Bilateral Fin-Lines", IEEE Trans. MTT, v. 29, pp. 669-675, July 1981.
7. Knorr, J.B., "Equivalent Reactance of a Shorting Septum in a Fin-Line: Theory and Experiment", IEEE Trans. MTT, v. 29, pp. 1196-1202, November 1981.
8. Mirshekar-Syahkal, D., and Davies, J.B., "Accurate Analysis of Couples Strip-Fineline Structure for Phase Constant, Characteristic Impedance, Dielectric and Conductor Losses", IEEE Trans. MTT, v. 30, pp. 906-910, June 1982.
9. Helard, M., Citerine, J., Picon, O., and Fouad Hanna, V., "Solution of Fin-Line Discontinuities Through the Identification of Its First Four Higher Order Modes", IEEE MTT-S Digest, pp. 387-389, 1983.
10. Sharma, A.K., and Hoefer, W.J.R., "Empirical Expressions for Fin-Line Design", IEEE Trans. MTT, v. 31, pp. 350-355, April 1983.
11. Sharma, A.K., and Hoefer, W.J.R., "Propagation in Coupled Unilateral and Bilateral Finlines", IEEE Trans. MTT, v. 31, pp. 498-501, June 1983.

12. Harrington, R.F., Field Computation by Moment Methods, Macmillan, 1968.
13. Demidovich, B.P., and Maron, I.A., Computational Mathematics, Mir, 1976.
14. Brown, R.G., Sharpe, R.A., Hughes, W.L., and Post, R.E., Lines, Waves, and Antennas, Wiley, 1973.
15. Miller, G.S., An Experimental Investigation of Several Fin-Line Discontinuities, M.S. Thesis, Naval Postgraduate School, Monterey, California, 1980.

INITIAL DISTRIBUTION LIST

	No. Copies
1. Library, Code 0142 Naval Postgraduate School Monterey, California 93943	2
2. Department Chairman, Code 62 Department of Electrical and Computer Engineering Naval Postgraduate School Monterey, California 93943	1
3. Professor Jeffery B. Knorr, Code 62Ko Department of Electrical and Computer Engineering Naval Postgraduate School Monterey, California 93943	2
4. Dr. Yi-Chi Shih, Code 62Zq Department of Electrical and Computer Engineering Naval Postgraduate School Monterey, California 93943	1
5. Dr. Hung-Moo Lee, Code 62Lh Department of Electrical and Computer Engineering Naval Postgraduate School Monterey, California 93943	1
6. CPT John C. Deal, USA Department of Electrical Engineering United States Military Academy West Point, New York 10996	2
7. COL Stanely E. Reinhart, Jr. Department of Electrical Engineering United States Military Academy West Point, New York 10996	1

DUDLEY KNOX LIBRARY



3 2768 00350094 3